AWARD NUMBER: W81XWH-11-1-0775

TITLE: Investigating the Regulation and Potential Role of Nonhypoxic Hypoxia-Inducible Factor 1 (HIF-1) in Aromatase Inhibitor-Resistant Breast Cancer."

PRINCIPAL INVESTIGATOR: Armina A. Kazi

CONTRACTING ORGANIZATION: University of Maryland, Baltimore
Baltimore, Maryland 21201

REPORT DATE: December 2015

TYPE OF REPORT: Final Annual Summary

PREPARED FOR: U.S. Army Medical Research and Materiel Command
Fort Detrick, Maryland 21702-5012

REPORT DOCUMENTATION PAGE

Form Approved
OMB No. 0704-0188

PLEASE DO NOT RETURN YOU DRESS.

REPORT DATE	2. REPORT TYYPE	3. DATES COVERED
December 2015	Final Annual Summary	15SEP2011 - 14SEP2015

TITLE AND SUBTITLE

Investigating the Regulation and Potential Role of Nonhypoxic Hypoxia-Inducible Factor 1 (HIF-1) in Aromatase Inhibitor-Resistant Breast Cancer."

5a. CONTRACT NUMBER
W81XWH-11-1-0775

5b. GRANT NUMBER
BC103931

5c. PROGRAM ELEMENT NUMBER

6. AUTHOR(S)
Armina A. Kazi

E-Mail: aakazi@loyola.edu

5d. PROJECT NUMBER

5e. TASK NUMBER

5f. WORK UNIT NUMBER

7. PERFORMING ORGANIZATION NAME(S) AND ADDRESS(ES)
University of Maryland, Baltimore
685 W. Baltimore Street
Baltimore, MD 21201

8. PERFORMING ORGANIZATION REPORT NUMBER

9. SPONSORING / MONITORING AGENCY NAME(S) AND ADDRESS(ES)

U.S. Army Medical Research and Materiel Command
Fort Detrick, Maryland 21702-5012

10. SPONSOR/MONITOR'S ACRONYM(S)

11. SPONSOR/MONITOR'S REPORT NUMBER(S)

12. DISTRIBUTION / AVAILABILITY STATEMENT

Approved for Public Release; Distribution Unlimited

13. SUPPLEMENTARY NOTES

14. ABSTRACT
Prior to this study, aromatase inhibitor (AI, ex. letrozole) resistance was associated with increased dependence on growth factors and decreased dependence on ERα. However, the role that such molecular changes play in AI resistance and the mechanism by which they elicit their effects were not known. Results from this study demonstrated that nonhypoxic expression of HIF-1 mediates HER2's effects on letrozole-resistance. Specifically, HER2-activated PI3K/Akt pathway increases HIF-1α protein synthesis in letrozole-resistant breast cancer cells. HIF-1α, in turn, upregulates expression of target proteins, such as BCRP and vimentin. BCRP and vimentin contribute to letrozole resistance through their effects on maintaining cacer stem cell characteristics and invasion and metastatic potential. Consequently, in addition to confirming the therapeutic potential of targeting HER2, this current study provides evidence that detecting and direct targeting of HIF-1 (ex. via EZN-2968)could also improve clinical diagnosis, prevention, and/or treatment of acquired AI resistance

15. SUBJECT TERMS
Breast cancer, aromatase inhibitors (ex. letrozole), drug resistance, cancer stem cells, nonhypoxic regulation

16. SECURITY CLASSIFICATION OF:			17. LIMITATION OF ABSTRACT	18. NUMBER OF PAGES	19a. NAME OF RESPONSIBLE PERSON
a. REPORT	b. ABSTRACT	c. THIS PAGE			USAMRMC
Unclassified	Unclassified	Unclassified	Unclassified	75	19b. TELEPHONE NUMBER *(include area code)*

Table of Contents

Page

INTRODUCTION

This research aims to understand the factors and molecular mechanisms involved in drug-resistant breast cancer, specifically aromatase inhibitor resistant breast cancer. Although aromatase inhibitors (AIs; i.e., letrozole) have been shown to be highly effective in treating estrogen receptor positive (ER+) breast cancer, a significant percentage of patients either do not respond to AIs or become resistant to them. Previous studies suggest that resistance to AIs involves a switch from dependence on ER signaling to dependence on growth factor-mediated pathways, such as human epidermal growth factor receptor-2 (HER2). The mechanism by which HER2 is involved in AI resistance remains mostly unclear. It is, therefore, important to elucidate the HER2-mediated pathway that contributes to AI resistance, and to identify other relevant factors involved that can be used as biomarkers of AI resistance or targets for therapy. One such factor may include HIF-1, a heterodimeric transcription factor made up of an inducible alpha (α) subunit and a constitutively expressed beta (β) subunit. HIF-1 regulates genes important for cell survival, metabolic adaptation, and angiogenesis. Oxygen (O_2) tension is a well-known regulator of HIF-1α, but other factors independent of O_2 can also regulate it. Thus, the purpose of this study is to determine the potential role of nonhypoxic HIF-1 in aromatase inhibitor resistant breast cancer, and whether it could be used as a diagnostic marker and therapeutic target. In vitro breast cancer cell studies, as well as and in vivo xenograft tumore studies will be conducted to test this hypothesis. In addition, EZN-2968, a specific RNA antagonist that specifically targets HIF-1α and is currently in phase 1 clinical trials will be investigated as a potential therapeutic drug.

KEY WORDS:

Breast cancer, letrzole, aromatase inhibitor resistance, hypoxia inducible factor 1 (HIF-1)

ACCOMPLISHMENTS—Overall project summary

Specific Aim 1: To determine the role of ERα and HER2 in the regulation of nonhypoxic HIF-1α expression and activity in letrozole-resistant breast cancer cells (LTLTCa cells).

Task 1: HER2, ERα, HIF-1α, HIF-1β, and β-actin protein expression in MCF-7Ca, LTLTCa, and MCF-7/HER2 (Hc7) cells under basal, nonhypoxic conditions will be determined by western blot analysis.

Experiments: *Experiments to accomplish this task were reported in the 2012 annual summary and published in Kazi et al. 2014. As shown in* ***Figure 1****, western blot analyses confirmed the molecular profiles of previously known letrozole-resistant LTLTCa cells (ERα-/HER2+) and of its letrozole-sensitive parental MCF-7Ca cells (ERα+/HER2-). In addition, they demonstrated that HIF-1α protein was also upregulated in LTLTCa cells by at least 2.5-fold ($p<0.001$) compared to MCF-7Ca cells. This increase was regardless of oxygen tension (i.e., hypoxic 1% O_2 or nonhypoxic 20% O_2) or cell confluency (50% or 95%). In contrast, expression of HIF-1α's dimer partner HIF-1β, which has been previously shown to be constitutively expressed in cells (Semenza et al. 2010; Laugherner et al . 2001), was similar in both cell lines (****Figure 2A****).*

Task 2: Effect of inhibiting ERα and/or HER2 on HIF-1α protein expression in MCF-7/HER2 cells will be determined by western blot analysis

Experiments: *Experiments to accomplish this task were reported in the 2012 annual summary and published in Kazi et al. 2014. Since LTLTCa an MCF-7Ca cells differ in their ERα and HER2 expression, experiments were conducted to determine the effect of inhibiting ERα and/or HER2 on HIF-1α protein expression in known ERα+/HER2+ MCF-7/HER2 (also known as Hc7) cells. Shown in* ***Figure 2C****, MCF-7/HER2 (Hc7) cells were treated with either vehicle or HER2 kinase inhibitor lapatinib and/or ERα antagonist ICI182,780. Both inhibitors were confirmed to inhibit their targets. Inhibition of HER2 activity and/or ERα decreased HIF-1α expression (0.1-fold vs. vehicle, $p<0.001$).*

Additional experiment: *Since HIF-1α expression was associated with both ERα- (LTLTCa cells in Figures 1 and 2) and ERα+ (MCF-7/HER2 cells in Figure 2), additional western blot analyses were done on AC1 and AC1-ExR cells. AC1 cells are like MCF-7Ca cells, except that the transfection of aromatase gene in AC1 cells was done by the laboratory of Dr. Angela Brodie and leads to higher aromatase levels. AC1-ExR cells were derived from AC1 xenograft tumors that, through long term treatment, developed resistance to another aromatase inhibitor exemestane. As shown in* ***Figure 2B,*** *AC1-ExR cells compared to AC1 cells, express similar levels of ERα and higher levels of HER2. In these cells, HIF-1α protein expression was also higher.*

Task 3: HIF-1α phosphorylation state in LTLTCa cells will be determined via λ-phosphatase treatment of protein followed by western blot analysis.

Experiments: *Experiments for this task were accomplished and explained in 2012 annual summary Shown in Figure 3, protein phosphorylation is detected as a change in protein migration after λ-phosphatase treatment. In LTLTCa cells, phosphorylation of HIF-1α was detected only after treatment with cobalt chloride (CoCl2), a hypoxia mimetic that prevents degradation of (i.e., stabilizes) HIF-1α protein.*

Task 4: Effect of inhibiting ERα and/or HER2 on HIF-1α phosphorylation state in MCF-7/HER2 cells will be studied via λ-phosphatase treatment of protein followed by western blot analysis.
Experiments*: Experiments for this task were accomplished and explained in 2012 annual summary. Since inhibition of ERα and/or HER2 significantly reduced HIF-1α expression in MCF-7/HER2 cells to almost undetectable levels, changes in phosphorylation are not observable.*

Additional experiments: *To further explore the nonhypoxic regulation of HIF-1α in LTLTCa cells, additional experiments were done and include in Kazi et al. 2014. First RT-PCR was conducted to determine whether increased HIF-1α protein levels were due to increased gene transcription. As shown in* ***Figure 4A****, while HER2 and ERα mRNA levels were elevated and reduced, respectively, in LTLTCa cells vs. MCF-7Ca cells, HIF-1α mRNA levels were not different. Second, treatment of LTLTCa and MCF-7Ca cells with transcriptional inhibitor actinomycin D for different times prior to conducting RT-PCR analysis, indicated that HIF-1α mRNA stability was similar in both cell lines (****Figure 4B****). Third, LTLTCa cells were treated for 3 h with either vehicle or hypoxia mimetic and HIF-1α stabilizer CoCl2 and then subjected to treatment with protein synthesis inhibitor cyclohexamide from 0-60 min (****Figure 4C****). Western blot analysis of HIF-1α protein showed that HIF-1α protein produced prior to treatment with cyclohexamide rapidly degraded in the absence of CoCl2. Fourth, the role of specific kinase pathways on HIF-1α protein expression in LTLTCa cells was studied (****Figure 5****). While all the pathway inhibitors used were effective in blocking their target proteins (see right panel in figure), only inhibitors of HER2 (trastuzumab and lapatinib), the PI3K pathway (LY294002), or mTOR (Rad001) decreased HIF-1α protein levels in LTLTCa cells/ MAPK pathway inhibitor U0126 had no significant effect on HIF-1α protein.*

Conclusions for Specific Aim 1: *Previous results indicated a role for HER2 in regulating HIF-1 in LTLTCa cells (refer to project narrative). Current findings are in agreement with these results. Along with a loss of ERα and gain of HER2, letrozole-resistant breast cancer is now also associated with nonhypoxic expression of HIF-1α. Under nonhypoxic conditions, HIF-1α protein levels appears to be due to increased protein synthesis that likely involves activation of HER2/PI3K/mTOR pathway and independent of ERα status. Association of HIF-1 with HER2 was observed not only via correlating expression of both proteins in different cell lines but also determining the effects of HER2 inhibitors on HIF-1α.*

Specific Aim 2: To define HIF-1α's role in letrozole-resistant cell phenotype and in xenograft growth.
Task 5: Effect of HIF-1α inhibition on LTLTCa cell characteristics in vitro will be investigated

5.a) Dose experiment to determine the most effective, yet non-toxic dose of EZN-2968 that can inhibit HIF-1α protein expression in LTLTCa cells will be done by MTT assay and western blot analysis.
Experiments: *Experiments to accomplish this task for BCRP were completed and reported in the 2012 annual summary and in abstract #95 at the annual AACR meeting (2013). As expected, HIF-1α mRNA and protein were significantly decreased in LTLTCa cells after 48 h of treatment with either 1 uM HIF-1α siRNA from Qiagen or 10 uM EZN-2968, a HIF-1α-specific RNA antagonist from Enzon Pharmaceuticals (EZN-2968). This was compare to effects of 1 uM negative control Qiagen siRNA and 10 M EZN-3088, a negative control scrambled control oligo, respectively. HIF-1α mRNA was reduced to at least 0.6-fold (****Figure 6A****, $p<0.05$), while protein was reduced to at least 0.3-fold* ***(Figure 6B,*** *$p< 0.05$****)*** *by both inhibitors compared to their respective negative controls. Reduction of HIF-1α expression preceded effects on cell viability* ***(Figures 7A).*** *Cell viability remained unchanged after 48 h treatment compared to negative controls. However, it led to an eventual decrease in LTLTCa cell resistance to increasing doses of letrozole observable after 6 days (****Figure 7B,*** *$p<0.001$). Thus, 48 h treatment of LTLTCa cells with 1 μM Qiagen HIF-1α siRNA or 10μM EZN-2968 were used in subsequent experiments.*

5.b) Effect of EZN-2968 on cancer stem cell characteristics of LTLTCa cells will be studied:

5.b.i) Effect of EZN-2968 on side population percentage in LTLTCa cells will be determined by Hoecsht 33342 dye efflux and flow cytometry.

Experiments*: Experiments to accomplish this task were completed and reported in the 2012 annual summary and in abstract #95 at the annual AACR meeting (2013). Prior to starting these experiments, the the flow cytometry core lab at UMB switched from Hoechst 33342 staining to. Dye Cycle Violet to analyze side population cells. DyCycle Violet is a cell permeable DNA binding dye that is similar to Hoechst 33342 in structure and has been use in previous studies to identify side population cells that are cancer stem cells (Telford et al. 2010). Side population analysis indicated that specific inhibition of HIF-1α significantly decreased side population percentage within 48 h (**Figure 8**). Treatment with Qiagen HIF-1α siRNA reduced the side population percentage to 19.2±0.2% compared to 23.5±0.7% with Qiagen negative control ($p<0.01$). Similarly, EZN-2968 reduced the side population to 8.9 ±0.4% compared to 16.7±0.04% with EZN-3088 negative control ($p<0.01$). As a positive experimental control, the effect of inhibiting breast cancer resistance protein (BCRP), a known regulator of side population cells and cancer stem cells was also determined (Gilani et al. 2012). As expected, treatment of LTLTCa cells with either BCRP inhibitor K0143 or BCRP siRNA also decreased the percentage of side population cells.*

5.b.ii) Effect of EZN-2968 on CD44 and CD24 positivity of LTLTCa cells will be determined by flow cytometry.

Experiments: *Experiments to accomplish this task were completed and reported in the 2012 annual summary and in abstract #95 at the annual AACR meeting (2013). Previous studies have indicated that cancer stem cells, including breast cancer stem cells, within a cancer cell population can be distinguished by expression of cell surface markers CD44 and CD24 (Al—Hajj et al. and Sheridan et al.). CD44+/CD24- expression has been associated with breast cancer stem cells and invasive and metastatic potential. When this characteristic was studied in LTLTCa cells treated with HIF-1α-specific siRNA, it was observed that EZN-2968 treatment significantly decreased the percentage of CD44+/CD24- cells to 27.4± 0.8% compared to negative control EZN 3088 treated cells (46.1± 0.1%) **(Figure)**. Interestingly, Qiagen HIF-1α siRNA treatment had no effect.*

5.b.iii) Effect of EZN-2968 on mammosphere formation of LTLTCa cells will be determined.

Experiments: *Experiments to accomplish this task have been completed and reported in the 2012 and 2012 annual summaries and in abstract #95 at the annual AACR meeting (2013). Mammsophere assay cultures under low-attachment conditions were conducted to isolate the cancer stem cell subpopulation with LTLTCa cells and observe their tumor (mammosphere)-forming potential. In separate experiments, LTLTCa cells were treated with either negative control or HIF-1α inhibitor (Qiagen HIF-1α siRNA or EZN-2968) for 48 h prior to plating cells under mammosphere conditions for 14 days. The number of mammsopheres were then quantified to represent number of cancer stem cells. Results indicate that both Qiagen HIF-1α siRNA treatment and EZN-2968 treatment of LTLTCa cells decreased mammosphere formation compared to negative control treatment by ~35-65% ($p< 0.01$, **Figure 10**). In contrast, upregulation of HIF-1α by CoCl2 treatment, increased mammosphere formation compared to negative control siRNA-treated cells (**Figure 10A**, $p <0.01$).*

5.b.iv) Effect of EZN-2968 on microtentacle scoring in LTLTCa cells will be determined by transfection with vector expressing membrane-localized GFP followed by fluorescence microscopy.

Experiments: *Experiments to accomplish this task have been completed and reported in the 2014 annual summary. Microtentacles, first observed by the laboratory of Dr. Stuart Martin, are vimentin- and tubulin-associated protrusions produced when breast cancer cells are in single suspension in vitro and circulating in blood vessels in vivo (Whipple et al. 2008; Charpentier et al. 2013). Increased microtentacle formation has been correlated with aggressive breast cancer subtypes and increased cancer stem cells as they may promote invasion and metastasis Charpentier et al. 2013). In this current study, the effect of upregulating and downregulating HIF-1α expression on microtentacle formation was determined. LTLTCa cells were treated with either vehicle (no CoCl2 +EZN 3088), 100 uM cobalt chloride (CoCl2, hypoxia mimetic that upregulates HIF-1α protein expression), 10 uM EZN-2968 (no CoCl2), or 100 uM CoCl2+10 uM EZN 2968 for 72 h. Microtentacle-expressing cells were then counted using an updated procedure from the laboratory of Dr. Stuart Martin at UMB, which involves staining cells with Cell Mask Orange. Upregulation of HIF-1α significantly increased the number of microtentacle-expressing cells, while down regulation of HIF-1α by EZN-2968 inhibited both basal number of cells exhibiting microtentacles, as well as the CoCl2-induced number of cells* ***(Figure 11)****.*

5.b.v) Effect of EZN-2968 on cytoskeletal components of microtentacles (vimentin and detyrosinated tubulin) will also be assessed by immunofluorescence

Experiments: *Experiments to accomplish this task were completed and reported in the 2013and 2014 annual summaries. To provide more easily quantitative analysis of the effect of EZN-2968 on microtentacle-associated cytoskeletal components vimentin and detryosinated tubulin, western blot analysis and real-time RT-PCR were done instead of immunofluorescence. As shown in* ***Figure 12A****, EZN-2968 significantly decreased vimentin protein expression by ~0.5-fold ($p<0.05$)but had no effect on detryosinate tubulin (glu-tubulin) protein compared to negative control EZN 3088. Real-time RT-PCR was then done to look at effects of HIF-1α inhibition (by Qiagen HIF-1α siRNA or EZN-2968) on mRNA expression of vimentin, as well as other factors also associated with metastasis and invasion. In agreement with Western blot analysis results, EZN-2968 (as well as Qiagen HIF-1α siRNA) also significantly decreased vimentin mRNA expression by ~0.5-fold compared to negative controls (****Figure 12B****). Interestingly, other the factors studied did not shown consistent effects and so were inconclusive.*

Additional experiments*: Additional experiments were done to further confirm the regulation of microtentacles by HIF-1α and to correlate EZN-2968's effects on vimentin expression with its effects on invasion and migration potential. As shown in* ***Figure 13A****, upregulating HIF-1α protein either via incubation of cells in 1% or by treatment of cells with hypoxia mimetic CoCl2 correlated with increased expression of vimentin protein (A) and mRNA (B) and microtentacle expression. Vimentin is associated with invasion and migration of cancer cells (Satelli et al. 2011). Inhibition of either HIF-1α (via EZN-2968 or Qiagen HIF-1α siRNA) or vimentin (via Qiagen vimentin siRNA) reduced the number of DAPI-stained LTLTCa cells that migrated through a matrigel transwell within 24 h compared to negative controls (****Figure 14****). In agreement with these results, Qiagen vimentin siRNA that specifically targets vimentin expression also decreased invasive potential of LTLTCa cells.*

Task 6: Effect of HIF-1α inhibition on LTLTCa cell characteristics in vivo in xenograft models will be investigated.

6.a) Dose response experiment to determine the most effective, yet non-toxic dose of EZN-2968 that can inhibit HIF-1α protein expression in letrozole-resistant MCF-7Ca tumor xenografts will be done along with western blot analysis.

6.b) To determine ability of EZN-2968 to prolong letrozole sensitivity will be conducted using MCF-7Ca xenograft tumor model.

6.c) To determine ability of EZN-2968 to inhibit letrozole-resistant tumor growth using letrozole-resistant MCF-7Ca xenograft tumor model.

Experiments for 6.a to 6.c: *These tasks were not able to be completed. By the time the xenograft animal experiments were to be done, pharmaceutical-grade EZN-2968 was no longer available from Enzon Pharmaceuticals. Experiments were then conducted using an alternative HIF-1α inhibitor, PX-478. Previously published studies indicated that PX-478 based on previously published studies (Jacoby et al. 2010; Spivak-Kroitzman et al. 2013). As was done with EZN-2968, rior to attempting to use PX-478 in vivo, studies were conducted to determine its efficacy in LTLTCa cells in vitro. In* ***Figure 15****, Western blot results indicated that PX-478, using concentrations that have been shown to be effective by other studies (Spivak-Kroitzman et al. 2013), did not significantly decrease HIF-1α protein expression in LTLTCa cells with or without the presence of hypoxia mimetic drug CoCl2. In* ***Figure 16****, MTT assays showed that PX-478 treatment trended do decrease cell viability with and without hypoxia mimetic drug CoCl2, but the decrease was minimal and not consistent with increasing dose. Lastly, in* ***Figure 17****, mammosphere assays showed that PX-478 did not significantly decrease the number of mammospheres nor their morphology as compared to untreated cells. Thus, PX-478 did not significantly alter the cancer stem cell population of LTLTCa cells. Due to the lack of significant effects of PX-478 on a variety of LTLTCa cell characteristics in vitro, its success in vivo was questionable and so xenograft tumor experiments were not pursued.*

6.d) To temporally correlate protein expression changes with tumor growth effects, protein expression of ERα, HER2, phosphorylated ERK1/2 and Akt, and HIF-1α in letrozole-treated tumors will be analyzed by western blot analysis.

Experiments: *Experiments to accomplish this task have been completed and reported in the 2013 annual summary. Frozen comparably-sized MCF-7Ca xenograft tumors collected previously during a xenograft experiment conducted in early 2012 for another project were analyzed (****Figure 18****). In this xenograft tumor experiment, representative MCF-7Ca xenograft tumors were collected from mice that were either continued to be treated with androstenedione (control) for 8 weeks or were then treated with letrozole for 1-16 weeks. In agreement with previous results (Jelovac et al. 2005), HER2 protein expression was increased within 2-4 weeks of letrozole treatment compared to androstenedione control (****Figure 18****). As expected, based on in vitro results (****Figures 1 and 2****), HIF-1α protein expression was also low in androestenedione (control) MCF-7Ca tumors and increased after 2-4 weeks of letrozole treatment, when HER2 also increased.*

Conclusions for Specific Aim 2: *Previous studies from our laboratory and others have indicate the importance of cancer stem cells in aromatase inhibitor (ex. letrozole) drug resistant breast cancer. Current findings indicate that cancer stem cell characteristics of LTLTCa cells is mediated by HIF-1α. In vitro experiments demonstrated that inhibition of HIF-1α decreased percentage of side population and CD44/CD24-expressing cells, mammosphere formation, and microtentacle formation. In addition, it decreased the invasive potential of LTLTCa cells. These studies further suggested that EZN-2968 protein expression results from xenograft tumors correlate with in vitro studies, and further support a role of HIF-1 in acquired letrozole resistance. Though HIF-1 protein expression studies on xenograft tumors correlated with in vitro studies, additional in vivo experiments*

investigating the effects of HIF-1 inhibition on tumor growth were not able to be done due to discontinued availability of EZN-2968 and due to ineffectiveness of alternative PX-478 in vitro. In vitro results for PX-478 indicated that its use in xenograft tumor studies using would likely not yield positive results. Though the search for an alternative pharmacological/clinical drug that directly targets HIF-1 has proven difficult, the search is ongoing. It would be ideal to find another drug in clinical development that can directly and specifically target HIF-1α. However, drugs that are known to indirectly (ex. as secondary effect) affect HIF-1α are being explored as well.

Specific Aim 3: To identify HIF-1 target genes that serve as markers of letrozole resistance.

Task 7: To compare expression between in MCF-7Ca and LTLTCa cells of known HIF-1 targets involved in cancer

7.a) To compare protein expression of known HIF-1 targets in MCF-7Ca and LTLTCa cells by western blot analysis.

Experiments: *Experiments to accomplish this task have been completed and reported in the 2012 and 2013 annual summaries, respectively, and in Gilani et al. 2012. Factors proposed for study have all been associated with cancer stem cell characteristics, invasive and metastatic potential, and drug resistance. Thus, candidate factors should be overexpressed in LTLTCa cells. Also, since HIF-1 is a transcription factor that activates transcription of target genes, mRNA expression candidate factors should decrease with HIF-1α inhibition. Based on this criteria, only BCRP and vimentin protein expression were analyzed by western blot analysis. BCRP and vimentin were the only 2 factors that met these two criteria (refer to results described in task 7.b and 9). As shown in* ***Figures 13 and 19****, both vimentin protein and BCRP protein expression were significantly increased in LTLTCa cells vs. MCF-7Ca cells. BCRP protein and mRNA expression was 1.8-fold and 3-fold, respectively, higher in LTLTCa cells vs. MCF-7Ca cells. Vimentin protein and mRNA expression was 2.1-fold higher in LTLTCa cells vs. MCF-7Ca cells. As mRNA expression of the other genes studied (refer to task 9) were either not upregulated in LTLTCa cells vs. MCF-7Ca cells, or were not consistently inhibited by HIF-1α siRNAs (Qiagen and EZN-2968), their protein expression was not analyzed for this task.*

7.b) To compare mRNA expression of known HIF-1 targets in MCF-7Ca and LTLTCa cells by real-time RT-PCR analysis.

Experiments: *Experiments to accomplish this task have been completed and reported in the 2012 and 2013 annual summaries and in Kazi et al. 2014. RT-PCR analyses of known HIF-1 target genes in MCF-7Ca vs. LTLTCa cells have been done.* ***Figure 20*** *demonstrated significant overexpression of vimentin (1.3-fold±0.09 vs. MCF-7Ca 1.0±0.02), angiopoietin like factor 4 (1.9-fold±0.05 vs. MCF-7Ca 1.0±0.02), endothelin 1 (3.0-fold±0.14 vs. MCF-7Ca 1.0±0.03), fibronectin (35.8-fold±1.74 vs. MCF-7Ca 1.0±0.07), and BCRP (2-fold±0.6 vs. MCF-7Ca 1.0±0.2) mRNA expression in LTLTCa cells compared to MCF-7Ca cells. As HIF-1 is a transcription factor that activates target genes, these upregulated genes were studied further in task 9. In contrast, LTLTCa cells express equal levels of TWIST mRNA as in MCF-7Ca cells and decrease levels of CXCR, MMP-2, and Kit ligand mRNA expression were significantly decreased in LTLTCa cells compared to MCF-7Ca cells. These genes were not studied further in this project, but will likely be investigated in the future in a separate project.*

Task 8: To determine whether HIF-1α binds to promoters of genes overexpressed in LTLTCa cells by chromatin immunoprecipitation.

Experiments: *Based on RT-PCR (Figures 13, 19, and 20) and Western blot analyses (****Figures 13 and 19****), binding of HIF-1α to BCRP and vimentin gene promoters was determined. The experiment to accomplish this task for BCRP was completed and reported in the project narrative and in Kazi et al. 2014. As shown in* ***Figure 21****, HIF-*

*1 binding to a region of the BCRP gene promoter that contains a hypoxia response element (HRE, 5'-GCGTG-3') occurs under basal conditions in LTLTCa cells and is significantly decreased by treatment with HER2 inhibitor lapatinib. Experiments to accomplish this task for vimentin were completed and reported in the 2014 annual summary. A potential HRE was located at nucleotide position 1082 on the vimentin 5'-flanking sequence and untranslated region (Rittling and Baserga. 1987). Chromatin immunoprecipiation (ChIP) analysis of HIF-1 binding to this promoter region demonstrated that although input samples showed successful isolation of the promoter region by ChIP, HIF-1 binding to this region under normoxic conditions was not detected. (**Figure 23**). These results may indicate that HIF-1 indirectly regulates vimentin expression by regulating another transcription factor. Both TWIST (Sun et al. 2009) and Snail (Zhang et al. 2013) transcription factors are known to be direct HIF-1 target genes. In turn, both Snail (Kaufhold et al. 2014) and Twist (Yang et al. 2004) are known to regulate vimentin expression.. Although TWIST and Snail were not upregulated LTLTCa vs. MCF-7Ca cells (**Figure 20**), their functions as transcription factors may be upregulated in LTLTCa cells. Investigation of regulation of TWIST and Snail function by nonhpoxic HIF-1 in aromatase inhibitor resistant breast cancer cells will be conducted in a separate future project.*

As mRNA expression of other genes studied (refer to task 9) were either not upregulated in LTLTCa cells vs. MCF-7Ca cells, or were not consistently inhibited by HIF-1α siRNAs (Qiagen and EZN-2968), their protein expression was not analyzed further for this task. These other genes will likely be studied in the future as part of a separate project investigating possible causes of the discrepancies between Qiagen siRNAs and EZN-2968.

Task 9: To determine whether EZN-2968 decreases expression of known HIF-1 targets in LTLTCa cells.
Experiments: *Experiments to accomplish this task have been completed and reported in the 2012 and 2013 annual summaries and in abstract #95 at the annual AACR meeting (2013). The effect of HIF-1α inhibition by both Qiagen HIF-1α siRNA and EZN-2968 on mRNA expression of the known HIF-1 target genes found to be upregulated in LTLTCa cells was determined by RT-PCR and Western blot analysis. As expected, both Qiagen HIF-1α siRNA and EZN-2968 significantly decreased HIF-1α mRNA expression in LTLTCa cells (**Figures 6 and 12**). However, among the known HIF-1 target genes identified in task 7.b, only vimentin (**Figure 12**) and BCRP (**Figure 6**) mRNA expression was decreased by both Qiagen HIF-1α siRNA and EZN-2968. mRNA expression of angiopoietin like factor 4, endothelin 1, and fibronectin were not consistently inhibited along with HIF-1α mRNA (**Figure 12**). Furthermore in some cases, there was an increase in mRNA expression when HIF-1α mRNA expression was reduced. Thus, these genes were not studied further in this project. Investigations into their differential regulation by HIF-1 will be conducted in a separate future project.*

Task 10: To determine importance of identified HIF-1 target genes in letrozole-resistant cells by inhibiting target genes via specific pharmacological inhibitors or siRNA followed by in vtiro cancer cell assays (as specific aim 2)
Experiments: *Experiments to accomplish this task have completed and were reported in the 2012 and 2013 annual summaries and published in Gilani et al. 2012. BCRP has been previously associated with cancer stem cells, particularly their characteristics of side population and mammosphere formation. Regarding the importance of BCRP in letrozole-resistant cells , experiments showed that inhibition of BCRP via either pharmacological inhibitor K0143 or Qiagen BCRP siRNA decreased percentage of side population, to 0.45% vs. 21% in vehicle-treated ($p<0.01$) and to 2.5% vs. 24% Qiagen negative control siRNA-treated cells, respectively. Similarly, BCRP siRNA treatment (which was shown to effectively inhibit BCRP mRNA expression in **Figure 24A**) resulted in decreased LTLTCa mammosphere formation frequency, compared to negative control siRNA (**Figure 24B**) and consistent with effects of pharmacological BCRP inhibitors K0143 and FTC (**Figure 24C**). Vimentin is a cytoskeletal protein overexpressed in a number of epithelial cancers, and is associated with*

accelerated tumor growth, invasion, and poor prognosis (Satelli et al. 2011). Pertinent to current findings, overexpression of vimentin is associated with highly aggressive and metastatic breast cancer cells and increased microtentacle formation (Whipple et al. 2008; Matrone et al. 2010). Thus, studies have been conducted to determine the role of vimentin in LTLTCa cells. Current results indicate that there is a correlation between HIF-1α and vimentin expression and metastatic potential, as indicated by microtentacle formation and invasion and migration ability. In ***Figure 14****, increased expression of HIF-1α in less aggressive and metastatic MCF-7Ca cells correlated with 1) at least an 8-fold increase in vimentin mRNA and protein expression. and 2) a ~50% increase in the percentage of cells exhibiting microtentacles. In* ***Figure 7,*** *treatment of LTLTCa cells with either HIF-1α siRNA (by Qiagen or EZN-2968) or vimentin siRNA (Qiagen), inhibited invasion and migration ability as determined by transwell migration through a matrigel and DAPI staining. As expected, vimentin siRNA also decreased microtentacle formation (****Figure 25****).*

Conclusions for Specific Aim 3: *Findings from experiments conducted in specific aim 2, suggested that the HER2-nonhypoxic HIF-1 signaling pathway in LTLTCa cells plays a role in acquired letrozole resistance via regulation of cell viability, cancer stem cell characteristics, and microtentacle formation. Since HIF-1 is a transcription factor that activates a wide variety of genes, it may be involved in letrozole resistance by regulating downstream target proteins directly involved in cell viability and cancer stem cell characteristics. Based on results, the signaling pathway that mediates letrozole resistant breast cancer likely includes BCRP and vimentin Among the various factors studied, only they met the criteria of being upregulated in LTLTCa cells and regulated by HIF-1. Furthermore, inhibition of BCRP and vimentin decreased cancer stem cell characteristics and invasion and metastatic characteristics of letrozole-resistant breast cancer. BCRP and vimentin could be useful diagnostic markers and therapeutic targets. This study, however, does not rule out the involvement of other factors, not included in the current list investigated.,*

PLAN FOR NEXT REPORTING PERIOD:

Nothing to report, though studies to look for alternative pharmacological drugs that work in vitro and in vivo will be continued.

IMPACT

Prior to this study, AI resistance was associated with increased dependence on growth factors and decreased dependence on ERα. However, the role that such molecular changes play in AI resistance and the mechanism by which they elicit their effects were not known. Results from this study demonstrated that nonhypoxic expression of HIF-1 mediates HER2's effects on letrozole-resistance. Specifically, HER2-activated PI3K/Akt pathway increases HIF-1α protein synthesis in LTLTCa cells. HIF-1α, in turn, upregulates expression of BCRP and vimentin, and contributes to letrozole resistance and stem cell characteristics of LTLTCa cells.

Nonhypoxic regulation of HIF-1 expression and activity in LTLTCa cells is due to HER2-activated PI3K/Akt pathway. This is consistent with findings by others indicating hypoxia independent upregulation of HIF-1α in cancer cells by loss of function of tumor suppressor genes and gain of function of oncogenes (Semenza. 2012). The oncogene HER2/neu, in particular has been previously associated with nonhypoxic HIF-1 (Laughner et al. 2001; Li et al. 2005). Laughner et al. and Li et al have demonstrated that transfection of HER2 into NIH/3T3 cells or activation of HER2 in MCF-7 cells led to activation of the PI3K/Akt pathway, and subsequent increased HIF-1 expression via protein synthesis and HIF-1 transcriptional activity. Our current results provide additional evidence that this HER2-PI3K/Akt pathway-HIF-1 signaling mechanism can occur endogenously in HER2+ cells in vitro and in vivo (xenograft tumors) and has physiological relevance (i.e., regulation of cancer stem cell characteristics) as well as potential clinical implication (i.e., AI resistance).

Inherent upregulation of HIF-1α protein expression under nonhypoxic conditions is another novel finding in AI-resistant breast cancer. There is precedence for associating HIF-1 expression with drug resistance in different cancer cell types, including chronic myeloid leukemia cells (Zhao et al. 2010), gastric cancer cells (Liu et al. 2007), non-small cell lung cancer cells (Song et al.. 2006), and even breast cancer cells (Flamant et al. 2010). However, these previous cases involved hypoxia-induced, HIF-1α rather than the nonhypoxic HIF-1. Our findings are also consistent with previous clinical evidence that HIF-1α is associated with letrozole resistance. Generali et al demonstrated that increase p-MAPK and HIF-1α protein expression were significant determinants of primary letrozole resistance in breast cancer patients. In contrast, increased ERα and decreased p-MAPK were significant determinants of response to letrozole treatment (Generali et al. 2009). The protein expression patterns observed by Generali et al. are similar to what is observed in letrozole-resistant LTLTCa and –sensitive MCF-7Ca cells, respectively. Although these clinical findings involve de novo letrozole resistance, they still correlate with, and likely pertain to, our laboratory's results on acquired letrozole resistance. These results combined suggest that HIF-1 is involved in both de novo and acquired AI resistance, and therefore could be therapeutically targeted to prevent and treat resistance to letrozole and the other AIs. HIF-1 may be contributing to letrozole resistance by mediating HER2's effects on target genes, such as BCRP and vimentin that are key proteins in the maintenance of cancer stem cell population and of invasion and metastasis. Based on this, a proposed model of acquired AI-resistance may involve the following scenario: under nonhypoxic conditions, when the breast cancer cell population and tumor size have been reduced by letrozole treatment and prior to significant tumor hypoxia, a switch from ERα- to growth factor (i.e., HER2)-mediated signaling occurs, which leads to increased HIF-1α expression and activation of HIF-1 target genes that contribute to AI resistance.

Consequently, determining HIF-1, BCRP, and vimentin protein expression could improve ability to identify ER+ breast cancer patients who are at risk for developing AI-resistant breast cancer. In addition, inhibition of HIF-1, BCRP, and/or vimentin expression and/or activity could prolong cancer cell sensitivity to AIs and prevent recurrence and metastasis. Indeed, a number anti-cancer drugs in clinical use are also known to

inhibit HIF-1 (Semenza. 2010). They include HER2 inhibitor, trastuzumab (Laughner et al. 2001) and lapatinib. Furthermore, as demonstrated in this study that HIF-1 is regulated mainly via PI3K/Akt pathway, inhibition of downstream affecter of this pathway using mTOR inhibitors such as rapamycin, temsirolimus/CCI-779 and everolimus/RAD-001, can also be considered (Laughner et al. 2001; Majumder et al., 2004; Faivre et al. 2006; Thomas et al. 2006). Lastly, novel to this study, EZN-2968, a specific HIF-1α RNA antagonist, which has previously been shown to reduce cancer cell viability and xenograft tumor growth and was currently under phase I clinical trial (Greenberger et al. 2008), appeared to be a promising drug to prevent and treat aromatase inhibitor resistance breast cancer in vitro. Despite the loss of EZN-2968 availability for in vivo studies and the failure of alternative drug PX-478 in vitro, the findings of this study suggest that HIF-1 targeting therapy should continue to be explored to treat breast cancer.

CHANGES/PROBLEMS

Unfortunately, EZN-2968 is no longer available from Enzon Pharmaceuticals. An alternative drug that can inhibit HIF-1α and shown to be effective in vivo was explored but proven not to be effective in vitro, so was not tested in vivo. Additional exploration of alternative HIF-1α inhibitors is ongoing.

SUPPORTING DATA: Figures and Figure legends

REPORTABLE OUTCOMES

Abstracts and Presentations:

- Rabia Gilani, Armina Kazi*, Amanda Schech, Saranya Chumsri, Preeti Shah, Angela Brodie. The involvement of HER2, HIF-1, and BCRP in cancer stem cell characteristics of letrozole-resisant breast cancer cells. Abstract #787 peer-reviewed and presented at American Association of Cancer Researchers (AACR) 2012 Annual Meeting. *co-first author and presenting author.
- Armina Kazi, Amanda Schech, Saranya Chumsri, Preeti Shah, Gauri Sabnis, Yael Gau, Angela Brodie. Inhibition of non-hypoxic HIF-1 expression in letrozole-resistant breast cancer cells reduces their cancer stem cell characteristics. Abstract #95 peer-reviewed and presented at American Association of Cancer Researchers (AACR) 2013 Annual Meeting.
- Armina Kazi, Gauri Sabnis, Qun Zhou, Akina Tamaki, Spencer Todd, Saranya Chumsri, Amanda Schech, Preeti Shah, Angela Brodie. HER2 regulated miRNA expression in letrozole resistant breast cancer. Abstract #7633 peer-reviewed and presented at American Association of Cancer Researchers (AACR) 2014 Annual Meeting.

Published Manuscripts:

- Gilani RA, Kazi AA*, Shah P, Schech AJ, Chumsri S, Sabnis G, Jaiswal AK, Brodie AH. The importance of HER2 signaling in the tumor-initiating cell population in aromatase inhibitor-resistant breast cancer. Breast Cancer Res Treat. 2012 Oct;135(3):681-92. *Co-first author.
- Armina A Kazi, Rabia A Gilani, Amanda J Schech, Saranya Chumsri, Gauri J Sabnis, Preeti Shah, Olga Goloubeva, Shari Kronsberg and Angela H Brodie. Nonhypoxic regulation and role of hypoxia-inducible factor 1 in aromatase inhibitor resistant breast cancer. Breast Cancer Research. 2014.

Employment:

- Have received and maintained tenure-track assistant professor position Loyola University Maryland.

New research collaborations that will be used to apply for R15 in 2016.

- I have continued with a clinical project at Greenbaum Cancer Center investigating the response of postmenopausal obese and overweight patients with ER+ breast cancer to neoadjuvant aromatase inhibitor therapy. My role in this clinical trial is to analyze HIF-1 and miRNA (particularly miRNAs that are associated with HER2 and HIF-1) profiles in patient samples.

REFERENCES

1. Kazi A, Gilani R, Schech A, Chumsri S, Sabnis G, Shah P, Goloubeva O, Kronsberg S, and Brodie A. Nonhypoxic regulation and role of hypoxia-inducible factor 1 in aromatase inhibitor resistant breast cancer. Breast Cancer Research. 2014

2. Semenza GL. Hypoxia-inducible factors: mediators of cancer progression and targets for cancer therapy. Trends Pharmacol Sci. 2012 Apr;33(4):207-14.

3. Laughner E, Taghavi P, Chiles K, Mahon PC, Semenza GL. HER2 (neu) signaling increases the rate of hypoxia-inducible factor 1alpha (HIF-1alpha) synthesis: novel mechanism for HIF-1-mediated vascular endothelial growth factor expression. Mol Cell Biol. 2001 Jun;21(12):3995-4004.

4. Telford W. Stem cell side population analysis and sorting using DyeCycle Violet. Curr Protoc. Cytom. 2010 Jan; Chapter 9 Unit 9.

5. Gilani RA, Kazi AA, Shah P, Schech AJ, Chumsri S, Sabnis G, Jaiswal AK, Brodie AH. The importance of HER2 signaling in the tumor-initiating cell population in aromatase inhibitor-resistant breast cancer. Breast Cancer Res Treat. 2012 Oct;135(3):681-92.

6. Al-Hajj M1, Wicha MS, Benito-Hernandez A, Morrison SJ, Clarke MF.Prospective identification of tumorigenic breast cancer cells. Proc Natl Acad Sci. 2003 Apr 1;100(7):3983-8.

7. Sheridan C, Kishimoto H, Fuchs RK, Mehrotra S, Bhat-Nakshatri P, Turner CH, Goulet R Jr, Badve S, Nakshatri H. CD44+/CD24- breast cancer cells exhibit enhanced invasive properties: an early step necessary for metastasis. Breast Cancer Res. 2006;8(5):R59.

8. Whipple RA, Balzer EM, Cho EH, Matrone MA, Yoon JR, Martin SS. Vimentin filaments support extension of tubulin-based microtentacles in detached breast tumor cells. Cancer Res. 2008 Jul 15;68(14):5678-88.

9. Charpentier M, Martin S. Interplay of Stem Cell Characteristics, EMT, and Microtentacles in Circulating Breast Tumor Cells. Cancers (Basel). 2013 Nov 14;5(4):1545-65.

10. Satelli A, Li S. Vimentin in cancer and its potential as a molecular target for cancer therapy. Cell Mol Life Sci. 2011 Sep;68(18):3033-46.

11. Jacoby JJ1, Erez B, Korshunova MV, Williams RR, Furutani K, Takahashi O, Kirkpatrick L, Lippman SM, Powis G, O'Reilly MS, Herbst RS. Treatment with HIF-1alpha antagonist PX-478 inhibits progression and

spread of orthotopic human small cell lung cancer and lung adenocarcinoma in mice. J Thorac Oncol. 2010 Jul;5(7):940-9.

12. Spivak-Kroizman T, Hostetter G, Posner R, Aziz M, Hu C, Demeure M, Von Hoff D, Hingorani S, Palculict T, Izzo J,Kiriakova G, Abdelmelek M, Bartholomeusz G, James B, Powis G. Hypoxia triggers Hedgehog-mediated tumor stromal interactions in pancreatic cancer. Cancer Res. 2013 Jun 1; 73(11): 3235–3247.

13. Jelovac D, Sabnis G, Long BJ, Macedo L, Goloubeva OG, Brodie AM. Activation of mitogen-activated protein kinase in xenografts and cells during prolonged treatment with aromatase inhibitor letrozole. Cancer Res. 2005 Jun 15;65(12):5380-9.

14. Rittling SR, Baserga R. Functional analysis and growth factor regulation of the human vimentin promoter. Mol Cell Biol. 1987.

15. Sun S, Ning X, Zhang Y, Lu Y, Nie Y, Han S, Liu L, Du R, Xia L, He L, Fan D. Hypoxia-inducible factor-1alpha induces Twist expression in tubular epithelial cells subjected to hypoxia, leading to epithelial-to-mesenchymal transition. Kidney Int. 2009.

16. Zhang L, Huang G, Li X, Zhang Y, Jiang Y, Shen J, Liu J, Wang Q, Zhu J, Feng X, Dong J, Qian C. Hypoxia induces epithelial-mesenchymal transition via activation of SNAI1 by hypoxia-inducible factor -1α in hepatocellular carcinoma. BMC Cancer. 2013.

17. Kaufhold S, Bonavida B. Central role of Snail1 in the regulation of EMT and resistance in cancer: a target for therapeutic intervention. J Exp Clin Cancer Res. 2014.

18. Yang J, Mani SA, Donaher J, Ramaswamy S, Itzykson R, Come C, Savagner P, Gitelman I, Richardson A, Weinberg RA. Twist, a Master Regulator of Morphogenesis, Plays an Essential Role in Tumor Metastasis. Cell. 2004.
19. Semenza GL. Hypoxia-inducible factors: mediators of cancer progression and targets for cancer therapy. Trends Pharmacol Sci. 2012 Apr;33(4):207-14.

20. Matrone MA, Whipple RA, Balzer EM, Martin SS. Microtentacles tip the balance of cytoskeletal forces in circulating tumor cells. Cancer Res. 2010 Oct 15;70(20):7737-41.

21. Li YM, Zhou BP, Deng J, Pan Y, Hay N, Hung MC. A hypoxia-independent hypoxia-inducible factor-1 activation pathway induced by phosphatidylinositol-3 kinase/Akt in HER2 overexpressing cells. Cancer Res. 2005 Apr 15;65(8):3257-63.

22. Zhao F, Mancuso A, Bui TV, Tong X, Gruber JJ, Swider CR, Sanchez PV, Lum JJ, Sayed N, Melo JV, Perl AE, Carroll M, Tuttle SW, Thompson CB. Imatinib resistance associated with BCR-ABL upregulation is dependent on HIF-1alpha-induced metabolic reprogramming. Oncogene. 2010 May 20;29(20):2962-72.

23. Song X, Liu X, Chi W, Liu Y, Wei L, Wang X, Yu J. Hypoxia-induced resistance to cisplatin and doxorubicin in non-small cell lung cancer is inhibited by silencing of HIF-1alpha gene. Cancer Chemother Pharmacol. 2006 Dec;58(6):776-84.

24. Flamant L, Notte A, Ninane N, Raes M, Michiels C. Anti-apoptotic role of HIF-1 and AP-1 in paclitaxel exposed breast cancer cells under hypoxia. Mol Cancer. 2010 Jul 13;9:191.

25. Generali D, Buffa FM, Berruti A, Brizzi MP, Campo L, Bonardi S, Bersiga A, Allevi G, Milani M, Aguggini S, Papotti M, Dogliotti L, Bottini A, Harris AL, Fox SB. Phosphorylated ERalpha, HIF-1alpha, and MAPK signaling as predictors of primary endocrine treatment response and resistance in patients with breast cancer. J Clin Oncol. 2009 Jan 10;27(2):227-34.

26. Majumder PK, Febbo PG, Bikoff R, Berger R, Xue Q, McMahon LM, Manola J, Brugarolas J, McDonnell TJ, Golub TR, Loda M, Lane HA, Sellers WR. mTOR inhibition reverses Akt-dependent prostate intraepithelial neoplasia through regulation of apoptotic and HIF-1-dependent pathways. Nat Med. 2004 Jun;10(6):594-601.

27. Faivre S, Kroemer G, Raymond E. Current development of mTOR inhibitors as anticancer agents. Nat Rev Drug Discov. 2006 Aug;5(8):671-88.

28. Greenberger LM, Horak ID, Filpula D, Sapra P, Westergaard M, Frydenlund HF, Albaek C, Schrøder H, Ørum H. A RNA antagonist of hypoxia-inducible factor-1alpha, EZN-2968, inhibits tumor cell growth. Mol Cancer Ther. 2008 Nov;7(11):3598-608.

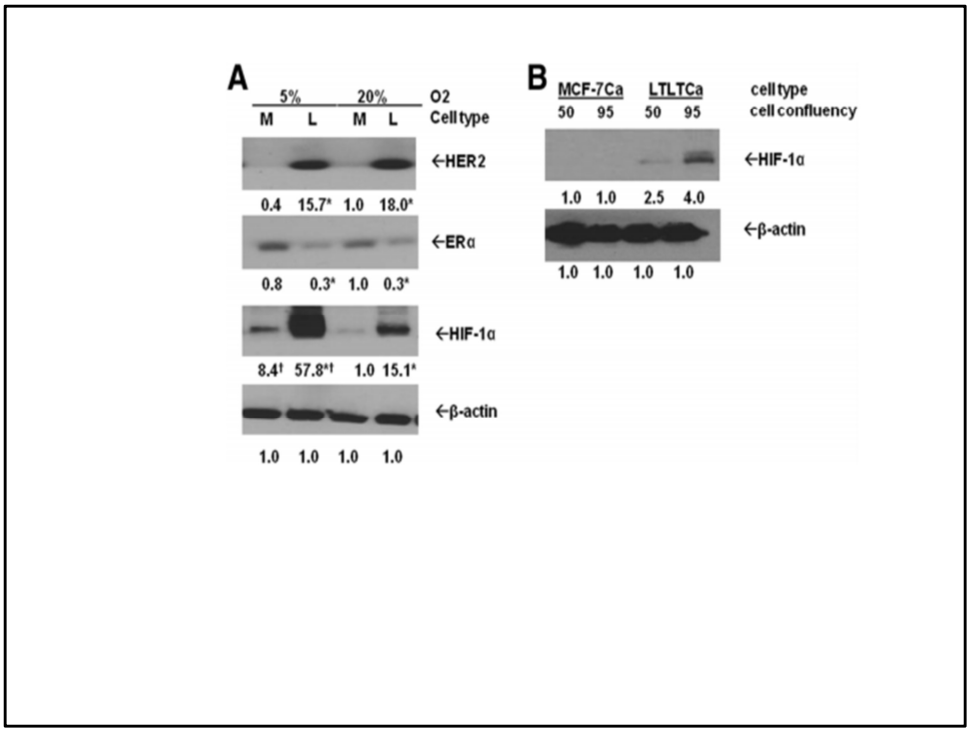

Figure 1 Comparison of protein expression in parental MCF-7Ca and LTLTCa cells under different oxygen tension and cell confluency.

A) Parental MCF-7Ca and LTLTCa cells were plated and cultured in their respective passage media under either 5% O2 (in vivo normoxic/ physiological conditions) or 20% O2 (normal, nonhypoxic cell culture conditions). Total protein was extracted and HER2, ERα, HIF-1α and β-actin were analyzed by Western blot analysis. Shown are representative blots and overall densitometry results of n = 6 independent cell samples/group. Densitometry results are expressed as mean fold-change in protein levels compared to MCF-7Ca cells in 20% O2 after normalization to β-actin (mean ± SD of n = 6 independent cell samples/group; *versus MCF-7Ca and † versus 20% O2; HER2 effect of cell type P = 0.0002, effect of % O2 P = .5749, interaction between cell type and % O2 P = .7337; ERα effect of cell type P < 0.0001, interaction between cell confluency and cell type P = 0.0006, two-way ANOVA). ANOVA, analysis of variance; ERα, estrogen receptor alpha; HER2, human epidermal growth factor receptor 2; HIF-1α, hypoxia inducible factor 1 α subunit; n, number; SD, standard deviation.

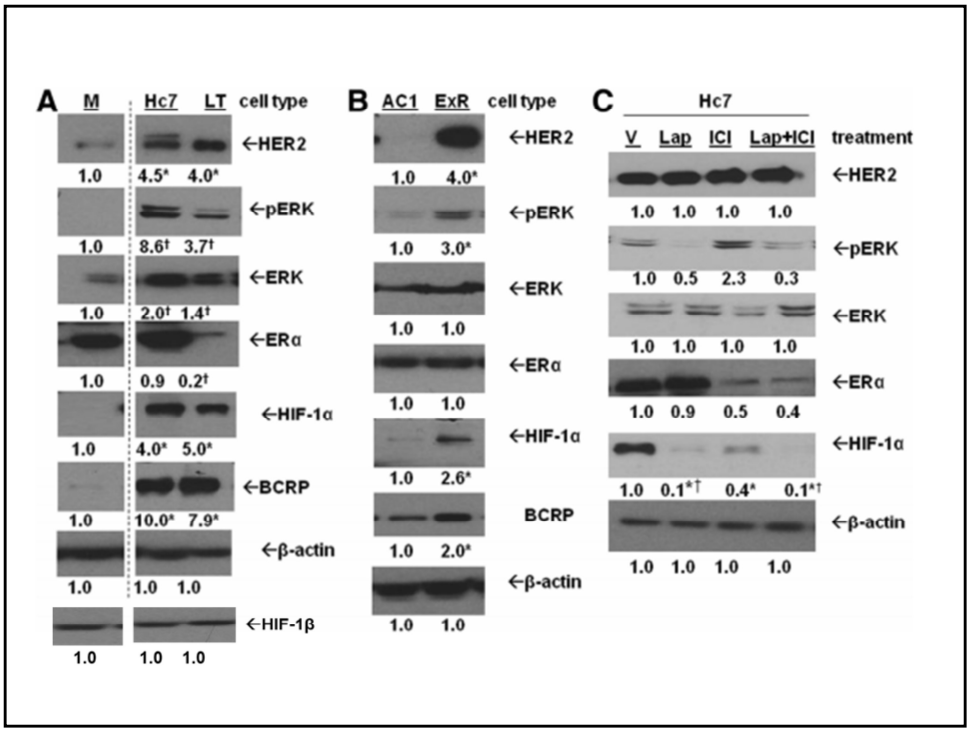

Figure 2 Protein expression in HER2+ cells and exemestane-resistant cells.
A) MCF-7Ca (M), Hc7 and LTLTCa (LT) cells were plated in their respective passage media. Total protein was extracted and HER2, phosphorylated- and total-ERK, ERα, HIF-1α, BCRP, HIF-1β, and β-actin protein were analyzed by Western blot. Shown are representative blots and overall densitometry results of n = 6 independent cell samples/group. Densitometry results are expressed as mean fold-change compared to MCF-7Ca after normalization to ERK (mean ± SD of n = 6 independent cell samples/group; *versus MCF-7Ca, P <0.05; † versus MCF-7Ca, P <0.001, one-way ANOVA). Dashed lines indicate omitted lane in between M and Hc7 of the same blots. B) AC1 (AC1) and AC1-ExR (ExR) cells were plated in their respective passage media. Total protein was extracted and HER2, phosphorylatedand total-ERK, ERα, HIF-1α and β-actin protein were analyzed by Western blot. Shown are representative blots and overall densitometry results of n = 6 independent cell samples/group. Densitometry results are expressed as mean fold-change compared to vehicle-treated cells after normalization to β-actin (mean ± SD of n = 6 independent cell samples/group; *versus vehicle, P <0.0001, two-sided t-test). C) MCF-7/HER2 cells were treated with either vehicle (V), 1 μM lapatinib (Lap), 100 nM ICI 182,780 (ICI) or 1 μM lapatinib + 100 nM ICI 182,780 (Lap + ICI) for 24 hours. Total protein was extracted and HER2, phospho- and total-ERK1/2, ERα, HIF-1α and β-actin were analyzed by Western blot. Shown are representative blots and overall densitometry results of n = 6 independent cell samples/group. Densitometry results are expressed as mean fold-change compared to vehicle-treated cells after normalization to β-actin (mean ± SD of n = 6 independent cell samples/group; *versus vehicle, P <0.0001, one-way ANOVA). ANOVA, analysis of variance; BCRP, breast cancer resistant protein; ERα, estrogen receptor alpha; HER2, human epidermal growth factor receptor 2; HIF-1α, hypoxia inducible factor 1 α subunit; n, number; SD, standard deviation.

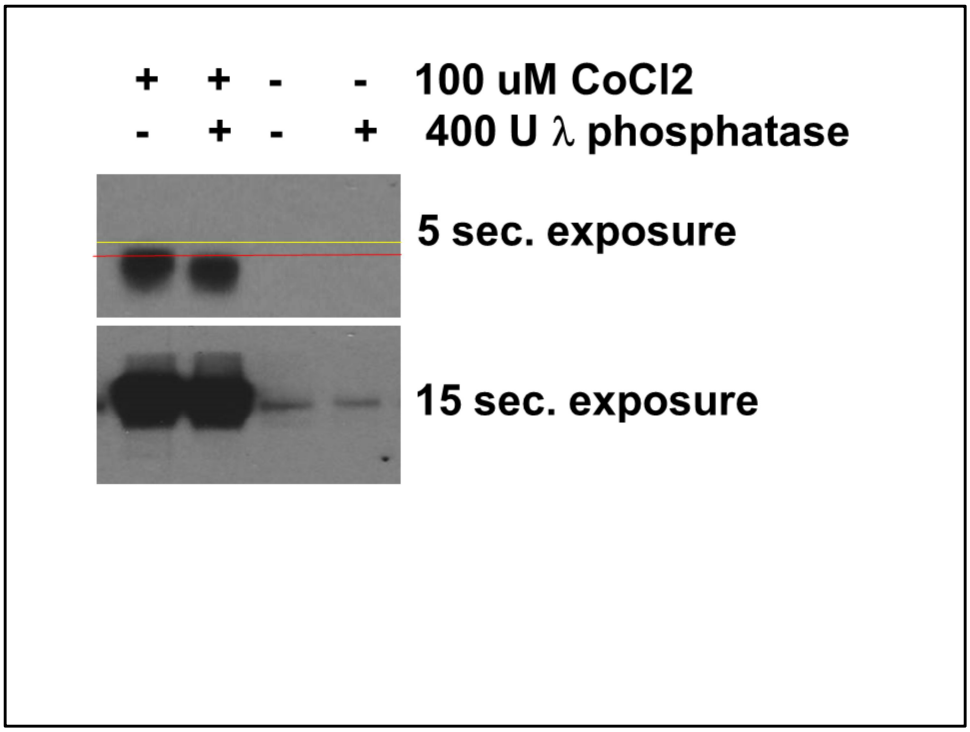

Figure 3. HIF-1α protein phosphorylation in LTLTCa cells.

LTLTCa cells were treated either with vehicle or cobalt chloride (CoCl2) for 24 h. Total protein was extracted and then either left untreated or treated with 400 U of λ phosphatase for 30 min. at 30° C prior western blot analysis for HIF-1α protein. Shown are western blot results at 5 sec. and 15 sec. exposure. Red and yellow lines correspond to changes in HIF-1α protein band migration.

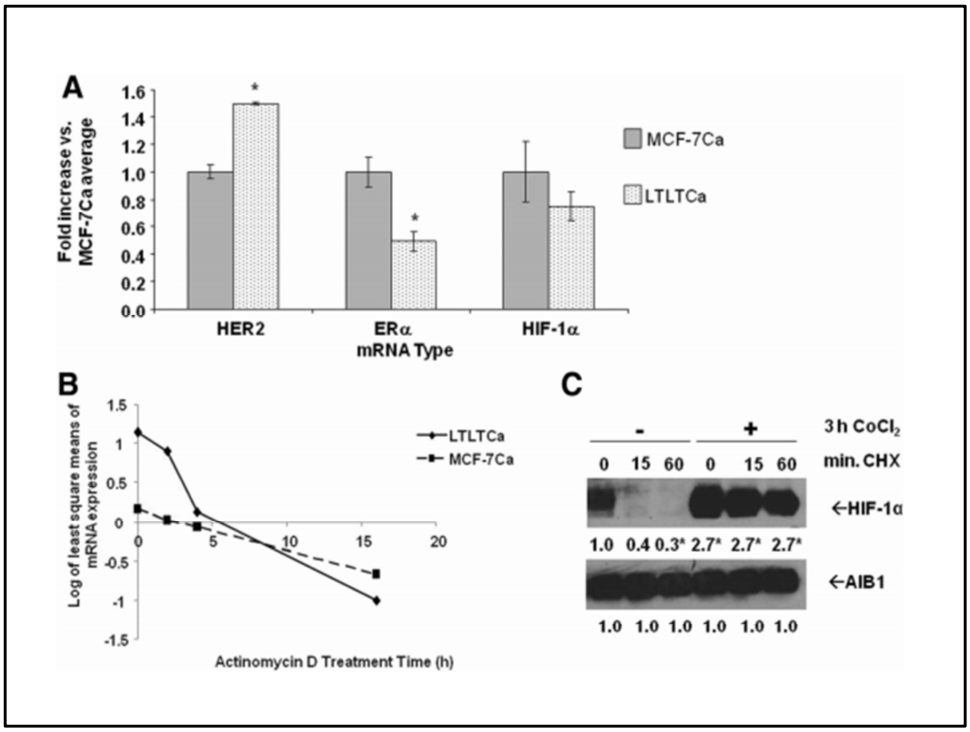

Figure 4 Comparison of HIF-1α mRNA expression and stability in LTLTCa and MCF-7Ca cells. A) LTLTCa and MCF-7Ca cells were plated and cultured in their respective passage media under normal cell culture (nonhypoxic) conditions. Total RNA was extracted and HER2, ERα, HIF-1α and 18S rRNA were analyzed by real-time RT-PCR analysis. Results shown are expressed as the mean fold-change in mRNA levels compared with MCF-7Ca cells after normalization to 18S rRNA (mean ± SD of n = 6 independent cell samples/group; *versus MCF-7Ca; effect of gene type P <0.0001, effect of cell type P = 0.1376, interaction between gene type and cell type P <0.0001; *MCF-7Ca versus LTLTCa for specific gene, P <0.0001; two-way ANOVA). B) LTLTCa and MCF-7Ca cells were treated with vehicle or 0.5 µg/ml actinomycin D for 0 to 16 hours. Total RNA was extracted and HIF-1α mRNA underwent real-time RT-PCR. Results are expressed as least square means of log transformed averages of mRNA expression at various timepoints (trend over time) after normalization to corresponding vehicle-treated samples and analysis by linear mixed effect model, adjusting for experiment, cell line and cell line*time interaction (means ± SD of n = 6 independent samples/group; P <0.001 for effect of cell line, time, their interaction and experiment). C) LTLTCa cells were treated with vehicle or 100 µM CoCl2 for three hours and then with 100 uM cycloheximide for 0 to 60 minutes. Whole cell protein was extracted and underwent Western blot for HIF-1α and AIB1 protein. Shown are representative blots and overall densitometry results of n = 6 independent cell samples/group. Densitometry results are expressed as mean fold-change in protein levels compared to vehicle-treated-0 minutes cycloheximide cells after normalization to AIB1 (mean ± SD of n = 6 independent cell samples/group; *versus no CoCl2-0 minutes CHX, P <0.0001, one-way ANOVA). ANOVA, analysis of variance; ERα, estrogen receptor alpha; HER2, human epidermal growth factor receptor 2; HIF-1α, hypoxia inducible factor 1 α subunit; n, number; SD, standard deviation.

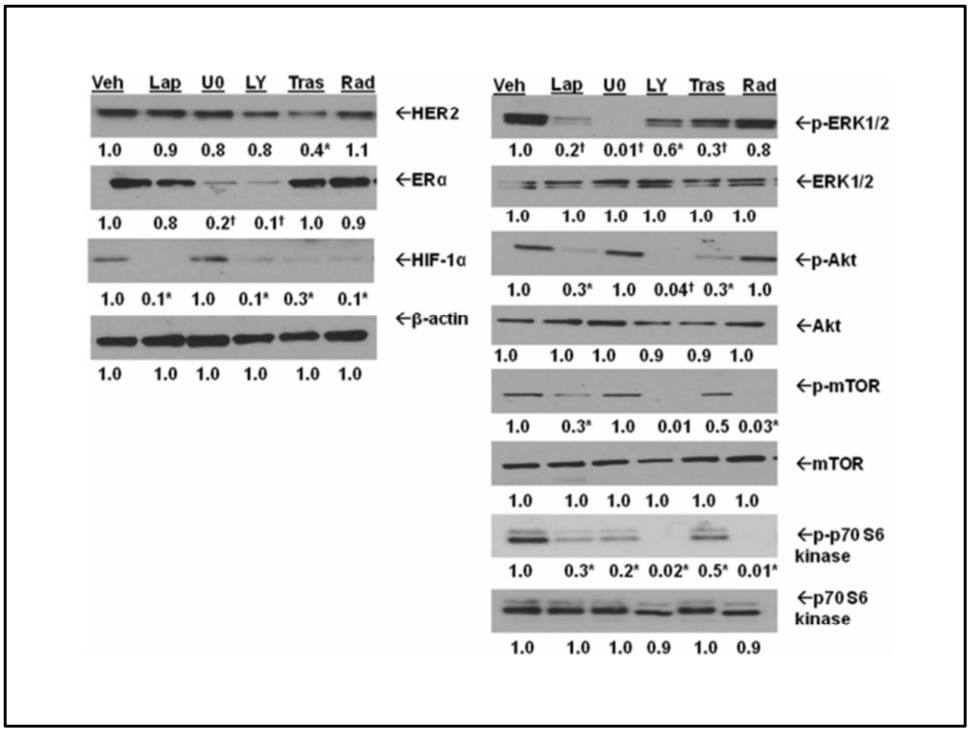

Figure 5. Regulation of HIF-1α protein in LTLTCa cells. A) LTLTCa cells were treated with either vehicle, 1 µM lapatinib, 20 µM MAPK pathway inhibitor U0126, 20 µM LY294002 PI3K pathway inhibitor, 500 µg/ml trastuzumab or 100 nM RAD001 for 24 hours. Total protein was extracted and HER2 ($P = 0.128$), phospho- and total-ERK1/2 ($P < 0.0001$ for p-ERK), phospho- and total-Akt ($P < 0.0001$ for p-Akt), phospho- and total mTOR ($P = 0.0071$), phospho- and total p70 S6 kinase ($P < 0.0001$), ERα ($P < 0.0001$), HIF-1α ($P = 0.0003$), and β-actin were analyzed by Western blot. Shown are representative blots and overall densitometry results of n = 6 independent cell samples/group. Densitometry results are expressed as mean fold-change in protein levels compared to vehicle-treated cells after normalization to β-actin (mean ± SD, n = 6 independent cell samples/group; *versus vehicle, $P < 0.05$; † versus vehicle, $P < 0.001$, one-way ANOVA). ANOVA, analysis of variance; ERα, estrogen receptor alpha; HER2, human epidermal growth factor receptor 2; HIF-1α, hypoxia inducible factor 1 α subunit; n, number; SD, standard deviation; mTOR, mammalian target of rapamycin.

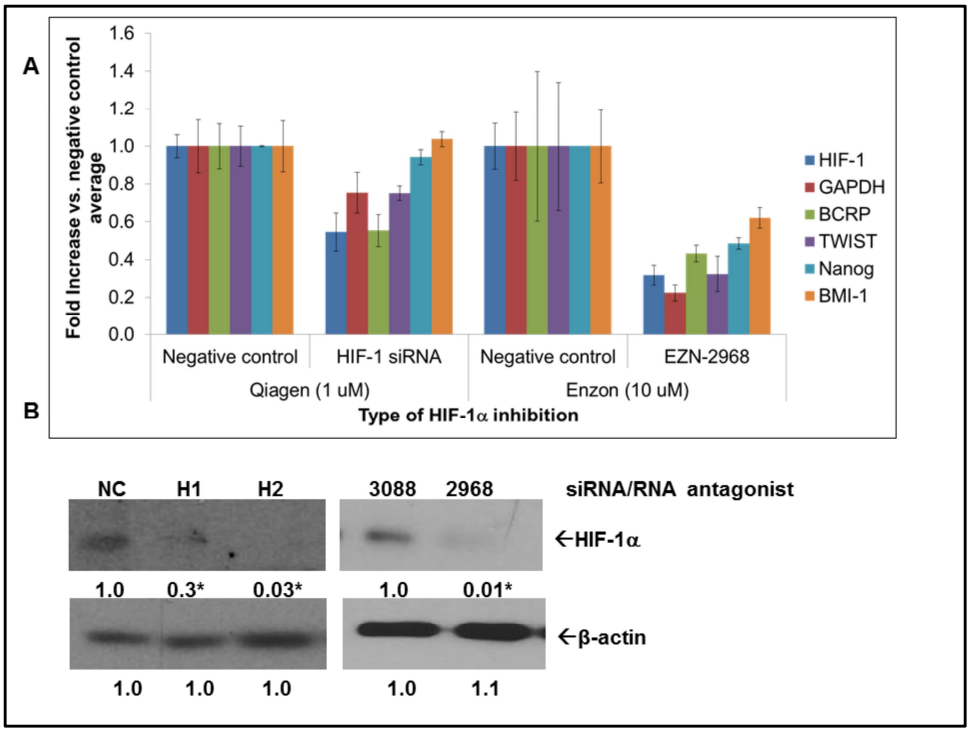

Figure 6. Confirmation of HIF-1α siRNA and EZN-2968 efficacy in LTLTCa cells.

LTLTCa cells were treated with either negative control siRNA , HIF-1α siRNA , negative control EZN 3088 or EZN-2968 for 48 h. A, . Total mRNA was extracted and HIF-1α, BCRP, GAPDH, Nanog, BMI-1, and TWIST mRNA, and 18S rRNA were analyzed by real-time RT-PCR. Real-time results are expressed as the fold-change in mRNA levels compared with negative control after normalization to 18S rRNA (mean ± SEM, n = 4 samples/group). B, Total protein was extracted and HIF-1α and β-actin protein were analyzed by Western blot. Densitometry results are expressed as fold-change compared to negative control after normalization to β-actin (mean ± SEM, n = 6 independent cell samples/group; * vs. negative, $p < 0.05$).

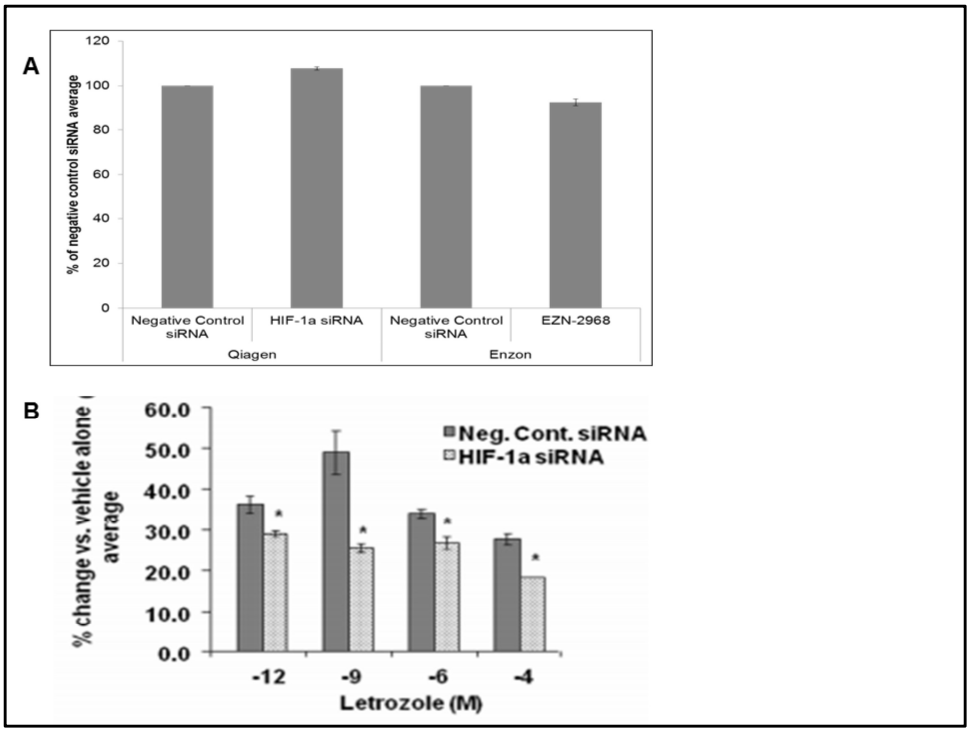

Figure 7. Confirmation that HIF-1α siRNA and EZN-2968 effects on HIF-1 occur prior to loss of cell viability.

A, LTLTCa cells were plated in passage media and then treated with either negative control siRNAs (Qiagen or Enzon), Qiagen HIF-1α siRNA, or EZN-2968 for HIF-1α for 48 h. Cell viability of cells was measured by MTT assay after 48 h treatment with negative control siRNAs, Qiagen HIF-1α siRNA, or EZN-2968 in the presence of 1 μM letrozole. Results are expressed as percent of negative control (mean ± SEM, n = 5 samples/group). B, Viability of the cells was measured by the MTT assay after 48 hours treatment with negative control or HIF-1 alpha siRNA and subsequently 6 day treatment with increasing doses of letrozole. Results are expressed as percent of 0 μM letrozole (vehicle) (mean ± SD, n = 4 independent cell samples/group; *versus 0 μM letrozole, P <0.001; overall P <0.0001 one way ANOVA). ANOVA, analysis of variance; BCRP, breast cancer resistant protein; HIF-1α, hypoxia inducible factor 1 α subunit; MTT, 3-[4,5-dimethylthiazol-2-yl]-2,5 diphenyl tetrazolium bromide; n, number; SD, standard deviation.

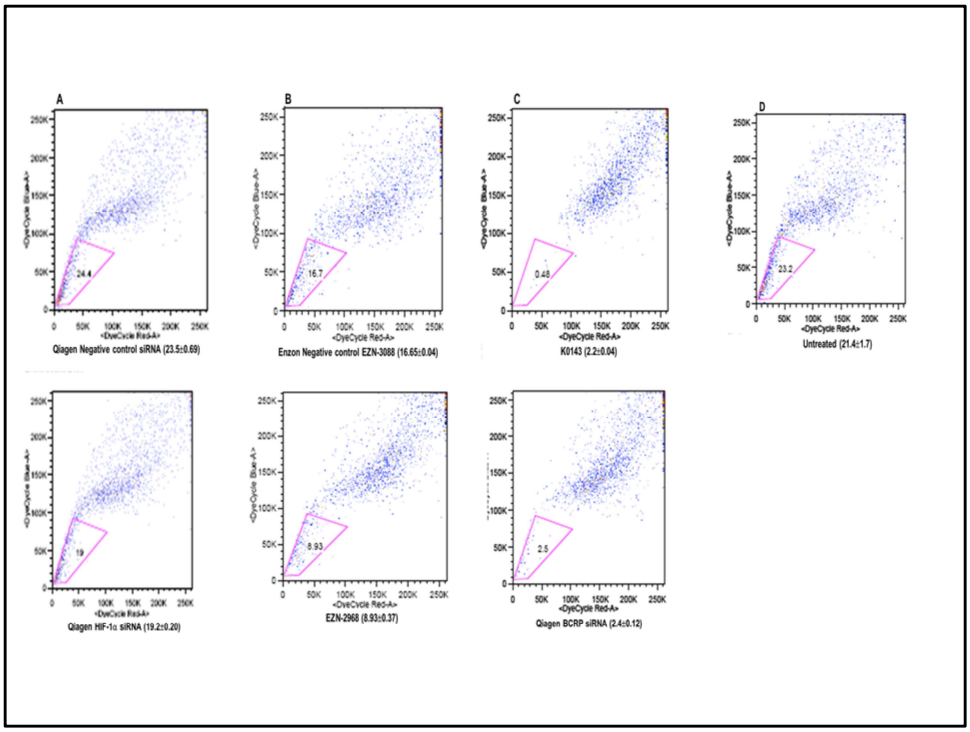

Figure 8. Effect of HIF-1α and BCRP siRNA and EZN-2968 on side population percentage of LTLTCa cells.

LTLTCa cells were treated with A) 1 μM Qiagen negative control siRNA or HIF-1α siRNA; B) or 10 μM Enzon negative control siRNA or EZN-2968; or C) BCRP inhibitors 1 μM K0143 or Qiagen BCRP siRNA treatment for 4 8h. Cells were stained with Vybrant DyeCycle violet. Cells were then acquired using BD LSRII and analyzed. Plots show representative side population fractions as designated by polygons and quantified as percentages (n=3, $p < 0.01$).

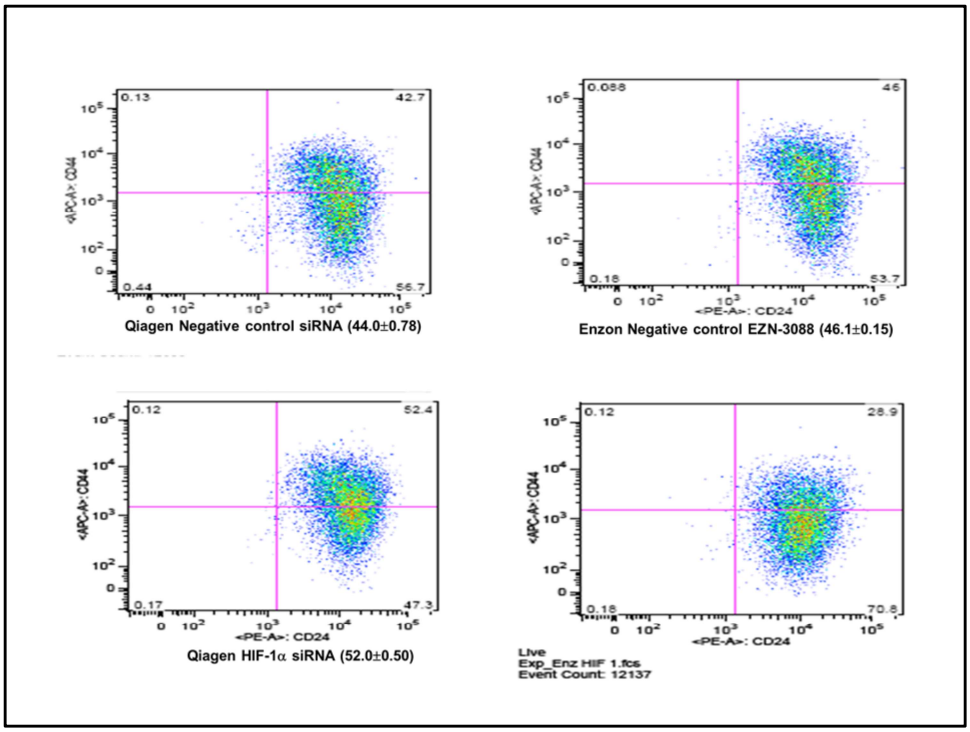

Figure 9. Effect of HIF-1α siRNA on CD44:CD24 positivity of LTLTCa cells.

LTLTCa cells were treated with A) 1 μM Qiagen negative control siRNA or B) HIF-1α siRNA or with 10 μM Enzon negative control siRNA or EZN-2968 for 72 h. Cells were stained with APC-conjugated CD44 and PE-conjugated CD24 antibody. Cells were then acquired using BD LSRII and analyzed by FlowJo software. Plots show representative CD44:CD24 positivity percentage ratios (n=3, $p < 0.05$).

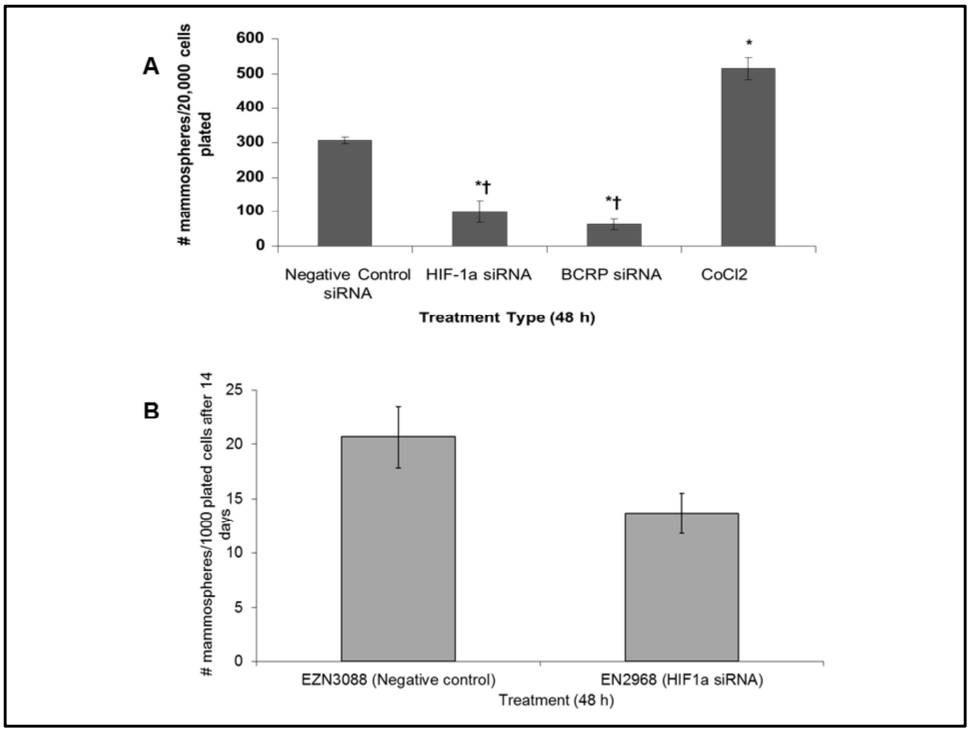

Figure 10. Effect of HIF-1αand/or BCRP siRNA on mammosphere formation in LTLTCa cells.

A, LTLTCa cells were plated in passage media and then treated with vehicle alone (control), negative control siRNA, HIF-1α siRNA, BCRP siRNA, or CoCl2 for 48 h. Cells were then collected and resuspended in mammosphere media on low-attachment cell culture wells. Results are expressed as number of mammospheres counted per 80,000 cells plated (mean ± SEM, n = 6 samples/group; * vs. vehicle, $p < 0.01$; † vs. control, negative control, and CoCl2). B, LTLTCa cells were plated in passage media and then treated with 10 μM EZN-3088 negative control siRNA, or 10 μM EZN-2968 HIF-1α -specific LNA for 48 h. Cells were then collected and resuspended in mammosphere media on low-attachment cell culture wells. Results are expressed as number of mammospheres counted per 1,000 cells plated after 14 days in culture (mean ± SEM, n = 6 samples/group; * vs. vehicle, $p < 0.05$; † vs. -3088 negative control). EZN-2968 was confirmed to decrease BCRP expression (0.35- and 0.15-fold vs. negative control, $p < 0.01$; data not shown).

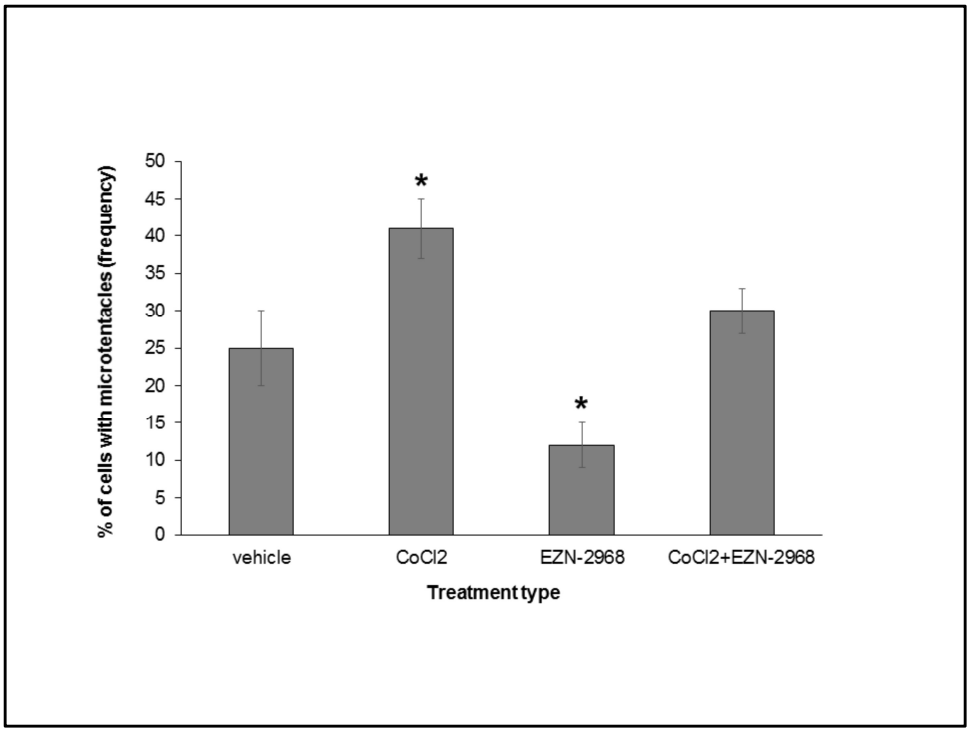

Figure 11. Effect of CoCl2 and EZN-2968 on microtentacle formation in LTLTCa cells.

LTLTCa cells were plated in passage media and then treated with 100 μM cobalt chloride (CoCl2) and/or 10 μM HIF-1α -specific LNA EZN-2968 for 48 h. Cells were then collected, stained with Cell Mask Orange, and resuspended in Ibidi slides for microtentacle scoring. Results are expressed as percent of cells counted with microtentacles per 100 total cells counted (i.e., frequency). (n =4 samples per treatment; *, p< 0,05 vs. vehicle).

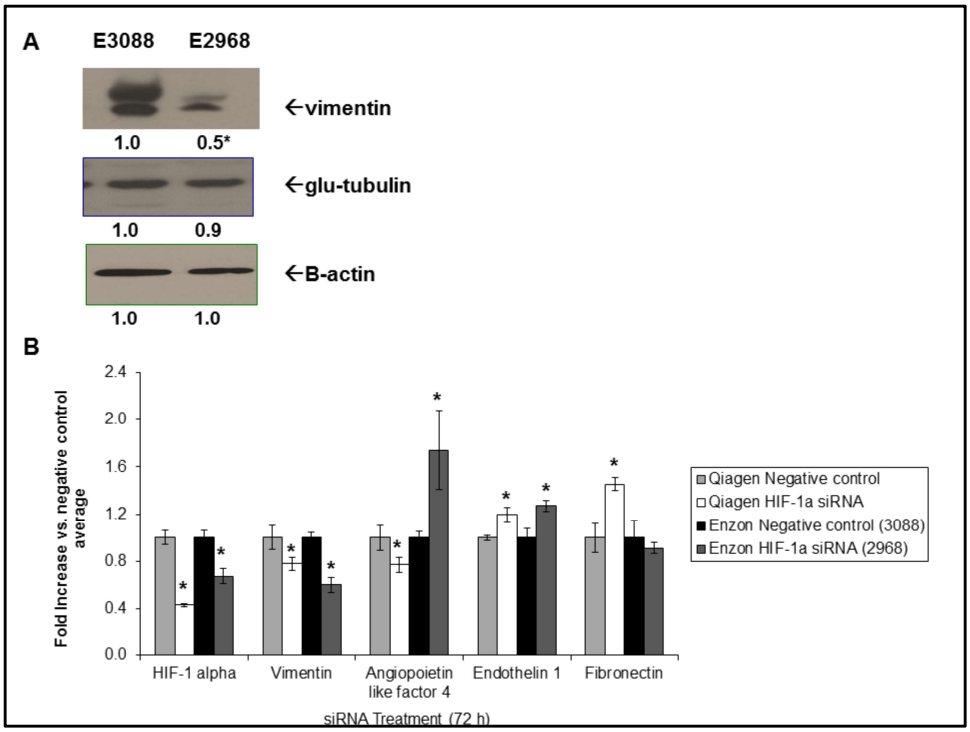

Figure 12. Effect of HIF-1α siRNA on mRNA expression in LTLTCa cells.
A, LTLTCa cells were treated with either negative control siRNA (EZN-3088) or HIF-1α siRNA (EZN-2968) for 72 h. Total protein was extracted and vimentin, glu-tubulin (detryosinated tubulin), and B-actin protein was analyzed by Western blot analysis. Shown are representative blots and overall densitometry results of n = 4 independent cell samples/group. Densitometry results are expressed as mean fold-change in protein levels compared to E3088-treated cells after normalization to β-actin (mean ± SD, n = 4 independent cell samples/group; *versus vehicle, P <0.05; t-test. B, LTLTCa cells were treated with either negative control siRNA (Qiagen or EZN-3088) or HIF-1α siRNA (Qiagen or EZN-2968) for 48 h. Total mRNA was extracted and HIF-1α, vimentin, angiopoietin like factor 4, endothelin 1, and fibronectin mRNA, and 18S rRNA were analyzed by real-time RT-PCR. Real-time results are expressed as the fold-change in mRNA levels compared with negative control after normalization to 18S rRNA (mean ± SEM, n = 4 samples/group, p<0.05)).

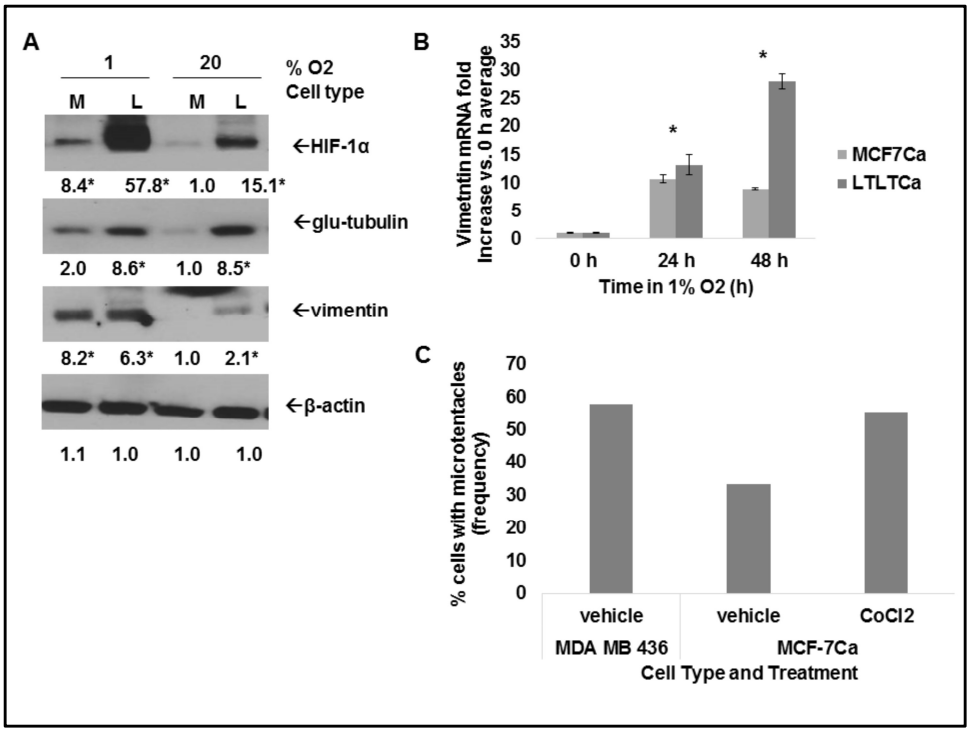

Figure 13. Expression of cytoskeletal proteins in MCF-7Ca and LTLTCa cells, and effect of HIF-1$^{\alpha}$ upregulation either by hypoxia or CoCl2 on cytoskeletal proteins vimentin and glu-tubulin (detyrosinated tubulin) and on microtentacle formation.

A. MCF-7Ca and LTLTCa cells were plated in their respective passage media and allowed to attach under normal cell culture conditions (20% O2). 24 h prior to protein extraction, cells either remained under normal cell culture conditions (20% O2) or transferred to hypoxia conditions (1% O2). Total protein was extracted and HIF-1$^{\alpha}$, glu-tubulin, vimentin, and β-actin protein were analyzed by Western blot. Densitometry results are expressed as fold-change compared to MCF-7Ca at 20% O2 after normalization to β-actin (mean ± SEM, n = 6 independent cell samples/group; * vs. MCF-7Ca at 20% O2, $p < 0.01$). B, MCF-7Ca and LTLTCa cells were plated in their respective passage media and allowed to attach under normal cell culture conditions (20% O2). 24 h or 48 h prior to RNA extraction, cells either remained under normal cell culture conditions (20% O2) or transferred to hypoxia conditions (1% O2). Total mRNA was extracted and vimentin and 18S rRNA were analyzed by real-time RT-PCR. Real-time results are expressed as the fold-change in mRNA levels compared with 0 h (cells that remained at 20% O2) after normalization to 18S rRNA (mean ± SEM, n = 6 samples/group, *, $p < 0.01$ compared to 0 h). C, MDA MB 436 and MCF-7Ca cells were plated and cultured in their respective passage media under normal cell culture conditions. When cells were 80-90% confluency, they were treated with either vehicle or 100 uM CoCl2 for 2 h prior to microtentacle scoring. Results are expressed as percent of cells counted with microtentacles (i.e., frequency).

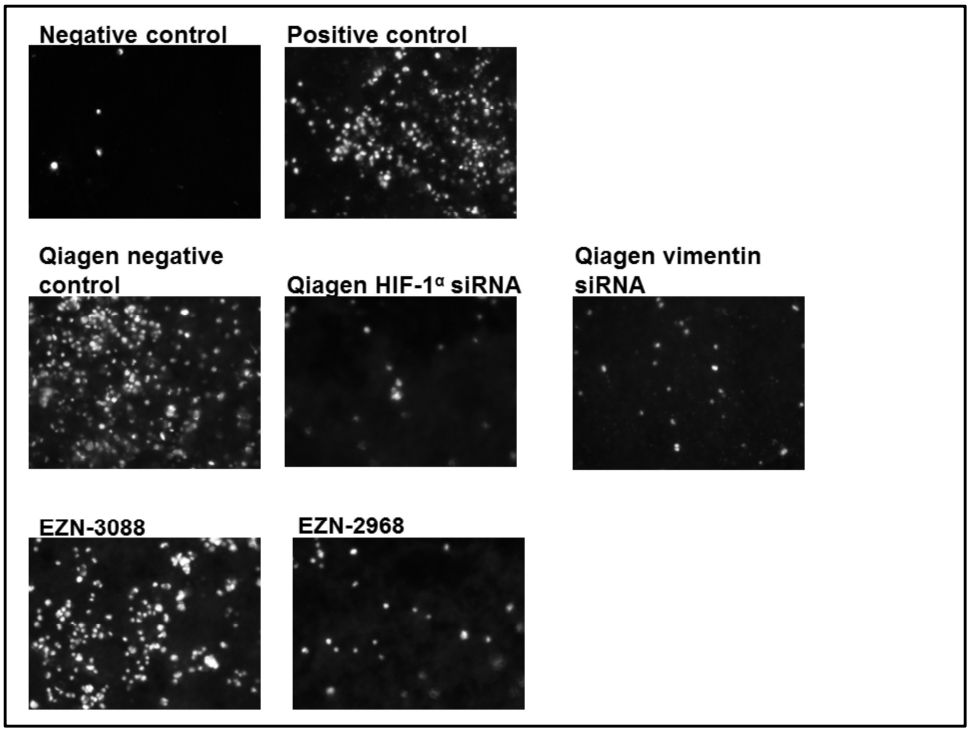

Figure 14. Effect of HIF-1α inhibition on invasive potential of LTLTCa cells
LTLTCa cells (n=3 per treatment group) were plated in passage media and treated with either no siRNA (negative and positive control), negative control siRNA (Qiagen or EZN-3088) or HIF-1α siRNA (Qiagen or EZN-2968), or vimentin siRNA (Qiagen) for 48 h after which cells were serum deprived overnight. Cells were then collected and seeded in matrigel transwells containing either serum free media (negative control) or passage media (remaining positive control and treatment groups). After 24 h, cells were fixed to membranes and cells that have invaded and migrated through matrigel transwell were stained with 1:2500 DAPI (white spots). Images were taken of each sample and representative images are shown. Negative control samples were not treated with siRNA and were incubated with serum free media in the transwell prior to imaging. Positive control samples were not treated with siRNA and were incubated with passage media in the transwell prior to imaging

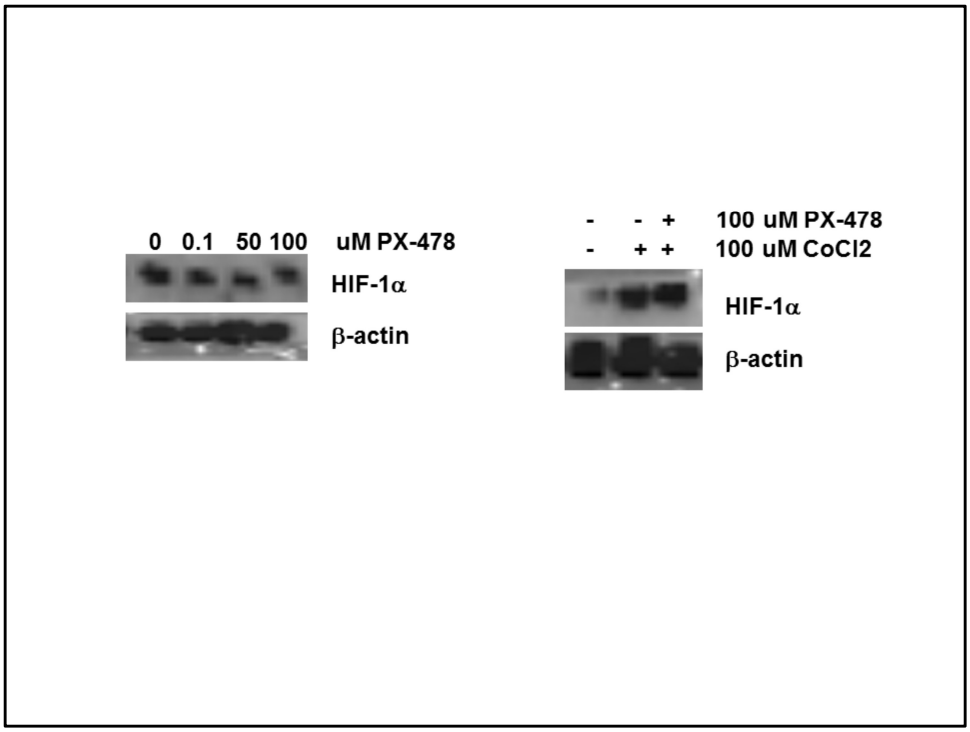

Figure 15. Effect of PX-478 on HIF-1 protein expression in LTLTCa cells.

A. LTLTCa cells were plated in passage media and were treated with either vehicle or 0.1, 10, 50, or 100 uM PX-478 for 48 h. B, LTLTCa cells were plated in passage media and were treated with either vehicle or with 100 M hypoxia mimetic cobalt chloride (CoCl2) and/or 100 uM PX-478 for 48 h. A and B, Proteins were collected and purified from cells and subjected to Western blot analysis for HIF-1 and -actin expression. Shown are representative immunoblots of n =6 samples per treatment.

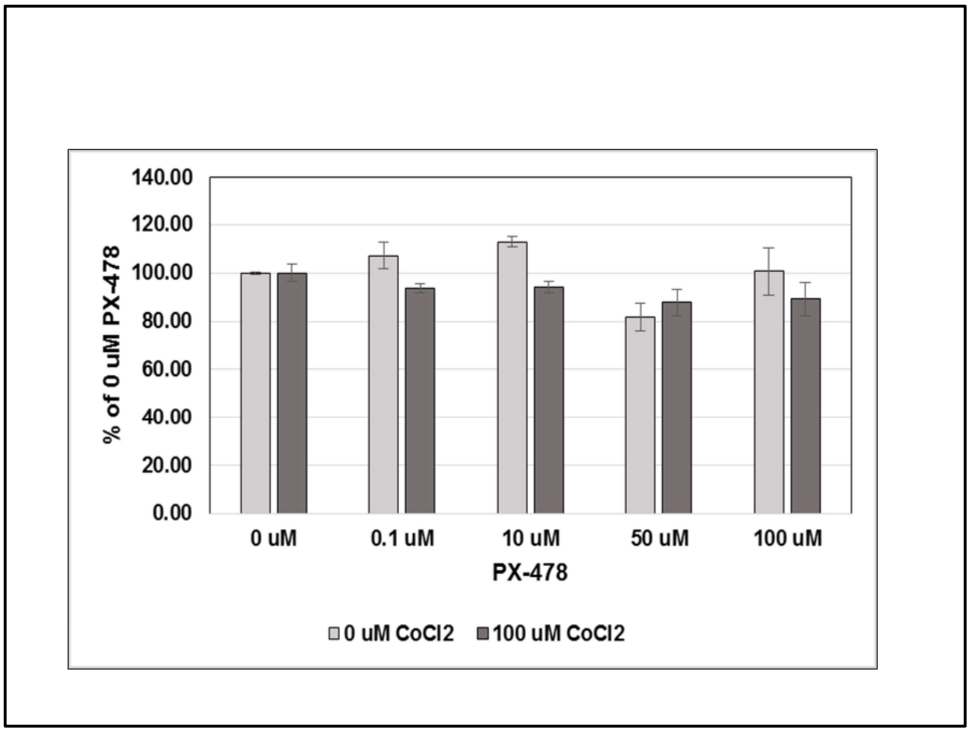

Figure 16. Effect of PX-478 on LTLTCa cell viability.

LTLTCa cells were plated in passage media and were treated with either vehicle or with 100 μM hypoxia mimetic cobalt chloride (CoCl2) and/or 0.1, 10, 50, or 100 uM PX-478 for 5 days. Number of viable cells were determined by the colorimetric MTT assay. Cells were incubated with 10% v/v MTT solution for 2.5 h, after which the resulting precipitate was dissolved into solution with DMSO and analyzed spectrophotometrically. Data shown are average % of absorbance compared to vehicle-treated (0 uM CoCl2, 0 uM PX-478) group of n =6 samples per treatment.

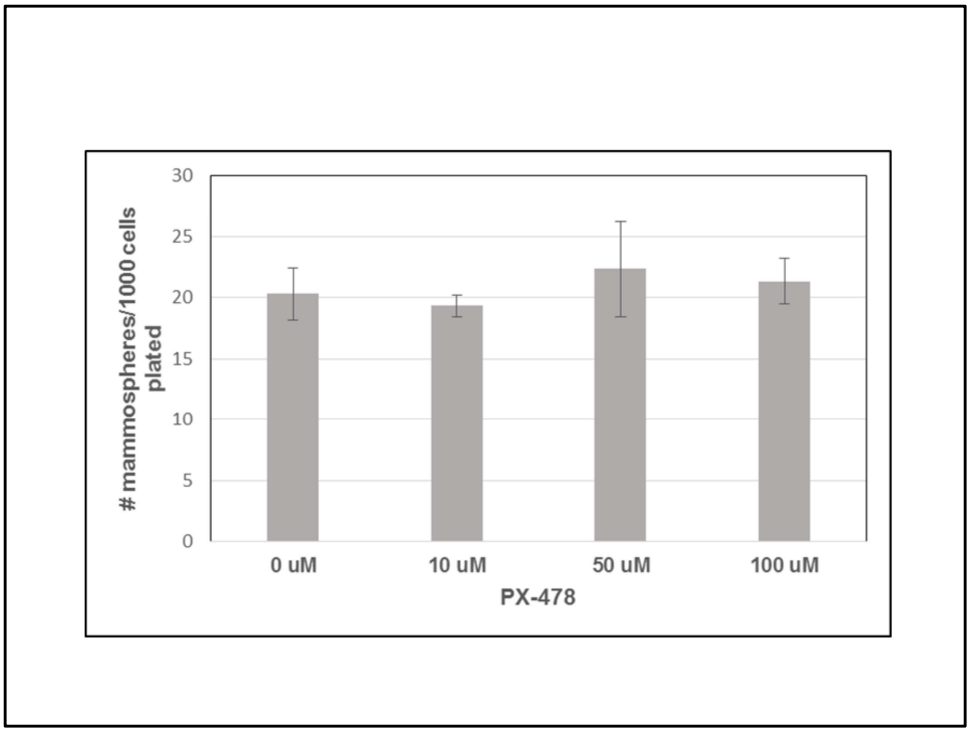

Figure 17. Effect of PX-478 on LTLTCa cell mammosphere formation.

LTLTCa cells were plated in passage media and were treated with either vehicle or with 100 uM PX-478 for 3 days prior to being plated in mammosphere media onto ultra-low attachment plates. Additional media was added after 7 days and the number of mammospheres were counted after 14 days. Data shown are average number of mammospheres of n =6 samples per treatment.

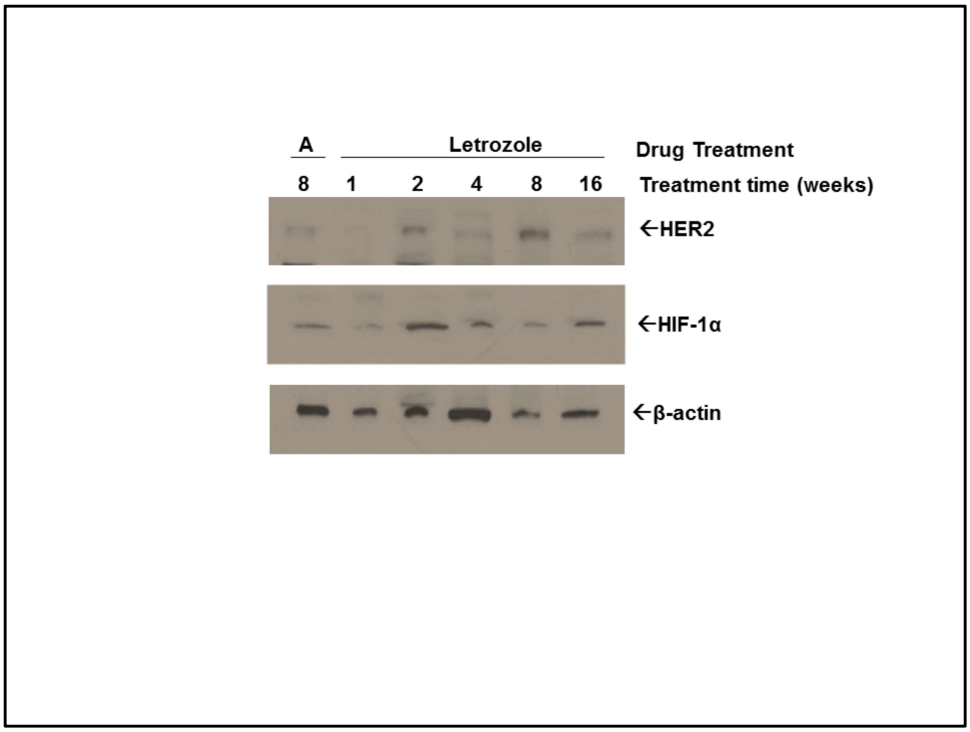

Figure 18. Effect of letrozole treatment on protein expression in MCF-7Ca xenograft tumors.

Total protein was extracted and HER2, HIF-1$^{\alpha}$, and β-actin protein were analyzed by Western blot from tumors obtained from a previously conducted xenograft tumor experiment. In this previous experiment, MCF-7Ca xenografts were grown in female ovariectomized mice. When tumors reached measurable size ~300 mm^3, mice were treated with 100 μg/day androstenedione (A; n=2) or letrozole (100 μg/day androstenedione and 10 μg/d letrozole. At certain timepoints of treatment (1-16 weeks) 2 representative mice from each group were euthanized and tumors were collected and store in -80 C. Shown are representative western blots.

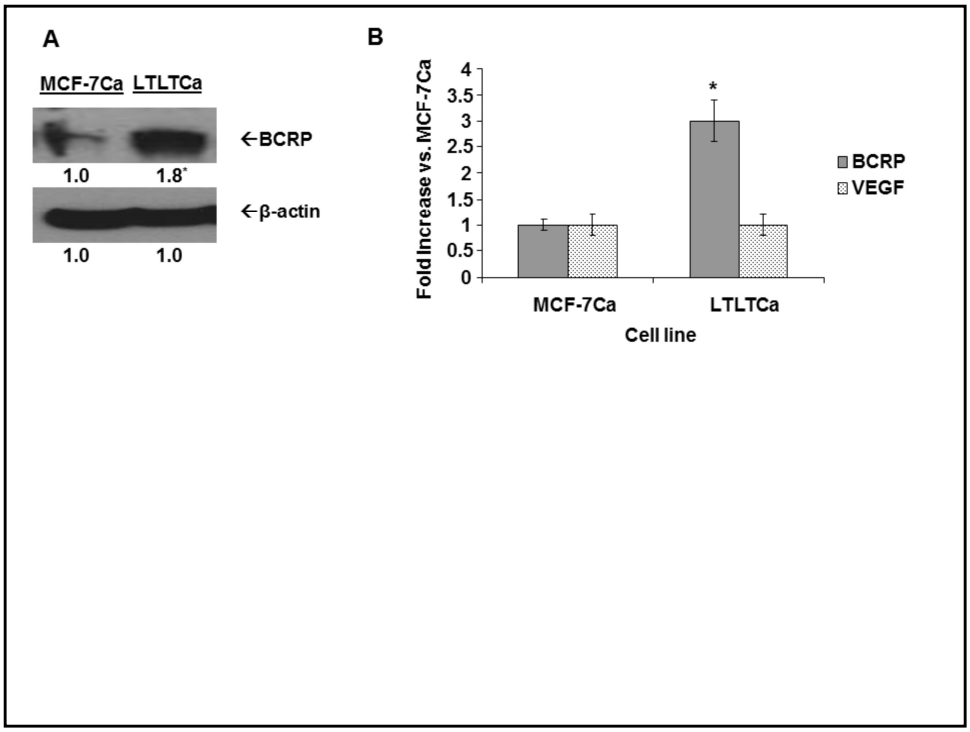

Figure 19. Comparison of BCRP protein and mRNA expression and stability in LTLTCa and MCF-7Ca cells

LTLTCa and parental MCF-7Ca cells were plated and cultured in their respective passage media under normal cell culture (nonhypoxic) conditions. A, Total protein was extracted and BCRP and β-actin were analyzed by Western blot analysis. Densitometry results are expressed as fold-change compared to MCF-7Ca cells after normalization to β-actin (mean ± SEM, n = 6 independent cell samples/group; * vs. MCF-7Ca, $p < 0.01$). B, Total RNA was extracted and BCRP mRNA, VEGF mRNA, and 18S rRNA were analyzed by real-time RT-PCR analysis. Results are expressed as the fold-change in mRNA levels compared with MCF-7Ca cells after normalization to 18S rRNA (mean ± SEM, n = 6 samples/group; * vs. MCF-7Ca, $p < 0.01$).

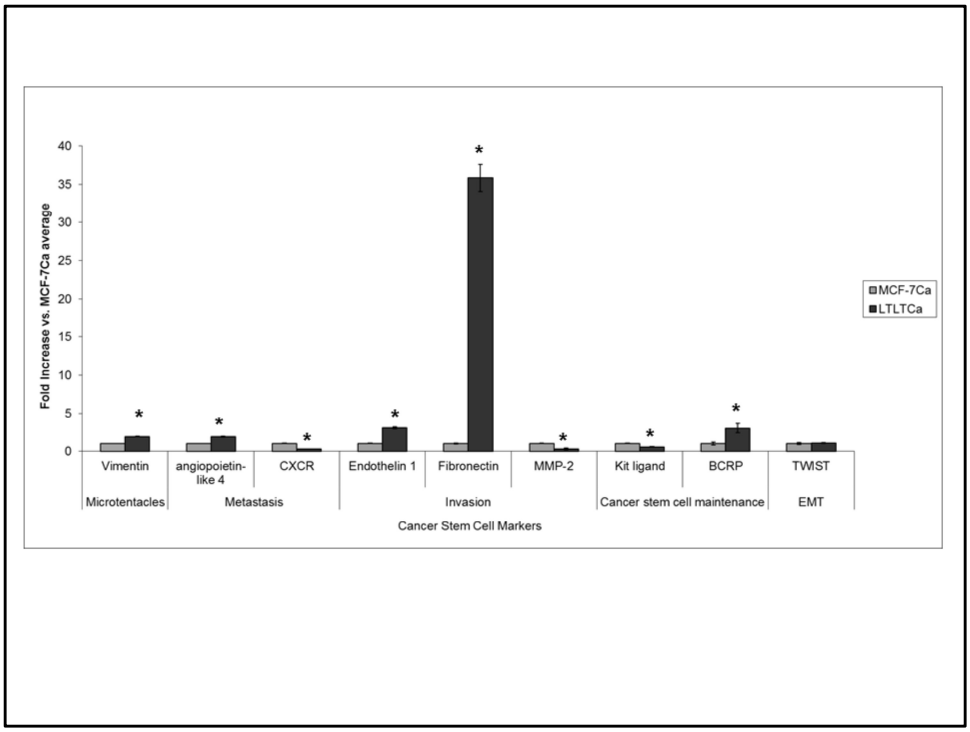

Figure 20. Comparison of mRNA expression in LTLTCa and MCF-7Ca cells.

LTLTCa and parental MCF-7Ca cells were plated and cultured in their respective passage media under normal cell culture (nonhypoxic) conditions. A, Total RNA was extracted and vimentin, angiopoietin-like 4, CXCR, endothelin 1, fibronectin, MMP-2, kit ligand, BCRP, and Twist mRNA, and 18S rRNA were analyzed by real-time RT-PCR analysis. Results are expressed as the fold-change in mRNA levels compared with MCF-7Ca cells after normalization to 18S rRNA (mean ± SEM, n = 6 samples/group; * vs. MCF-7Ca, $p < 0.05$).

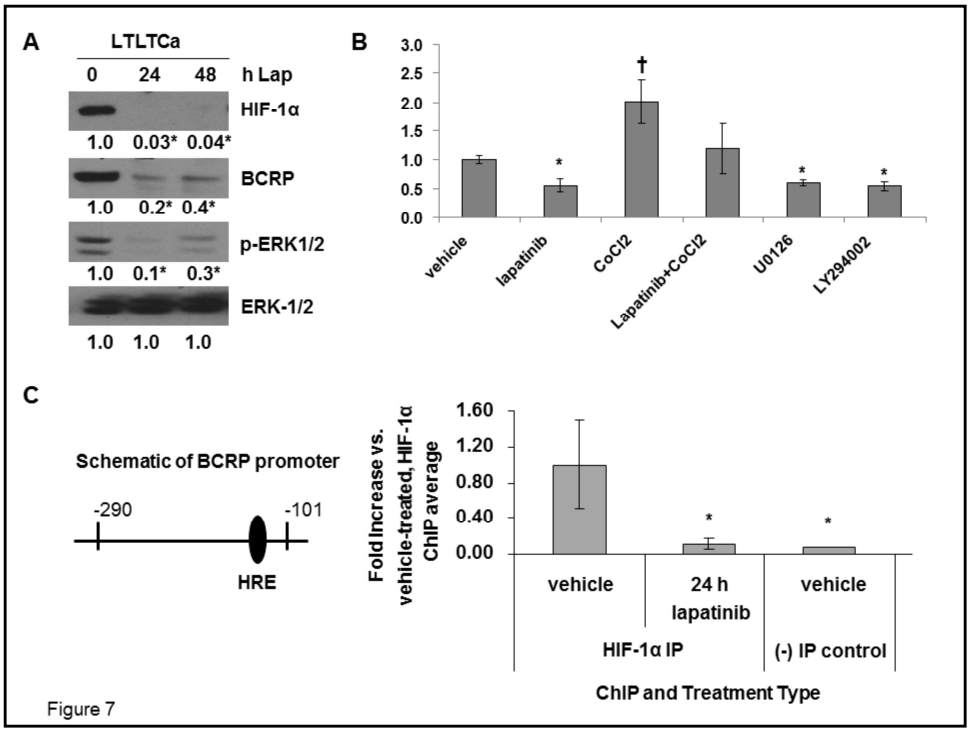

Figure 21. Effect of lapatinib and Cocl2 on BCRP protein and mRNA expression and on HIF-1$^{\alpha}$ binding to the BCRP promoter

A-B, LTLTCa were treated with vehicle, 1 μM lapatinib, and/or 100 μM CoCl2 for 24-48 h and protein, mRNA, and protein-DNA complexes were analyzed. A, LTLTCa cells were treated with lapatinib for 0-48 h. Total protein was extracted and HIF-1α, BCRP, p-ERK1/2, and ERK were analyzed by Western blot analysis. Densitometry results are expressed as fold-change compared to 0 h after normalization to ERK (mean ± SEM, n = 6 independent cell samples/group; * vs. 0 h lapatinib, $p < 0.01$). B, Total RNA was extracted and BCRP mRNA and 18S rRNA were analyzed by real-time RT-PCR analysis. Real-time results are expressed as the fold-change in mRNA levels compared with vehicle after normalization to 18S rRNA (mean ± SEM, n = 6 samples/group; * vs. vehicle, $p < 0.05$; † vs. lapatinib, U0126, or LY294002, $p < 0.05$). C, Protein-DNA complexes from LTLTCa cells were analyzed by ChIP analysis. Immunoprecipitation was carried out using either an antibody HIF-1α or an equivalent volume of normal mouse serum (-IP control). Primers for the –290 to –101 region of the human BCRP promoter, which contains the HRE to which HIF-1 binds, were used for real-time PCR. ChIP real-time PCR results are expressed as the fold increase, compared with vehicle-treated cells (means ± SEM, n = 6 per group; * vs.vehicle-HIF-1 IP, $p < 0.05$).

Figure 22. Human vimentin promoter (A31892.1). Potential hypoxia response elements (5'-CGTG-3') have been identified in yellow.

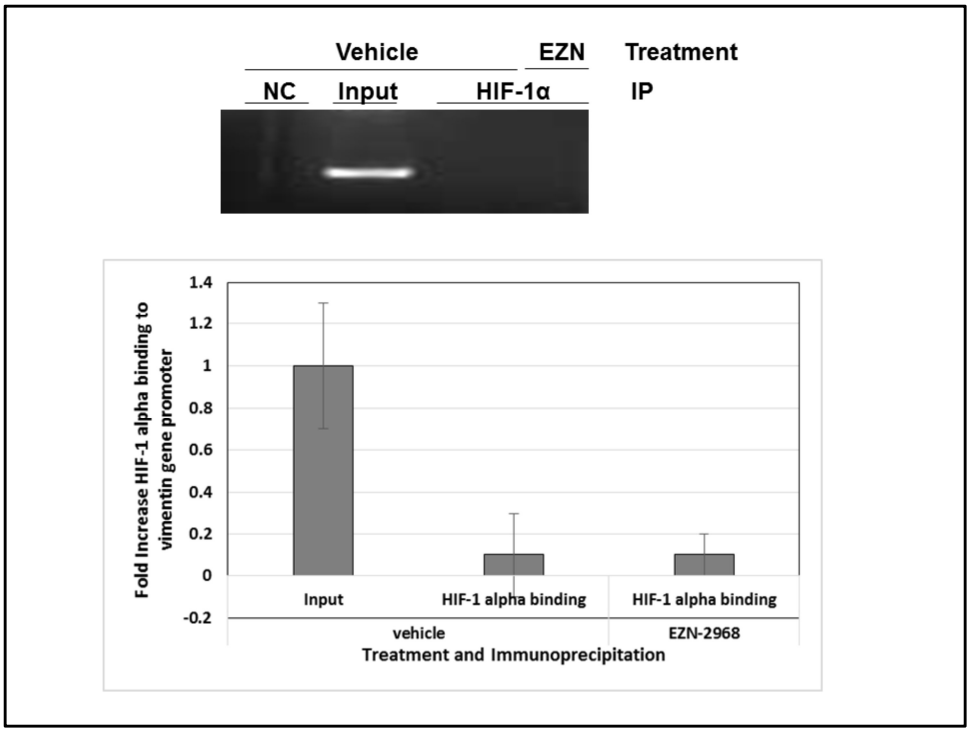

Figure 23. Binding of HIF-1$^{\alpha}$to vimentin promoter in LTLTCa cells.

LTLTCa cells were plated in their respective passage media and allowed to attach under normal cell culture conditions (20% O2), prior to being treated with either vehicle or 10 µM EZN-2968 (EZN) for 48 h. Protein-DNA complexes from LTLTCa cells were analyzed by ChIP analysis. Immunoprecipitation was carried out using a HIF-1 alpha antibody or an equivalent volume of negative control normal mouse serum (NC). Primers for the region of the human vimentin promoter, which contains the HRE to which HIF-1 binds, were used for real-time PCR. ChIP real-time PCR results are shown both as representative image and as quantitative graph in which binding is expressed as the fold increase, compared with input samples of vehicle-treated cells (means ± SEM, n = 3 per group; * vs. input DNA, $p < 0.05$).

.

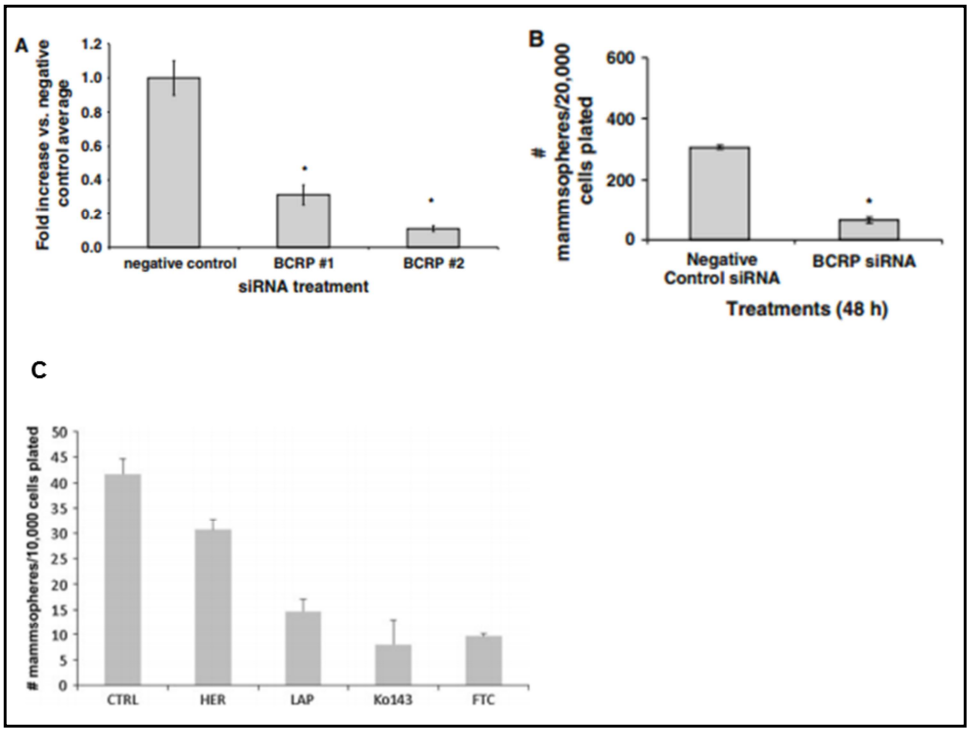

Figure 24. Effect of BCRP inhibition on mammosphere formation in LTLTCa cells. A, LTLT-Ca cells were plated in passage media and then treated with two siRNAs for BCRP for 48 h. Total mRNA was extracted and BCRP mRNA and 18S rRNA were analyzed by real-time RT-PCR. Real-time results are expressed as the fold change in mRNA levels compared with negative control after normalization to 18S rRNA (mean ± SEM, n = 6 samples/group; asterisk vs. vehicle, p\0.01). B, LTLT-Ca cells were plated in passage media and then treated with negative control siRNA or BCRP siRNA for 48 h. Cells were then collected and resuspended in mammosphere media on low-attachment cell culture wells. Results are expressed as number of mammospheres counted per 40,000 cells plated (mean ± SEM, n = 6 samples/group; asterisk vs. negative control, p< 0.01). After 48 h treatment with either vehicle (control), HER2 inhibitors (1 lM lapatinib or 500 lg/mL trastuzumab), or BCRP inhibitors (1 lM of either Ko1453 or FTC), LTLT-Ca cells were plated onto ultra-low-attachment plates containing mammosphere culture media. After 14 days in culture, formed mammospheres were imaged and counted. The mean mammosphere counts. (mean ± SEM, n = 3 independent cell samples/group, p\0.01.) are shown.

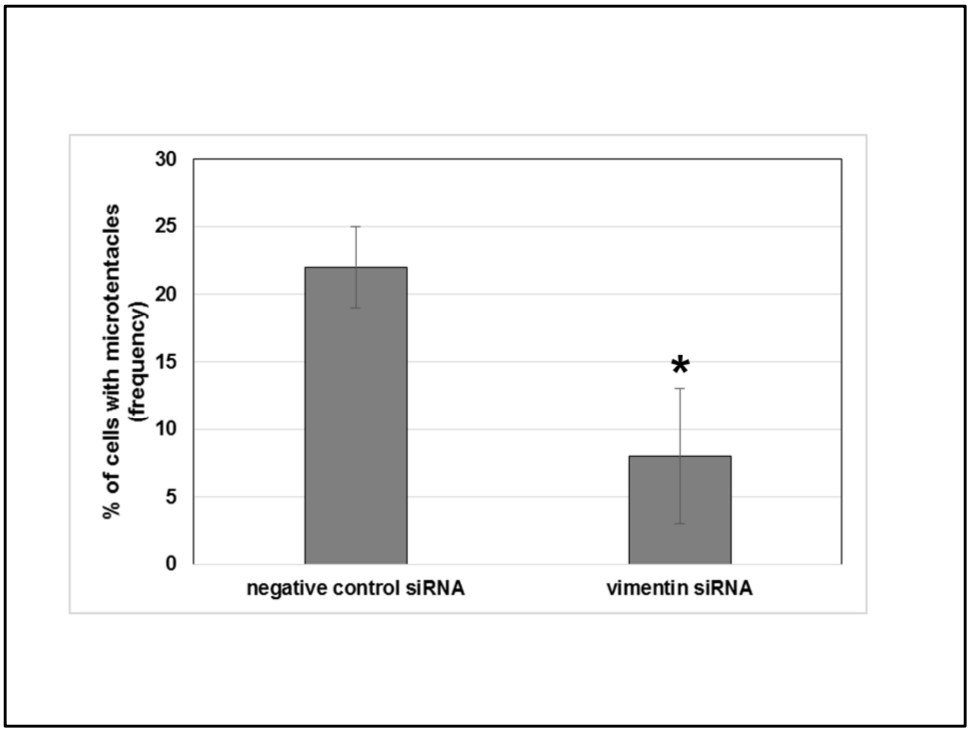

Figure 25. Effect of vimentin siRNA on microtentacle formation in LTLTCa cells.

LTLTCa cells were plated in passage media and then treated with 10 μM Qiagen vimentin-specific siRNA for 48 h. Cells were then collected, stained with Cell Mask Orange, and resuspended in Ibidi slides for microtentacle scoring. Results are expressed as percent of cells counted with microtentacles per 100 total cells counted (i.e., frequency). (n =5 samples per treatment; *, p< 0,05 vs. negative control).

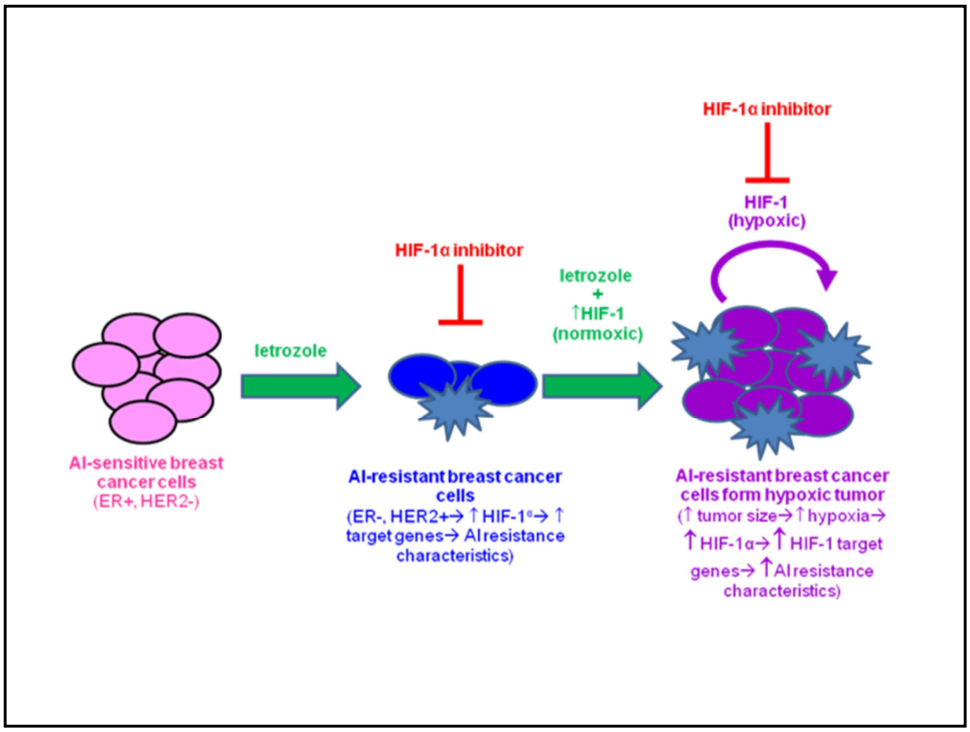

Figure 26. Proposed model of regulation and role of HIF-1α in AI resistant breast cancer.

Breast Cancer Res Treat (2012) 135:681–692
DOI 10.1007/s10549-012-2148-8

PRECLINICAL STUDY

The importance of HER2 signaling in the tumor-initiating cell population in aromatase inhibitor-resistant breast cancer

Rabia A. Gilani · Armina A. Kazi · Preeti Shah · Amanda J. Schech · Saranya Chumsri · Gauri Sabnis · Anil K. Jaiswal · Angela H. Brodie

Received: 3 January 2012 / Accepted: 20 June 2012 / Published online: 10 August 2012

Abstract Aromatase inhibitors (AIs) are an effective therapy in treating estrogen receptor-positive breast cancer. Nonetheless, a significant percentage of patients either do not respond or become resistant to AIs. Decreased dependence on ER-signaling and increased dependence on growth factor receptor signaling pathways, particularly human epidermal growth factor receptor 2 (EGFR2/HER2), have been implicated in AI resistance. However, the role of growth factor signaling remains unclear. This current study investigates the possibility that signaling either through HER2 alone or through interplay between epidermal growth factor receptor 1 (EGFR/HER1) and HER2 mediates AI resistance by increasing the tumor initiating cell (TIC) subpopulation in AI-resistant cells via regulation of stem cell markers, such as breast cancer resistance protein (BCRP). TICs and BCRP are both known to be involved in drug resistance. Results from in vitro analyses of AI-resistant versus AI-sensitive cells and HER2-versus HER2+ cells, as well as from in vivo xenograft tumors, indicate that (1) AI-resistant cells overexpress both HER2 and BCRP and exhibit increased TIC characteristics compared to AI-sensitive cells; (2) inhibition of HER2 and/or BCRP decrease TIC characteristics in letrozole-resistant cells; and (3) HER2 and its dimerization partner EGFR/HER1 are involved in the regulation of BCRP. Overall, these results suggest that reducing or eliminating the TIC subpopulation with agents that target BCRP, HER2, EGFR/HER1, and/or their downstream kinase pathways could be effective in preventing and/or treating acquired AI resistance.

Keywords Breast cancer · Tumor initiating cells · Lapatinib · Aromatase inhibitor · Hormone or endocrine therapy · HER2 · BCRP

Rabia A. Gilani and Armina A. Kazi contributed equally to this study.

R. A. Gilani · A. A. Kazi · P. Shah · A. J. Schech · G. Sabnis · A. K. Jaiswal · A. H. Brodie
Department of Pharmacology and Experiment Therapeutics, University of Maryland School of Medicine, Baltimore MD 21201, USA

A. A. Kazi
Department of Biology, Loyola University Maryland, Baltimore, MD 21210, USA

S. Chumsri
Department of Medicine, University of Maryland School of Medicine, Baltimore, MD 21201, USA

S. Chumsri · G. Sabnis · A. K. Jaiswal · A. H. Brodie
University of Maryland Marelene and Steward Greenebaum Cancer Center, University of Maryland, Baltimore MD 21201, USA

A. H. Brodie (✉)
Department of Pharmacology and Experiment Therapeutics, University of Maryland School of Medicine, Health Science Facilities, Room 580G, 685 West Baltimore Street, Baltimore, MD 21201, USA
e-mail: abrodie@umaryland.edu

Introduction

Inhibition of estrogen synthesis via aromatase inhibitors (AIs, i.e., letrozole, anastrozole, and exemestane) is highly effective in treating estrogen receptor-positive (ER+) breast cancer and preventing contra-lateral breast cancer [1]. A significant percentage of ER+ patients, however, either do not respond to AIs or become resistant to them during treatment [2, 3]. Previous work by our laboratory indicates that acquired AI resistance involves a switch from

the dependence on ER signaling to the dependence on growth factor-mediated pathways, such as human epidermal growth factor receptor 2 (EGFR2)/HER2 and insulin-like growth factor receptor (IGFR) [2–4]. However, the mechanism by which growth factor signaling confers AI resistance remains unclear.

One possibility is that HER2 mediates expansion of the tumor initiating cell (TIC) population, as suggested in previous studies [5, 6]. TICs are a small distinct subset of cells within a heterogeneous tumor which have the ability to initiate and maintain tumor growth and to promote metastasis [7–12]. Pertinent to acquired AI resistance, TICs are known to play a role in radio- and chemo resistance [7–9], as the residual tumor cell population remaining after treatment with conventional chemotherapy or AIs exhibit a high proportion of TICs [7–9, 13–15]. The expansion of TICs or inability to eliminate them may contribute to acquire AI resistance in breast cancer.

HER2 may maintain and/or expand the TIC subpopulation within an AI-resistant tumor by regulating certain TIC effector genes, such as the breast cancer resistance protein (BCRP). BCRP maintains TICs in an undifferentiated state [13, 15]. It is also a membrane-associated transporter protein, the function of which is to efflux out various molecules from the cell, and has been linked to multi-drug chemoresistance of breast cancer cells [13, 15–17]. Furthermore, other studies have shown a correlation between BCRP and HER2 [6, 18–20] and ERα [21, 22]. Thus, the purpose of this current study was to (1) determine if the TIC subpopulation is increased in AI-resistant versus-sensitive cells; (2) analyze the TIC subpopulation in letrozole-resistant cells; (3) investigate the importance of HER2 and BCRP on the TIC phenotype in letrozole-resistant cells; (4) determine whether HER2 regulates BCRP; and (5) determine if EGFR/HER1 is also involved.

Materials and methods

Cell lines and reagents

Cell lines

Cell lines (and their ER/HER2 status) used are listed in Table 1. MCF-7Ca cells are MCF-7 cells stably transfected with the human aromatase gene (supplied by Dr. Chen, City of Hope, Duarte, CA) and maintained in DMEM 1× high glucose (Invitrogen) supplemented with 5 % fetal bovine serum (FBS), 1 % penicillin/streptomycin (P–S), and 700 μg/mL G418. Long-term letrozole-treated (LTLT-Ca) cells are letrozole-resistant cells isolated from MCF-7Ca mouse xenograft tumors treated for 56 weeks with letrozole, and maintained in phenol red-free (PRF) modified IMEM (Invitrogen) supplemented with 5 % charcoal dextran-treated FBS (CDT-FBS), 1 % P–S, 750 μg/mL G418, and 1 μM letrozole. MCF-7 cells (ATCC) were maintained in DMEM 1 × high glucose (Invitrogen) supplemented with 5 % FBS and 1 % P–S. MCF-7/HER2 cells are MCF-7 cells transfected with the HER2 gene (supplied by Ann Hambruger, University of Maryland Baltimore, UMB) maintained in DMEM 1× high glucose (Invitrogen) supplemented with 5 % FBS, 1 % P–S, and 500 μg/mL hygromycin. AC1 cells are MCF-7 cells stably transfected with the human aromatase maintained in DMEM 1× high glucose (Invitrogen) supplemented with 5 % FBS, 1 % P–S, and 800 μg/mL G418. AC1-exemestane resistant (AC1-ExR) cells are a exemestane-resistant cells isolated from AC1 mouse xenograft tumors treated for ~10 weeks with exemestane maintained in PRF modified IMEM (Invitrogen) supplemented with 5 % CDT-FBS, 1 % P–S, 800 μg/mL G418, and 5 μM exemestane.

Table 1 Molecular profile and aromatase inhibitor-sensitivity of cell lines used

Cell Line	ERα status	HER2 status	AI-sensitivity
MCF-7Ca	+	−	Yes
LTLT-Ca	−	+	No (to letrozole)
MCF7	+	−	Yes
MCF7/HER2	+	+	ND
SUM149	−	−	ND
AC1	+	−	Yes
AC1-ExR	+	+	No (to exemestane)

ND not determined

Reagents

The following drugs were used: letrozole (Novartis); lapatinib (GlaxoSmithKline Pharmaceutical); trastuzumab (Genentech); BIBX1382 (Calbiochem); and BCRP inhibitors Ko143 and fumitremorgen C (FTC) were kindly provided by Dr. Douglas Ross (UMB). Use of Ko143 and FTC depended on availability from Dr. Ross' laboratory. The following antibodies were used in western blot analyses: HER2 (EMD Millipore); BCRP (EMD Millipore); ERα (Santa Cruz Biotechnology); and phosphorylated and total ERK1/2 or Akt, phosphorylated and total EGFR/HER1, and β-actin (all obtained from Cell Signaling Technology).

Side population (SP) analysis

SP analysis was performed either by Hoechst 33342 assay [6, 23] or using Vibrant DyeCycle Violet stain (Invitrogen). Briefly, after drug treatment, 1×10^6 cells/mL were suspended in prewarmed IMEM with 2 % FBS and 10 mM HEPES containing 5 μg of Hoechst 33342 (Sigma) or 1 μL

of DyeCycle Violet stock. Cells were incubated at 37 °C for 40 min (Dye Cycle) or 90 min (Hoechst). Cells were acquired using BD-LSRII. Data was analyzed by means of FlowJo software. Cells treated with BCRP inhibitor Ko143 were included in each SP analysis set as a control to demonstrate inhibition of dye efflux.

Aldehyde dehydrogenase (ALDH) assay

The Aldefluor assay was performed using the Aldefluor Assay kit from Stem Cell Technologies. ALDH stained cells were identified in cells by comparing the same sample with and without the ALDH inhibitor DEAB (diethylaminobenzaldehyde). Cells were acquired using BD LSRII and FACS CANTO. Data were analyzed by means of FlowJo software.

Mammosphere assay

The mammosphere assay was performed using reagents from Stem Cell Technologies according to the manufacturer's instructions. Single cells were suspended in complete Mammocult media as per the manufacturer's instructions and plated in ultra-low-attachment plates (Corning) at a density of 10,000–20,000 cells/mL. Media was replenished every 3 days. Mammospheres were counted after at least 7 days and up to 3–4 weeks. Spheres with a colony count of at least 50 cells were considered mammospheres.

Immunofluorescence (IF)

IF staining for Oct-4 was performed on sorted LTLT-Ca cells kept under non-adherent conditions for 2–3 days prior to cytospinning. Pelleted cells were fixed with 4 % paraformaldehyde and incubated with OCT4 antibody (Santa Cruz Biotechnology) and the corresponding fluorochrome-tagged secondary antibody (Invitrogen). Images were obtained and analyzed by means of Image J software.

RT-PCR

RNA extraction and reverse transcription (RT)

RNA was extracted and purified using the RNeasy Mini Kit (Qiagen). RNA was reverse transcribed to complementary DNA (cDNA) using 200 U of Moloney murine leukemia virus reverse transcriptase (Invitrogen) and incubating at 37 °C for 1 h.

Real-Time PCR

mRNA expression analyses were carried out by real-time PCR using a DNA Opticon system (MJ Research) and using DyNAmo SYBR green qPCR mix (New England Biolabs). Standard curves were generated by serially diluting the sample expected to have the most amount of PCR product. The yield of product for each unknown sample was calculated by applying its threshold cycle, or C(T), value to the standard curve by means of the Opticon Monitor analysis software (version 1.01, MJ Research). Values were normalized to corresponding 18S rRNA values and expressed as the fold increase relative to controls. Primers for HER2, BCRP, BMI-1, Nanog, and Twist were obtained from Sigma or Qiagen.

Growth and treatment of MCF-7Ca mouse xenograft tumors

All animal studies were performed according to the guidelines and approval of the Animal Care Committee of UMB. MCF-7Ca tumor xenografts of MCF-7Ca cells were grown in ovariectomized athymic nude mice as previously described [24]. Briefly, each mouse received subcutaneous (sc) inoculations in one site per flank of 100 μL of cell suspension containing $\sim 2.5 \times 10^7$ MCF-7Ca cells. All mice were supplemented throughout the experiment with 100 μg/day androstenedione (Δ4A) sc 5 days/week. Δ4A is converted to estrogen by aromatase expressed in MCF-7Ca cells. Tumor growth was monitored weekly and treatments began when the tumors reached ~ 300 mm^3. Mice were then randomly divided into either control (100 μg/day Δ4A) or letrozole (100 μg/day Δ4A + 10 μg/day letrozole) treatment groups. Letrozole and Δ4A were prepared using 0.3 % Hydroxypropylcellulose in saline solution. Mice were injected sc five times weekly with the indicated drugs. Tumors were collected at necropsy either at previously designated times (weeks 4, 8, and 16), or when tumors reached 2,000 mm^3 in size.

Western blot analysis

Cells

Plated cells were washed with ice-cold PBS and then lysed with radioimmunoprecipitation (RIPA) buffer containing protease and phosphatase inhibitors (Roche) by sonication and incubation for 20 min at 4 °C. Lysed samples were centrifuged at 14,000 rpm for 20 min at 4 °C to collect protein lysates (supernatant). 10–40 μg of protein underwent 10 % SDS–polyacrylamide gel electrophoresis and transferred to a polyvinylidene difluoride membrane (Fisher Scientific). The resulting blots were probed with specific mouse or rabbit primary antibodies and either goat anti-mouse or -rabbit secondary antibodies conjugated to horseradish peroxidase (Biorad), respectively. Blots were developed using SuperSignal West Pico Chemiluminescent Substrate (Thermo Scientific). Blots that were to be re-

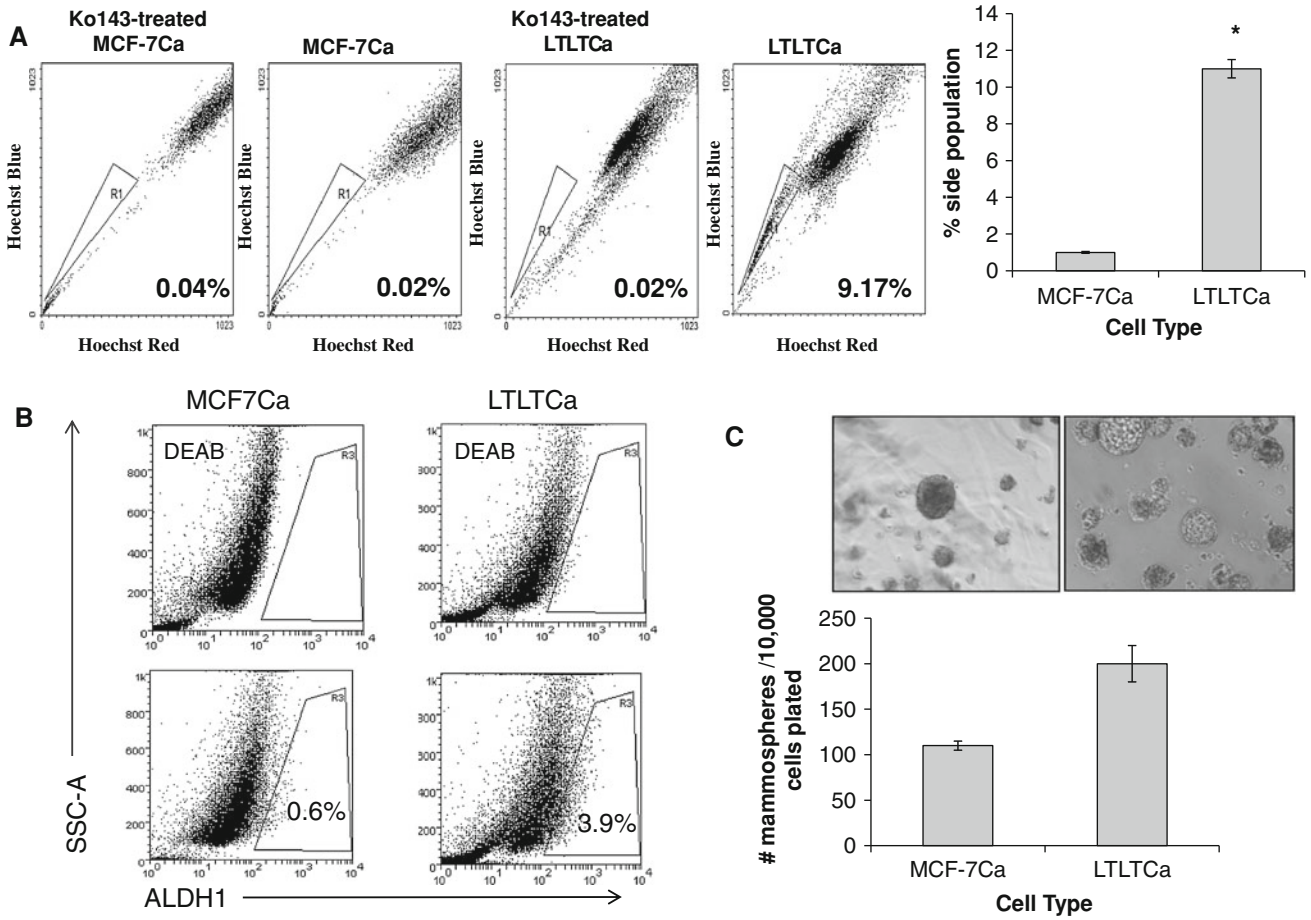

Fig. 1 Analysis of SP and ALDH in MCF-7Ca and LTLT-Ca cells. **a** Percentage of side population (SP) cells were analyzed in MCF-7Ca and LTLT-Ca cells by Hoechst staining and flow cytometry in the absence or presence of BCRP inhibitor Ko143. Plots show representative SP fractions as designated by *polygons* and quantified as percentages ($n = 3$ independent cell samples/group; $p < 0.01$). **b** Analysis of aldehyde dehydrogenase 1 (ALDH) by measuring the cellular fluorescence of bodipy-aminoacetate (BAAA) in the presence or absence of specific ALDH inhibitor DEAB. Plots show representative ALDH1-expressing cells, as designated by *polygons* and quantified as percentages ($n = 3$ independent cell samples/group; $p < 0.05$). **c** MCF-7Ca and LTLT-Ca cells were plated onto ultra-low-attachment plates containing mammosphere culture media. After 8 days in culture, formed mammospheres were imaged (*top panel*) and counted (*bottom panel*). Shown are representative images (*top panel*) and mean mammosphere counts. (Mean ± SEM, $n = 9$ independent cell samples/group, $p < 0.05$.)

probed were stripped with Restore Western Blot Stripping Buffer (Thermo Scientific) for 40 min at room temperature before incubation with another primary antibody.

MCF-7Ca xenograft tumors

Tumor samples were first homogenized in ice-cold DPBS containing protease inhibitors and centrifuged. The resulting tumor homogenate pellets were lysed with RIPA buffer. Tumor protein lysates were then collected and subjected to the same western blot analyses as cells.

Statistical analysis

All experiments were carried out at least 2–3 times each with replicates. Statistical analyses were performed by Student's *t* test (two samples), ANOVA (3+ samples) by means of Graph Pad Prism software.

Results

Letrozole-resistant LTLT-Ca cells exhibit higher percentage of TICs compared to letrozole sensitive MCF-7Ca cells

The TIC subpopulation can be distinguished from other cells within a cancer cell population by several characteristics: (1) exclusion of Hoechst dye from cells and identification as "side population" (SP) cells [25–27]; (2) increased ALDH1 expression [28]; (3) ability to form mammospheres in culture [29]; and (4) expression of

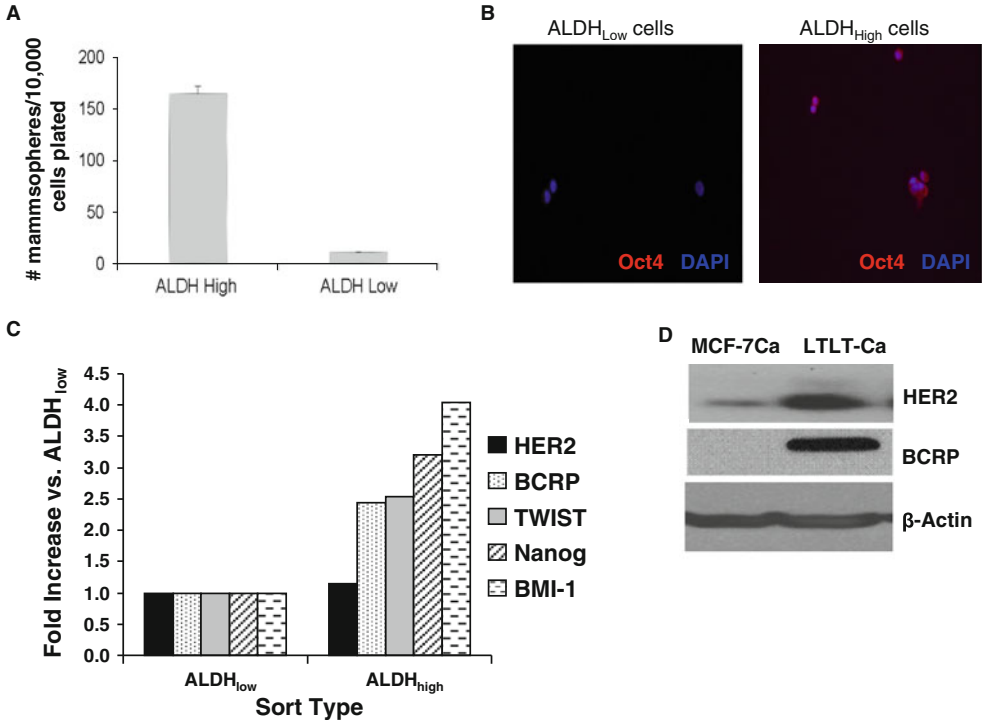

Fig. 2 mRNA expression in ALDH$_{low}$ and ALDH$_{high}$ LTLT-Ca cells and protein expression in LTLT-Ca versus MCF-7Ca cells. **a** LTLT-Ca cells were treated with aldefluor and then ALDH1$_{low}$ and ALDH1$_{high}$ cells (3–4 % lowest and highest) were sorted by fluorescence-activated cell sorting (FACS). Sorted cells were then plated under ultra-low-attachment conditions at a density of 10,000 cells/well. After ~3 weeks, formed mammospheres were counted. A representative graph of the average number of formed mammospheres ($n = 3$; $p < 0.01$) is shown. **b** ALDH1$_{low}$- and ALDH1$_{high}$-expressing LTLT-Ca cells were subjected to immunofluorescence with Oct-4 antibody (*red*) and DAPI nuclear stain (*blue*). Shown are representative immunofluorescence images. **c** Total mRNA was extracted from ALDH1$_{low}$- and ALDH1$_{high}$-expressing LTLT-Ca cells, and real-time RT-PCR analyses were done for HER2, BCRP, TWIST, Nanog, and BMI-1 mRNA and 18S rRNA. Real-time results are expressed as the fold change in mRNA levels compared with ALDH low after normalization to 18S rRNA (mean ± SEM, $n = 2$ pooled samples/group). **d** MCF-7Ca and LTLT-Ca cells were plated in their respective passage media. Total protein was extracted and HER2, BCRP, and β-actin protein were analyzed by western blot. Representative blots ($n = 6$ independent cell samples/group) are shown

known stem cell markers, such as BCRP [13, 15, 30], Nanog [31], and BMI-1 [32]. Letrozole-resistant LTLT-Ca, derived from long-term letrozole treated MCF-7Ca xenograft tumors, and letrozole-sensitive parental MCF-7Ca cells were, therefore, compared to each other based on these TIC parameters. LTLT-Ca cells were found to have higher percentage of SP cells (9.17 ± 2.0 % LTLT-Ca vs. 0.02 ± 0.01 % MCF-7Ca, $p < 0.01$) and ALDH-expressing cells (3.9 % LTLT-Ca vs. 0.6 % MCF-7Ca, $p < 0.01$) than MCF-7Ca cells (Fig. 1a, b). LTLT-Ca cells also formed significantly more mammospheres in culture than MCF-7Ca cells (Fig. 1c, $p < 0.05$). Thus, letrozole-resistant LTLT-Ca cells express more TIC characteristics than parental, letrozole-sensitive MCF-7Ca cells.

The TIC subpopulation in LTLT-Ca cells was further analyzed through isolation of the highest and lowest 3–4 % ALDH1-expressing cells (Fig. 2). These were designated as ALDH1$_{high}$ (i.e., TICs) and ALDH1$_{low}$ cells, respectively, and their ALDH expression levels were confirmed by immunofluorescence (data not shown). These subpopulations were then compared for their ability to form mammospheres and their expression of known stem cell markers and HER2. As expected, ALDH1$_{high}$ cells formed significantly more mammospheres (164.7 ± 7.5 vs. 11 ± 1, $p < 0.05$; Fig. 2a) and they expressed higher levels of stem cell markers OCT-4 (as shown by immunofluorescence, Fig. 2b), BCRP, BMI-1, and Nanog (>2.5–>3.3-fold as shown by RT-PCR, Fig. 2c) compared to ALDH1$_{low}$ cells. In addition, ALDH1$_{high}$ cells expressed higher mRNA levels of TWIST, an epithelial–mesenchymal transition marker and transcription factor known to regulate BMI-1 and of HER2 (>1.3 and >2.5-fold vs. ALDH1$_{low}$, Fig. 2c). HER2 overexpression in ALDH1$_{high}$ versus ALDH1$_{low}$ cells was additionally confirmed by flow cytometry (data not shown). Both HER2 and BCRP proteins were also increased in LTLT-Ca cells when compared overall to MCF-7Ca cells (Fig. 2d). These results demonstrate that the TIC population can be isolated from LTLT-Ca cells and that they express factors known to be involved in their regulation.

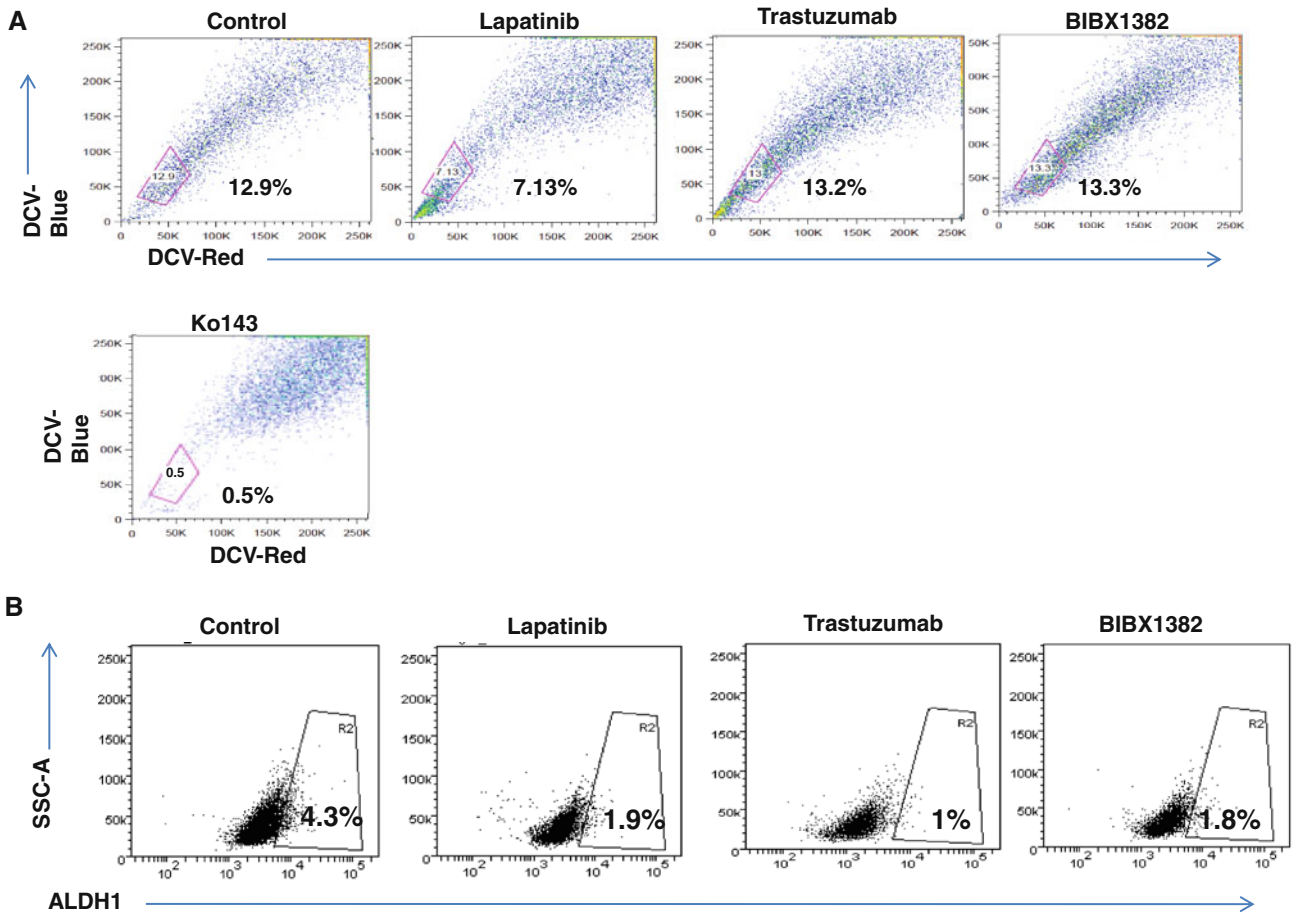

Fig. 3 Effect of HER2, BCRP, and/or EGFR inhibitors on percentage of side population (SP) cells and ALDH-expressing LTLT-Ca cells. **a** Percentage of side population (SP) cells were analyzed in MCF-7Ca and LTLT-Ca cells by Hoechst staining by flow cytometry after 48 h treatment with vehicle (*control*), 1 μM Ko143, 1 μM lapatinib, 500 μg/mL trastuzumab, or 10 nM BIBX 1382. Plots show representative SP fractions, as designated by *polygons* and quantified as percentages ($n = 3$ independent cell samples/group; $p < 0.01$). **b** Analysis of aldehyde dehydrogenase 1 (ALDH) by measuring the cellular fluorescence of bodipy-aminoacetate (BAAA) after 48 h treatment with vehicle (*control*), 1 μM lapatinib, 500 μg/mL trastuzumab, or 100 nM BIBX 1382. Plots show representative ALDH expressing cells, as designated by *polygons* and quantified as percentages ($n = 3$ independent cell samples/group; $p < 0.05$)

EGFR/HER1, HER2, and BCRP are involved in regulating the TIC phenotype in LTLT-Ca cells

HER2 and BCRP are examples of TIC-regulating factors [9, 13, 15, 18, 30, 33, 34]. To assess the importance of HER2 in regulating the TIC phenotype, the effects of HER2 inhibitors lapatinib (a EGFR/HER1-HER2 tyrosine kinase inhibitor), and trastuzumab (a HER2-specific monoclonal antibody) [35] were determined. Lapatinib treatment, in particular, has been previously shown to reduce TIC characteristics in breast cancer cells obtained from patients [9]. Since HER2 can be ligand-dependently activated through dimerization with EGFR/HER1 [36], and lapatinib can inhibit both HER2 and EGFR/HER1, the effect of highly specific and potent (at nM concentrations) EGFR/HER1 kinase inhibitor BIBX1382 [37] was also analyzed. The percentage of SP cells in LTLT-Ca remained unchanged by HER2-specific trastuzumab or EGFR/HER1-specific BIBX1382, but was decreased by dual inhibitor lapatinib (7.3 vs. 12.9 % control, Fig. 3a). ALDH1 expression, however, was decreased in LTLT-Ca cells by lapatinib, trastuzumab, and BIBX1382 (1.87, 0.99, and 1.8 vs. 4.34 % of vehicle-treated, respectively; Fig. 3b). Finally, 48 h treatment with either lapatinib or trastuzumab before plating in ultra-low-attachment conditions significantly decreased LTLT-Ca mammosphere formation ($p < 0.05$; Fig. 4), with greater effects observed in lapatinib-treated cells. The inhibitory effects of these drugs on TIC characteristics was not due to induction of cell death in the overall LTLT-Ca cell population, as trypan blue cell viability assays showed no significant differences between vehicle- and drug-treated cells within the same 48 h time frame (data not shown).

BCRP's importance was similarly assessed using specific and potent BCRP inhibitors FTC or FTC's less toxic, more potent analog Ko143 [38]. Consistent with studies in other breast cancer cell lines [6] and with BCRP's known function as a membrane-associated transporter protein that effluxes from cells a variety of molecules (i.e., Hoechst dye and chemotherapeutic drugs) [16], Ko143 treatment significantly reduced the percentage of SP cells (0.02 % Ko143 vs. 9.17 % in Fig. 1a; 0.24 % Ko143 vs. 7.91 % vehicle in Fig. 3a). Both FTC and Ko143 significantly decreased mammosphere formation by ~75 % compared to vehicle-treated LTLT-Ca cells ($p < 0.05$, Fig. 4). Similar reduction in mammosphere formation was observed after treatment of LTLT-Ca cells with BCRP siRNA to reduce BCRP expression (Fig. 5). Neither Ko143 nor FTC had an effect on ALDH1 expression (data not shown). Overall, these results demonstrate that both HER2 and BCRP are involved in regulating the TIC phenotype of LTLT-Ca cells. BCRP is important in SP and mammosphere formation, whereas HER2 is required for ALDH1, SP, and mammosphere formation in LTLT-Ca cells. These results indicate that EGFR/HER1 may also have a role in TICs.

EGFR/HER1 and HER2 are involved in regulation of BCRP

Since HER2 and BCRP are both overexpressed in LTLT-Ca cells (Fig. 2) and are important in the TIC phenotype (Figs. 3, 4), another objective of this study was to determine whether HER2 regulates BCRP expression in LTLT-Ca cells and whether EGFR/HER1 was also involved. The role of HER2 is supported by several pieces of evidence.

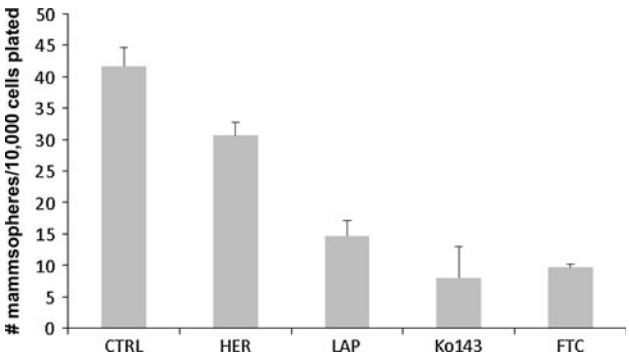

Fig. 4 Effect of HER2, BCRP, and/or EGFR inhibitors on mammosphere formation in LTLT-Ca cells. After 48 h treatment with either vehicle (*control*), HER2 inhibitors (1 μM lapatinib or 500 μg/mL trastuzumab), or BCRP inhibitors (1 μM of either Ko1453 or FTC), LTLT-Ca cells were plated onto ultra-low-attachment plates containing mammosphere culture media. After 14 days in culture, formed mammospheres were imaged and counted. The mean mammosphere counts. (mean ± SEM, $n = 3$ independent cell samples/group, $p < 0.01$.) are shown

First, other HER2-expressing cell lines also had elevated BCRP levels. HER2-transfected MCF-7 (MCF-7/HER2) cells overexpressed BCRP protein compared to HER2-/low expressing cells (i.e., MCF-7 and SUM149), and at comparable levels to LTLT-Ca cells (Fig. 6a). In addition, compared to exemestane-sensitive, HER2-, parental AC1 cells, another AI (exemestane)-resistant cell line (AC1-ExR) had elevated levels of both HER2 and BCRP protein (Fig. 6b) and increased mammosphere formation (Fig. 6c). Even though ERα is also known to regulate BCRP [22], BCRP protein was elevated in both ERα-/HER2 + LTLT-Ca cells and in ERα+/HER2 + MCF-7/HER2 and AC1-ExR cells (Fig. 6a, b). It was also elevated in cell lines with (AC1-ExR cells) or without (LTLT-Ca) increased EGFR/HER1 phosphorylation compared to their parental cell lines (Fig. 6a, b). Thus, upregulation of BCRP occurs independently of ERα expression and EGFR/HER1 activation.

Second, inhibition of HER2 signaling decreased BCRP expression. LTLT-Ca cells were treated for 24 h with lapatinib alone, trastuzumab alone, BIBX1382 alone, or

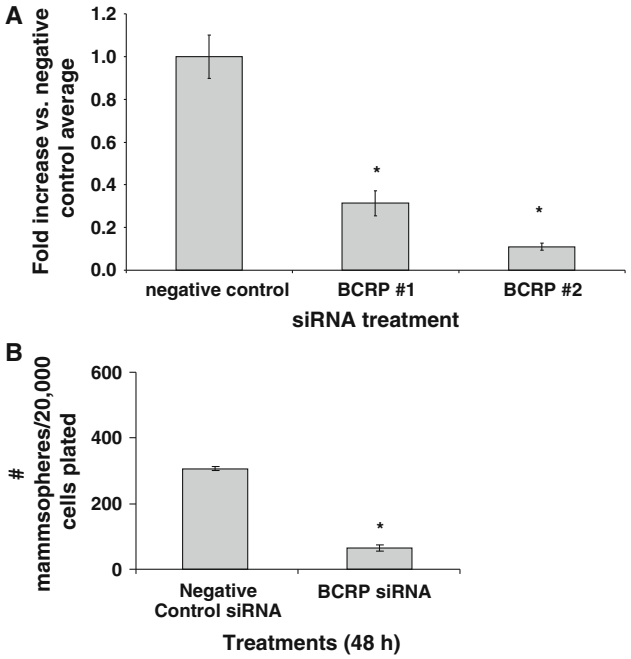

Fig. 5 Effect of BCRP siRNA on BCRP mRNA expression and mammosphere formation in LTLT-Ca cells. **a** LTLT-Ca cells were plated in passage media and then treated with two siRNAs for BCRP for 48 h. Total mRNA was extracted and BCRP mRNA and 18S rRNA were analyzed by real-time RT-PCR. Real-time results are expressed as the fold change in mRNA levels compared with negative control after normalization to 18S rRNA (mean ± SEM, $n = 6$ samples/group; *asterisk* vs. vehicle, $p < 0.01$). **b** LTLT-Ca cells were plated in passage media and then treated with negative control siRNA or BCRP siRNA for 48 h. Cells were then collected and resuspended in mammosphere media on low-attachment cell culture wells. Results are expressed as number of mammospheres counted per 40,000 cells plated (mean ± SEM, $n = 6$ samples/group; *asterisk* vs. negative control, $p < 0.01$)

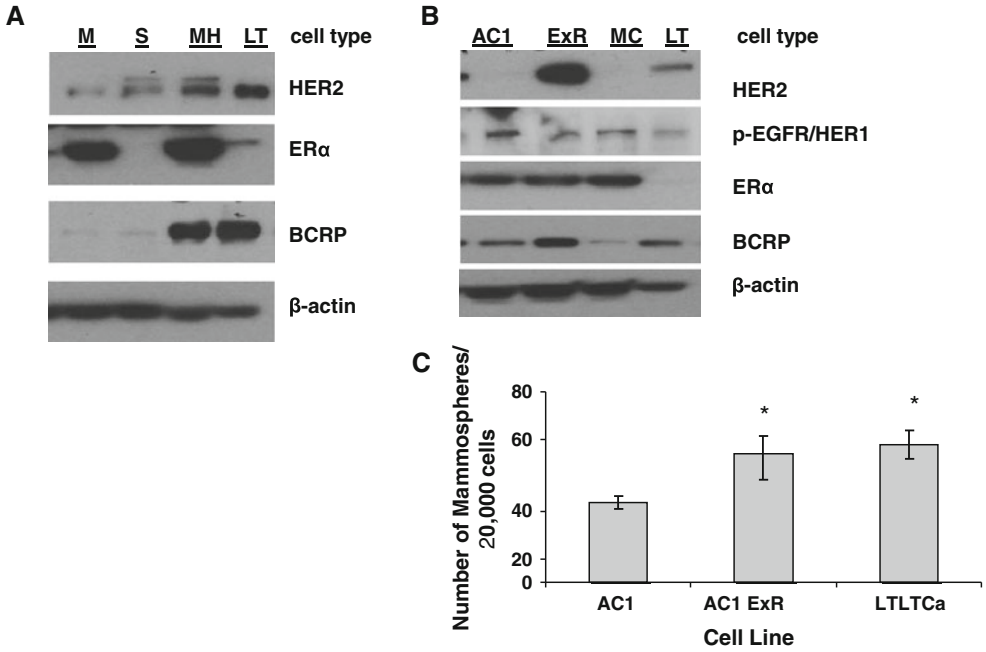

Fig. 6 Protein expression in HER2- and HER2+ cells and mammosphere formation in AC1-ExR cells. **a** MCF-7Ca (*MC*), SUM149 (*S*), MCF-7/HER2 (*MH*), and LTLT-Ca (*LT*) cells were plated in their respective passage media. Total protein was extracted and HER2, ERα, BCRP, and β-actin protein were analyzed by western blot. Representative blots ($n = 6$ independent cell samples/group) are shown. **b** AC1 (*AC1*), AC1-ExR (*ExR*), MCF-7Ca (*MC*), and LTLT-Ca (*LT*) cells were plated in their respective passage media. Total protein was extracted and HER2, phosphorylated EGFR/HER1 (p-EGFR/HER1), ERα, BCRP, and β-actin protein were analyzed by western blot. Representative blots ($n = 3$ samples/group) are shown. **c** AC1, AC1-ExR, and LTLT-Ca cells were resuspended and plated in mammosphere media onto ultra-low-attachment cell culture wells. After 8 days, formed mammospheres were counted. Results are expressed as number of mean mammospheres counted per 20,000 cells plated (mean ± SEM, $n = 3$ samples/group; *asterisk* vs. vehicle, $p < 0.05$ vs. AC1)

BIBX1382 and trastuzumab in combination (B + T). Cells were then subjected to western blot analyses to confirm efficacy and specificity of each treatment and to determine the effect of each on BCRP expression. Drug treatments affected HER2 and/or EGFR/HER1 expression and their downstream activation of MAPK (evidenced by p-ERK1/2) as expected: only cells treated with trastuzumab reduced HER2 protein expression; none affected EGFR/HER1 expression; and all decreased p-ERK1/2 protein expression with lapatinib alone and B + T having the greatest effects (Fig. 7a). Lapatinib and B + T were also the most effective treatments for reducing PI3K/Akt kinase pathway activation (as evidenced by p-Akt protein) and BCRP protein expression (Fig. 7a), consistent with other studies [20], RT-PCR analyses further showed that lapatinib's inhibitory effects on BCRP expression also occurred at the mRNA level and regardless of letrozole treatment (Fig. 7b).

Third, HER2 and BCRP upregulation occurred concurrently and before tumors became resistant to letrozole's growth inhibitory effects. Our previous studies have demonstrated that letrozole-treated MCF-7Ca xenografts acquire resistance to letrozole after 16–18 weeks of letrozole treatment [24]. This is preceded by upregulation of HER2 protein expression in tumors beginning at ~4 weeks of letrozole treatment [24]. In this current study, analysis of tumor samples acquired after 4 and 14 weeks of control treatment (Δ4A) demonstrated that BCRP protein levels remained unchanged (Fig. 8) despite significant growth of the tumor at this time (data not shown). In contrast, 4 weeks of letrozole treatment increased BCRP expression by 1.9- (not normalized) or 4.9-fold (normalized) compared control-treated tumors. BCRP expression increased even more compared to control after 8 and 24 weeks (3.5 or 4.9-fold and 3.7 or 4.1-fold vs. 4 weeks of control, respectively). Altogether, in vitro and in vivo results of this current study support a role for HER2, as well as EGFR/HER1 in the regulation of BCRP expression in LTLT-Ca cells.

Discussion

It has been previously established that resistance of ERα+ breast cancer cells to AIs involves a switch from ERα-dependent growth to growth factor-dependent growth [2, 3, 24, 39]. Particularly, in letrozole- and exemestane-resistant breast cancers, this switch involves overexpression of HER2 (Figs. 2, 7). How HER2 contributes to resistance to AIs, however, was unknown.

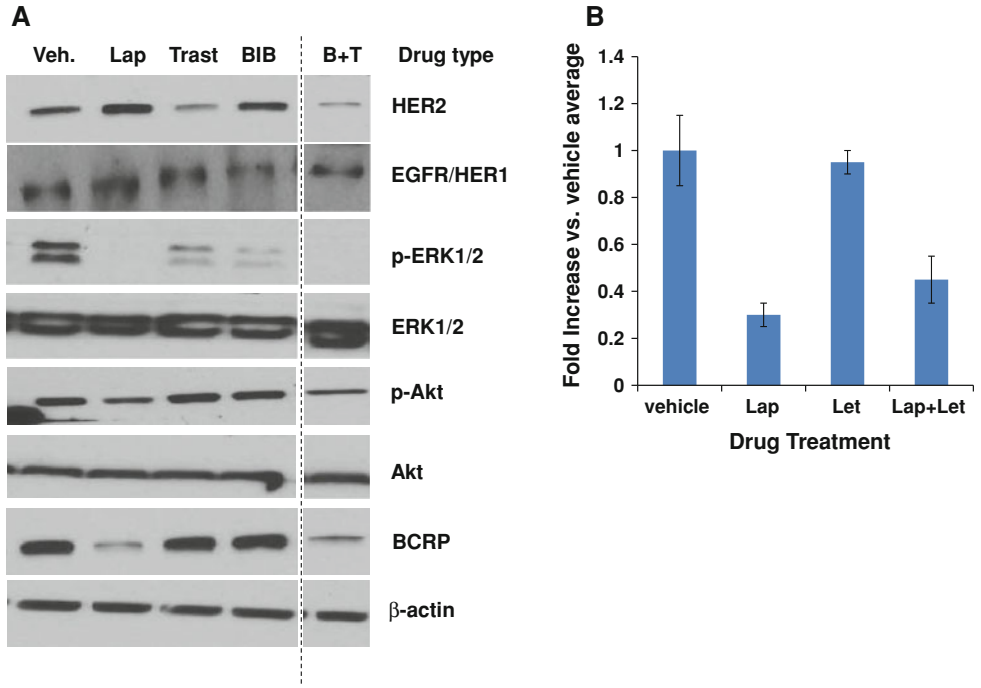

Fig. 7 Effect of HER2 and EGFR inhibitors on protein and/or mRNA expression in LTLT-Ca cells. **a** LTLT-Ca cells were treated for 24 h with either vehicle (*Veh*), 1 μM lapatinib, 500 μg/mL trastuzumab (*Trast*), 100 nM BIBX 1382 (*BIB*), or BIBX 1382 and trastuzumab in combination (*B* + *T*). Total protein was extracted and HER2, EGFR/HER1, phosphorylated- (p-ERK1/2) and total-ERK1/2, phosphorylated- and total-Akt, BCRP, and *β*-actin were analyzed by western blot ($n = 3$ independent cell samples/group). Representative blots are shown. *Dashed line* indicates omitted lane in between BIB and B + T lanes of the same blots. **b** LTLT-Ca cells were treated with either DMSO/ethanol vehicle or 1 μM lapatinib and/or 1 μM letrozole or 24 h. Total RNA was extracted and BCRP mRNA and 18S rRNA were analyzed by real-time RT-PCR analysis. Real-time results are expressed as the fold-change in mRNA levels compared with vehicle after normalization to 18S rRNA (mean ± SEM, $n = 6$ samples/group)

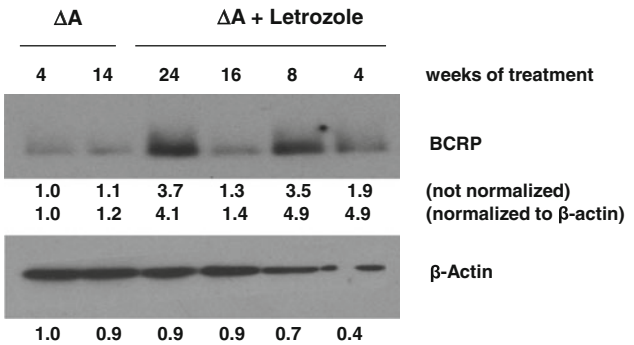

Fig. 8 Protein expression in xenograft MCF-7Ca tumors. Xenografts of MCF-7Ca cells were grown in mice as described in the Materials and Methods. After the tumors reached 300 mm^3, mice were treated with either control (100 μg/day Δ4A) or letrozole (100 μg/day Δ4A + 10 μg/day letrozole). At various pre-designated times or when the tumors reached 2,000 mm^3, tumors were collected at necropsy and BCRP and *β*-actin protein expression was analyzed by western blot

One possibility explored in this study is that HER2 confers resistance by regulating stem cell markers that, in turn, increase TICs within the overall cancer cell population. TICs have been linked to tumor relapse, metastasis, and resistance to chemotherapy in several cancer types, including breast cancer [40]. However, their role in endocrine therapy resistance, particularly AI resistance, has not been well studied. Dubrovska et al. [41] has recently demonstrated that tamoxifen-resistant cells have higher BCRP and ALDH expression, and higher clonogenic potential and tumourigenicity in vivo compared to tamoxifen-sensitive MCF7 cells. Our current study provides support for the relevance of TICs in AI resistance. LTLT-Ca and/or AC1-ExR cells exhibited higher levels of TIC characteristics, including expression of known stem cell markers, than their AI-sensitive parental cell lines (Figs. 1, 2, 3, 6).

Expression of stem cell marker and drug efflux transporter BCRP [42] in letrozole and exemestane-resistant cells is of notable significance. LTLT-Ca cells expressed higher BCRP levels and SP percentage compared to letrozole-sensitive MCF-7Ca cells, and inhibition of BCRP function decreased LTLT-Ca cell mammosphere formation and SP % (Figs. 2, 3). While non-TIC cells can also express BCRP and be designated as SP cells, these characteristics tend to be enriched in the TIC subpopulation [43, 44]. Thus, acquired resistance to letrozole or

exemestane may occur via increased effluxing of these AIs out of breast cancer cells, particularly TICs, and via increased presence of TICs in general.

Increased TICs and BCRP in AI-resistant cells appear to be regulated by HER2, as well as EGFR1/HER1. This is consistent with studies demonstrating EGFR/HER1 and/or HER2 overexpression in tamoxifen-resistant and long-term estrogen-deprived cells, as well as in breast TICs [40]. Patients with EGFR1/HER1- and HER2-overexpression tumors also have poorer clinical outcomes with tamoxifen treatment [36]. EGFR/HER1's role in AI-resistant breast cancer, however, appears to be secondary to that of HER2 and/or only in association with HER2 via dimerization. Its expression and activation was not consistently associated with letrozole- or exemestane-resistance or with BCRP expression (Fig. 6). Nevertheless, it cannot be ruled out that EGFR/HER1 may independently regulate stem cell markers and other TIC characteristics in AI-resistant cells not investigated in this study.

Taken together, the results of this study suggest that reducing or eliminating the TIC subpopulation with agents that target BCRP, HER2, EGFR/HER1, and/or their downstream kinase pathways (i.e., MAPK and PI3K/Akt pathways) could be effective in preventing and/or treating acquired AI resistance. Clinical studies have shown that treating patients with AIs in combination with either lapatinib or trastuzumab [45–47], or gefitinib (an EGFR tyrosine kinase inhibitor) [48] resulted in better clinical outcomes than treating with AIs alone. The number of such clinical studies are limited, however, and even fewer have directly compared these drugs to each other. One study has shown that trastuzumab combined with neoadjuvant anthracycline-taxane-based chemotherapy elicits a better pathological response in untreated ER-/HER2+ breast cancer patients than lapatinib combined with chemotherapy [49]. However, results of our current study suggests that the dual EGFR/HER1-HER2 kinase inhibitor lapatinib may be more effective than either HER2-specific trastuzumab or EGFR-specific gefitinib, or in treating ER+ breast cancer patients that have relapsed from AI treatment.

Acknowledgments This research was supported in part by RO1 CA 62483 and a Komen Scholars award to Angela Brodie. The authors would like to thank Dr Ferenc Livak for his help with flow cytometry.

Conflict of interest The authors declare that they have no conflict of interest.

References

1. Chumsri S, Howes T, Bao T, Sabnis G, Brodie A (2011) Aromatase, aromatase inhibitors, and breast cancer. J Steroid Biochem Mol Biol 125(1–2): 13–22. doi:10.1016/j.jsbmb.2011.02.001
2. Johnston SR, Martin LA, Leary A, Head J, Dowsett M (2007) Clinical strategies for rationale combinations of aromatase inhibitors with novel therapies for breast cancer. J Steroid Biochem Mol Biol 106(1–5):180–186. doi:10.1016/j.jsbmb.2007.05.019
3. Sabnis G, Brodie A (2011) Adaptive changes results in activation of alternate signaling pathways and resistance to aromatase inhibitor resistance. Mol Cell Endocrinol 340(2):142–147. doi:10.1016/j.mce.2010.09.005
4. Macedo LF, Sabnis GJ, Goloubeva OG, Brodie A (2008) Combination of anastrozole with fulvestrant in the intratumoral aromatase xenograft model. Cancer Res 68(9): 3516–3522. doi:10.1158/0008-5472.CAN-07-6807
5. Magnifico A, Albano L, Campaner S, Delia D, Castiglioni F, Gasparini P, Sozzi G, Fontanella E, Menard S, Tagliabue E (2009) Tumor-initiating cells of HER2-positive carcinoma cell lines express the highest oncoprotein levels and are sensitive to trastuzumab. Clin Cancer Res 15(6):2010–2021. doi:10.1158/1078-0432.CCR-08-1327
6. Nakanishi T, Chumsri S, Khakpour N, Brodie AH, Leyland-Jones B, Hamburger AW, Ross DD, Burger AM (2010) Side-population cells in luminal-type breast cancer have tumour-initiating cell properties, and are regulated by HER2 expression and signalling. Br J Cancer 102(5):815–826. doi:10.1038/sj.bjc.6605553
7. Creighton CJ, Li X, Landis M, Dixon JM, Neumeister VM, Sjolund A, Rimm DL, Wong H, Rodriguez A, Herschkowitz JI, Fan C, Zhang X, He X, Pavlick A, Gutierrez MC, Renshaw L, Larionov AA, Faratian D, Hilsenbeck SG, Perou CM, Lewis MT, Rosen JM, Chang JC (2009) Residual breast cancers after conventional therapy display mesenchymal as well as tumor-initiating features. Proc Natl Acad Sci USA 106(33):13820–13825. doi:10.1073/pnas.0905718106
8. Phillips TM, McBride WH, Pajonk F (2006) The response of CD24(−/low)/CD44+ breast cancer-initiating cells to radiation. J Natl Cancer Inst 98(24):1777–1785. doi:10.1093/jnci/djj495
9. Li X, Lewis MT, Huang J, Gutierrez C, Osborne CK, Wu MF, Hilsenbeck SG, Pavlick A, Zhang X, Chamness GC, Wong H, Rosen J, Chang JC (2008) Intrinsic resistance of tumorigenic breast cancer cells to chemotherapy. J Natl Cancer Inst 100(9):672–679. doi:10.1093/jnci/djn123
10. Nicolini A, Ferrari P, Fini M, Borsari V, Fallahi P, Antonelli A, Berti P, Carpi A, Miccoli P (2011) Stem cells: their role in breast cancer development and resistance to treatment. Curr Pharm Biotechnol 12(2):196–205
11. van Rhenen A, Feller N, Kelder A, Westra AH, Rombouts E, Zweegman S, van der Pol MA, Waisfisz Q, Ossenkoppele GJ, Schuurhuis GJ (2005) High stem cell frequency in acute myeloid leukemia at diagnosis predicts high minimal residual disease and poor survival. Clin Cancer Res 11(18):6520–6527. doi:10.1158/1078-0432.CCR-05-0468
12. Al-Hajj M, Becker MW, Wicha M, Weissman I, Clarke MF (2004) Therapeutic implications of cancer stem cells. Curr Opin Genet Dev 14(1):43–47. doi:10.1016/j.gde.2003.11.007
13. Mehta K (1994) High levels of transglutaminase expression in doxorubicin-resistant human breast carcinoma cells. Int J Cancer 58(3):400–406
14. Calcagno AM, Salcido CD, Gillet JP, Wu CP, Fostel JM, Mumau MD, Gottesman MM, Varticovski L, Ambudkar SV (2010) Prolonged drug selection of breast cancer cells and enrichment of cancer stem cell characteristics. J Natl Cancer Inst 102(21): 1637–1652. doi:10.1093/jnci/djq361
15. Dontu G, Al-Hajj M, Abdallah WM, Clarke MF, Wicha MS (2003) Stem cells in normal breast development and breast cancer. Cell Prolif 36(Suppl 1):59–72
16. Doyle LA, Ross DD (2003) Multidrug resistance mediated by the breast cancer resistance protein BCRP (ABCG2). Oncogene 22(47):7340–7358. doi:10.1038/sj.onc.1206938

17. Liu H, Cheng D, Weichel AK, Osipo C, Wing LK, Chen B, Louis TE, Jordan VC (2006) Cooperative effect of gefitinib and fumitremorgin c on cell growth and chemosensitivity in estrogen receptor alpha negative fulvestrant-resistant MCF-7 cells. Int J Oncol 29(5):1237–1246
18. Meyer zu Schwabedissen HE, Grube M, Dreisbach A, Jedlitschky G, Meissner K, Linnemann K, Fusch C, Ritter CA, Volker U, Kroemer HK (2006) Epidermal growth factor-mediated activation of the map kinase cascade results in altered expression and function of ABCG2 (BCRP). Drug Metab Dispos 34(4):524–533. doi:10.1124/dmd.105.007591
19. Zhang W, Ding W, Chen Y, Feng M, Ouyang Y, Yu Y, He Z (2011) Up-regulation of breast cancer resistance protein plays a role in HER2-mediated chemoresistance through PI3K/Akt and nuclear factor-kappa B signaling pathways in MCF7 breast cancer cells. Acta Biochim Biophys Sin (Shanghai) 43(8):647–653. doi:10.1093/abbs/gmr050
20. Perry J, Ghazaly E, Kitromilidou C, McGrowder EH, Joel S, Powles T (2010) A synergistic interaction between lapatinib and chemotherapy agents in a panel of cell lines is due to the inhibition of the efflux pump BCRP. Mol Cancer Ther 9(12): 3322–3329. doi:10.1158/1535-7163.MCT-10-0197
21. Wang H, Zhou L, Gupta A, Vethanayagam RR, Zhang Y, Unadkat JD, Mao Q (2006) Regulation of BCRP/ABCG2 expression by progesterone and 17beta-estradiol in human placental BeWo cells. Am J Physiol Endocrinol Metab 290(5):E798–E807. doi:10.1152/ajpendo.00397.2005
22. Zhang Y, Zhou G, Wang H, Zhang X, Wei F, Cai Y, Yin D (2006) Transcriptional upregulation of breast cancer resistance protein by 17beta-estradiol in ERalpha-positive MCF-7 breast cancer cells. Oncology 71(5–6):446–455. doi:10.1159/000108594
23. Goodell MA (2002) Multipotential stem cells and 'side population' cells. Cytotherapy 4(6):507–508. doi:10.1080/14653240276 1624638
24. Jelovac D, Sabnis G, Long BJ, Macedo L, Goloubeva OG, Brodie AM (2005) Activation of mitogen-activated protein kinase in xenografts and cells during prolonged treatment with aromatase inhibitor letrozole. Cancer Res 65(12):5380–5389. doi:10.1158/0008-5472.CAN-04-4502
25. Patrawala L, Calhoun T, Schneider-Broussard R, Zhou J, Claypool K, Tang DG (2005) Side population is enriched in tumorigenic, stem-like cancer cells, whereas ABCG2+ and ABCG2- cancer cells are similarly tumorigenic. Cancer Res 65(14):6207–6219. doi:10.1158/0008-5472.CAN-05-0592
26. Christgen M, Ballmaier M, Bruchhardt H, von Wasielewski R, Kreipe H, Lehmann U (2007) Identification of a distinct side population of cancer cells in the Cal-51 human breast carcinoma cell line. Mol Cell Biochem 306(1–2):201–212. doi:10.1007/s11010-007-9570-y
27. Goodell MA, Rosenzweig M, Kim H, Marks DF, DeMaria M, Paradis G, Grupp SA, Sieff CA, Mulligan RC, Johnson RP (1997) Dye efflux studies suggest that hematopoietic stem cells expressing low or undetectable levels of CD34 antigen exist in multiple species. Nat Med 3(12):1337–1345
28. Korkaya H, Paulson A, Iovino F, Wicha MS (2008) HER2 regulates the mammary stem/progenitor cell population driving tumorigenesis and invasion. Oncogene 27(47):6120–6130. doi:10.1038/onc.2008.207
29. Dontu G, Jackson KW, McNicholas E, Kawamura MJ, Abdallah WM, Wicha MS (2004) Role of notch signaling in cell-fate determination of human mammary stem/progenitor cells. Breast Cancer Res 6(6):R605–R615. doi:10.1186/bcr920
30. Calcagno AM, Salcido CD, Gillet JP, Wu CP, Fostel JM, Mumau MD, Gottesman MM, Varticovski L, Ambudkar SV (2010) Prolonged drug selection of breast cancer cells and enrichment of cancer stem cell characteristics. J Natl Cancer Inst 102(21):1637–1652. doi:10.1093/jnci/djq361
31. Jeter CR, Liu B, Liu X, Chen X, Liu C, Calhoun-Davis T, Repass J, Zaehres H, Shen JJ, Tang DG (2011) NANOG promotes cancer stem cell characteristics and prostate cancer resistance to androgen deprivation. Oncogene 30(36): 3833–3845. doi:10.1038/onc.2011.114
32. Liu S, Dontu G, Mantle ID, Patel S, Ahn NS, Jackson KW, Suri P, Wicha MS (2006) Hedgehog signaling and Bmi-1 regulate self-renewal of normal and malignant human mammary stem cells. Cancer Res 66(12):6063–6071. doi:10.1158/0008-5472.CAN-06-0054
33. Nakanishi T, Chumsri S, Khakpour N, Brodie AH, Leyland-Jones B, Hamburger AW, Ross DD, Burger AM (2010) Side-population cells in luminal-type breast cancer have tumour-initiating cell properties, and are regulated by HER2 expression and signalling. Br J Cancer 102(5):815–826. doi:10.1038/sj.bjc.6605553
34. Chen JS, Pardo FS, Wang-Rodriguez J, Chu TS, Lopez JP, Aguilera J, Altuna X, Weisman RA, Ongkeko WM (2006) EGFR regulates the side population in head and neck squamous cell carcinoma. Laryngoscope 116(3):401–406. doi:10.1097/01.mlg.0000195075.14093.fb
35. Ahn ER, Vogel CL (2012) Dual HER2-targeted approaches in HER2-positive breast cancer. Breast Cancer Res Treat 131(2): 371–383. doi:10.1007/s10549-011-1781-y
36. Saxena R, Dwivedi A (2012) ErbB family receptor inhibitors as therapeutic agents in breast cancer: current status and future clinical perspective. Med Res Rev 32(1): 166–215. doi:10.1002/med.20209
37. Solca FF, Baum A, Langkopf E, Dahmann G, Heider KH, Himmelsbach F, van Meel JC (2004) Inhibition of epidermal growth factor receptor activity by two pyrimidopyrimidine derivatives. J Pharmacol Exp Ther 311(2):502–509. doi:10.1124/jpet.104.069138
38. Allen JD, van Loevezijn A, Lakhai JM, van der Valk M, van Tellingen O, Reid G, Schellens JH, Koomen GJ, Schinkel AH (2002) Potent and specific inhibition of the breast cancer resistance protein multidrug transporter in vitro and in mouse intestine by a novel analogue of fumitremorgin C. Mol Cancer Ther 1(6):417–425
39. Masri S, Phung S, Wang X, Chen S (2010) Molecular characterization of aromatase inhibitor-resistant, tamoxifen-resistant and LTEDaro cell lines. J Steroid Biochem Mol Biol 118(4–5): 277–282. doi:10.1016/j.jsbmb.2009.10.011
40. O'Brien CS, Farnie G, Howell SJ, Clarke RB (2011) Breast cancer stem cells and their role in resistance to endocrine therapy. Horm Cancer 2(2):91–103. doi:10.1007/s12672-011-0066-6
41. Dubrovska A, Hartung A, Bouchez LC, Walker JR, Reddy VA, Cho CY, Schultz PG (2012) CXCR4 activation maintains a stem cell population in tamoxifen-resistant breast cancer cells through AhR signalling. Br J Cancer. doi:10.1038/bjc.2012.105
42. Konecny G, Pauletti G, Pegram M, Untch M, Dandekar S, Aguilar Z, Wilson C, Rong HM, Bauerfeind I, Felber M, Wang HJ, Beryt M, Seshadri R, Hepp H, Slamon DJ (2003) Quantitative association between HER-2/neu and steroid hormone receptors in hormone receptor-positive primary breast cancer. J Natl Cancer Inst 95(2):142–153
43. Hirschmann-Jax C, Foster AE, Wulf GG, Nuchtern JG, Jax TW, Gobel U, Goodell MA, Brenner MK (2004) A distinct "side population" of cells with high drug efflux capacity in human tumor cells. Proc Natl Acad Sci USA 101(39):14228–14233. doi:10.1073/pnas.0400067101
44. Natarajan K, Xie Y, Baer MR, Ross DD (2012) Role of breast cancer resistance protein (BCRP/ABCG2) in cancer drug resistance. Biochem Pharmacol 83(8): 1084–1103. doi:10.1016/j.bcp.2012.01.002

45. Johnston S, Pippen J Jr, Pivot X, Lichinitser M, Sadeghi S, Dieras V, Gomez HL, Romieu G, Manikhas A, Kennedy MJ, Press MF, Maltzman J, Florance A, O'Rourke L, Oliva C, Stein S, Pegram M (2009) Lapatinib combined with letrozole versus letrozole and placebo as first-line therapy for postmenopausal hormone receptor-positive metastatic breast cancer. J Clin Oncol 27(33):5538–5546. doi:10.1200/JCO.2009.23.3734
46. Fleeman N, Bagust A, Boland A, Dickson R, Dundar Y, Moonan M, Oyee J, Blundell M, Davis H, Armstrong A, Thorp N (2011) Lapatinib and trastuzumab in combination with an aromatase inhibitor for the first-line treatment of metastatic hormone receptor-positive breast cancer which over-expresses human epidermal growth factor 2 (HER2): a systematic review and economic analysis. Health Technol Assess 15(42):1–93, iii–iv. doi:10.3310/hta15420
47. Koeberle D, Ruhstaller T, Jost L, Pagani O, Zaman K, von Moos R, Oehlschlegel C, Crowe S, Pilop C, Thuerlimann B (2011) Combination of trastuzumab and letrozole after resistance to sequential trastuzumab and aromatase inhibitor monotherapies in patients with estrogen receptor-positive, HER-2-positive advanced breast cancer: a proof-of-concept trial (SAKK 23/03). Endocr Relat Cancer 18(2):257–264. doi:10.1530/ERC-10-0317
48. Cristofanilli M, Valero V, Mangalik A, Royce M, Rabinowitz I, Arena FP, Kroener JF, Curcio E, Watkins C, Bacus S, Cora EM, Anderson E, Magill PJ (2010) Phase II, randomized trial to compare anastrozole combined with gefitinib or placebo in postmenopausal women with hormone receptor-positive metastatic breast cancer. Clin Cancer Res 16(6):1904–1914. doi:10.1158/1078-0432.CCR-09-2282
49. Untch M, Loibl S, Bischoff J, Eidtmann H, Kaufmann M, Blohmer JU, Hilfrich J, Strumberg D, Fasching PA, Kreienberg R, Tesch H, Hanusch C, Gerber B, Rezai M, Jackisch C, Huober J, Kuhn T, Nekljudova V, von Minckwitz G (2012) Lapatinib versus trastuzumab in combination with neoadjuvant anthracycline-taxane-based chemotherapy (GeparQuinto, GBG 44): a randomised phase 3 trial. Lancet Oncol 13(2):135–144. doi:10.1016/S1470-2045(11)70397-7

Breast Cancer RESEARCH

RESEARCH ARTICLE Open Access

Nonhypoxic regulation and role of hypoxia-inducible factor 1 in aromatase inhibitor resistant breast cancer

Armina A Kazi[1,5], Rabia A Gilani[1], Amanda J Schech[1], Saranya Chumsri[2,3], Gauri Sabnis[1,3], Preeti Shah[1,3], Olga Goloubeva[3,4], Shari Kronsberg[4] and Angela H Brodie[1,3,6*]

Abstract

Introduction: Although aromatase inhibitors (AIs; for example, letrozole) are highly effective in treating estrogen receptor positive (ER+) breast cancer, a significant percentage of patients either do not respond to AIs or become resistant to them. Previous studies suggest that acquired resistance to AIs involves a switch from dependence on ER signaling to dependence on growth factor-mediated pathways, such as human epidermal growth factor receptor-2 (HER2). However, the role of HER2, and the identity of other relevant factors that may be used as biomarkers or therapeutic targets remain unknown. This study investigated the potential role of transcription factor hypoxia inducible factor 1 (HIF-1) in acquired AI resistance, and its regulation by HER2.

Methods: In vitro studies using AI (letrozole or exemestane)-resistant and AI-sensitive cells were conducted to investigate the regulation and role of HIF-1 in AI resistance. Western blot and RT-PCR analyses were conducted to compare protein and mRNA expression, respectively, of ERα, HER2, and HIF-1α (inducible HIF-1 subunit) in AI-resistant versus AI-sensitive cells. Similar expression analyses were also done, along with chromatin immunoprecipitation (ChIP), to identify previously known HIF-1 target genes, such as breast cancer resistance protein (BCRP), that may also play a role in AI resistance. Letrozole-resistant cells were treated with inhibitors to HER2, kinase pathways, and ERα to elucidate the regulation of HIF-1 and BCRP. Lastly, cells were treated with inhibitors or inducers of HIF-1α to determine its importance.

Results: Basal HIF-1α protein and BCRP mRNA and protein are higher in AI-resistant and HER2-transfected cells than in AI-sensitive, HER2- parental cells under nonhypoxic conditions. HIF-1α expression in AI-resistant cells is likely regulated by HER2 activated-phosphatidylinositide-3-kinase/Akt-protein kinase B/mammalian target of rapamycin (PI3K/Akt/mTOR) pathway, as its expression was inhibited by HER2 inhibitors and kinase pathway inhibitors. Inhibition or upregulation of HIF-1α affects breast cancer cell expression of BCRP; AI responsiveness; and expression of cancer stem cell characteristics, partially through BCRP.

Conclusions: One of the mechanisms of AI resistance may be through regulation of nonhypoxic HIF-1 target genes, such as *BCRP*, implicated in chemoresistance. Thus, HIF-1 should be explored further for its potential as a biomarker of and therapeutic target.

* Correspondence: abrodie@umaryland.edu
[1]Department of Pharmacology and Experimental Therapeutics, University of Maryland, Baltimore, MD 21201, USA
[3]School of Medicine, University of Maryland Marlene and Stewart Greenebaum Cancer Center, Baltimore, MD 21201, USA
Full list of author information is available at the end of the article

Introduction

Breast cancer is the most prevalent form of cancer among women in the United States and second leading cause of cancer related deaths [1]. Approximately 70% to 80% of breast cancers express estrogen receptor (ER+) and, consequently, are estrogen-dependent in their growth. Endocrine/hormonal therapies have proven effective in treating ER + breast cancers. Selective estrogen receptor modulators (SERMS), such as tamoxifen, inhibit estrogen action on breast cancer cells by blocking ER + signaling. Alternatively, aromatase inhibitors (AIs; for example, letrozole, anastrozole, and exemestane) reduce circulating levels of estrogen by inhibiting the conversion of androgens to estrogen by the enzyme aromatase [2,3]. Comparing the efficacy of tamoxifen versus AIs, a number of clinical studies have shown that AIs are superior in terms of disease free survival, time to recurrence and prevention of contralateral breast cancer [4,5]. In the adjuvant setting, AIs are less toxic with minimal adverse effects compared to chemotherapy and provide protection against development of contralateral breast cancer. AIs are now first-line treatments for ER + breast cancer in post-menopausal women [6]. However, a significant percentage (range 30% to 65%) of patients either does not respond to AIs [7] or becomes resistant to them [8-10].

Studies from this lab and others suggest that resistance to AIs occurs after a switch from dependence on ER signaling to dependence on growth factor-mediated pathways, such as human epidermal growth factor receptor-2 (HER2), a member of the membrane epidermal growth factor receptor (EGFR) family of receptor tyrosine kinases, and insulin-like growth factor receptor (IGFR) [9-11]. Pre-clinical [12] and clinical [10] studies have explored HER2 inhibitors, trastuzumab and lapatinib, as treatments for letrozole-resistant breast cancer. Preclinically, our laboratory has shown that trastuzumab alone or in combination with letrozole decreased HER2 expression, restored ERα expression, and inhibited tumor growth of MCF-7Ca xenografts that became resistant to letrozole [13]. Clinically, it has been shown that lapatinib in combination with letrozole significantly increased progression-free survival in patients versus letrozole alone as first-line therapy for hormone receptor- and HER2-positive postmenopausal metastatic breast cancer [10,14]. However, studies with *de novo* HER2+ breast cancer (that is, not HER2+ breast cancer of acquired AI resistance) indicate that resistance can develop to HER2 inhibitors as well [15,16]. Thus, although it has yet to be studied, there may be a risk of developing resistance to second-line HER2 inhibitor therapy in patients who have already acquired resistance to first-line AI therapy. As a membrane receptor, HER2 can affect many cellular pathways, some of which may not be directly involved in the development of AI resistance. Targeting another factor downstream of HER2 that more directly mediates effects specific and essential to the development of AI resistance may be as effective as targeting HER2 itself, while not having the same level of risk of producing second-line acquired resistance. Currently, the mechanism by which HER2 is involved in AI resistance remains unclear. It is, therefore, important to: 1) further elucidate the HER2-mediated pathway that contributes to AI resistance, particularly characteristics associated with AI resistant breast cancer cells; and 2) identify other potential factors involved that may serve as novel molecular biomarkers and therapeutic targets.

One factor that may be involved in HER2-mediated AI resistance is HIF-1, a heterodimeric transcription factor made up of an inducible alpha (α) subunit and a constitutively expressed beta (β) subunit [17]. HIF-1α is normally kept low in cells by proteosomal degradation, but lack of sufficient oxygen levels (hypoxia, for example, 1% to 2% O_2) prevents this degradation. This leads to increased intracellular HIF-1α protein levels, formation of HIF-1, and activation of HIF-1 target genes important for cell survival, metabolic adaptation and angiogenesis. Interestingly, HIF-1 expression and/or activation can also be regulated by growth factors, hormones and cytokines independent of O_2 levels. For example, ERα- and HIF-1-mediated signaling pathways are known to interact antagonistically [18,19] and cooperatively [20-23]. EGFR and HER2, as well as kinase signaling pathways, such as the MAPK and PI3K/Akt pathways, have also been shown to regulate HIF-1α expression and activity [22,24,25].

The role of hypoxia-regulated HIF-1 in cancer has been well studied. This is particularly relevant to sizable tumors whose cancer cells are too distant from existing blood vessels to get enough oxygen and nutrients [26]. Hypoxia and/or HIF-1 have been implicated in increased patient mortality and disease progression [27]. Their involvement in tumor formation and metastasis [28,29], and regulation of cancer stem cells [28,30] and stem cell markers, such as breast cancer resistant protein (BCRP) [27,30,31], has also been demonstrated. However, nonhypoxic regulation of HIF-1 and its importance in cancer remains largely unknown. Specific to this study, the regulation and role of nonhypoxic HIF-1 in breast cancer cell resistance to AIs, specifically letrozole, has yet to be explored. Using a letrozole-resistant cell line developed from xenograft tumors in our laboratory, this current study tested the overall hypothesis that nonhypoxic HIF-1 is an essential factor in HER2-mediated letrozole resistance. More specifically, in letrozole-responsive tumors, the switch from ERα to HER2-dependent signaling increases HIF-1α expression, independent of nutrient or oxygen availability. HIF-1 then acts as a key transcription factor activating target genes involved in processes that promote letrozole resistance.

Methods

Cells and reagents

Cell culture

Cell lines (and their ER/HER2 status) used are listed in Table 1. MCF-7Ca cells obtained from the laboratory of Dr. Chen through institutional agreement (City of Hope, Duarte, CA, USA) are MCF-7 cells stably transfected with the human placental aromatase gene [32,33]. Aromatase is the enzyme that converts androgens to estrogen. Transfection of the aromatase gene does not affect ER/HER2 status, ER activation, or estrogen-dependence of MCF-7 cells, but it does allow MCF-7 cells to proliferate in response to androgens (for example, androstenedione) and be sensitive to growth inhibitor effects of aromatase inhibitors [33]. MCF-7Ca cells were maintained in (D)MEM 1× high glucose (Invitrogen, Grand Island, NY) supplemented with 5% fetal bovine serum (FBS), 1% penicillin/streptomycin (P-S), and 700 μg/mL geneticin selective antibiotic (G418). Long-term letrozole-treated (LTLTCa) cells, developed in our laboratory [34], are letrozole-resistant breast cancer cells isolated from MCF-7Ca mouse xenograft tumors treated for 56 weeks with letrozole and that have become resistant to the growth inhibitory effects of letrozole. LTLTCa cells were maintained in phenol red–free (PRF) modified Improved Minimal Essential Media (IMEM) (Invitrogen, Grand Island, NY) supplemented with 5% charcoal dextran-treated FBS (CDT-FBS), 1% P-S, 750 μg/mL G418, and 1 μM letrozole. LTLTCa cells can be compared to MCF-7Ca cells in experiments since they originated from the MCF-7Ca cell population and their expression of ERα and HER2 returns to levels similar to that of MCF-7Ca cells after letrozole withdrawal [35]. MCF-7 cells obtained from American Type Culture Collection (ATCC) were maintained in (D)MEM 1× high glucose (Invitrogen, Grand Island, NY) supplemented with 5% FBS and 1% P-S. Hc7 cells were developed in our laboratory; they are MCF-7 cells transfected with the *HER2* gene and overexpress HER2 [36]. Hc7 cells were maintained in (D)MEM 1× high glucose (Invitrogen, Grand Island, NY) supplemented with 5% FBS, 1% P-S, and 500 μg/ml hygromycin. AC1 cells are another set of MCF-7 cells stably transfected with the human placental aromatase gene [37]. Similar to MCF-7Ca cells, AC1 cells are ER+/HER2-, proliferate in response to estrogen or androstenedione, express the aromatase enzyme and are sensitive to aromatase inhibitors [38]. AC1 cells, however, were created in our laboratory rather than Dr. Chen's, and they express higher levels of aromatase (data not shown). AC1 cells are maintained in (D)MEM 1x high glucose (Invitrogen, Grand Island, NY) supplemented with 5% FBS, 1% P-S, and 800 μg/mL G418. AC1-exemestane resistant (AC1-ExR) cells, developed in our laboratory, are exemestane-resistant cells isolated from AC1 mouse xenograft tumors treated for approximately 10 weeks with exemestane maintained in PRF modified IMEM (Invitrogen, Grand Island, NY) supplemented with 5% CDT-FBS, 1% P-S, 800 μg/mL G418, and 5 μM exemestane.

For experiments determining the effect of oxygen tension on protein expression, MCF-7Ca and LTLTCa cells were plated in passage media and incubated either under normal (20% O_2 at 37°C) or more physiological (5% O_2; using a hypoxia chamber) cell culture conditions for 24 hours. MCF-7 cells used to generate MC-7Ca and AC1 cells were obtained from the ATCC and, thus, did not require ethical approval or patient consent.

Table 1 ERα and HER2 status and aromatase inhibitor-sensitivity of cell lines used

Cell line	ERα status	HER2 status	AI-sensitivity
MCF-7Ca	+	-	Yes
LTLT-Ca	-	+	No (to letrozole)
MCF7	+	-	Yes
MCF7 / HER2	+	+	ND
AC1	+	-	Yes
AC1-Ex R	+	+	No (to exemestane)

ERα, estrogen receptor alpha; HER2, human epidermal growth factor receptor 2; ND: not determined.

Reagents

The following drugs were used: letrozole (Novartis, NY, USA); lapatinib (GlaxoSmithKline Pharmaceutical, Brentford, Middlesex, United Kingdom); trastuzumab (Genentech, San Francisco, CA); exemestane (Pfizer, NY, USA); cycloheximide (#C1988), actinomycin D (#A9415), and cobalt chloride ($CoCl_2$; #C8661) (all from Sigma, St. Louis, MO). The following antibodies were used in western blot analyses: HER2 (#04-1127) and BCRP (EMD Millipore, Billerica, MA); HIF-1α (#610959; BD Biosciences); ERα (#8644; Cell Signaling Technology, Danvers, MA); phosphorylated and total ERK1/2, Akt (#4058 and #4685), mTOR (#2971 and #2972) and p70 S6 kinase (#9205 and #9202) all from Cell signaling Technology, Danvers, MA); and β-actin (#4970; Cell Signaling Technology, Danvers, MA).

Western blot analysis

Plated cells were washed with ice-cold PBS and then lysed with radioimmunoprecipitation (RIPA) buffer containing protease (#11836145001) and phosphatase inhibitors (#4906837001) (both from Roche Applied Sciences, Indianapolis, IN) by sonication and incubation for 20 minutes at 4°C. Lysed samples were centrifuged at 14,000 rpm for 20 minutes at 4°C to collect protein lysates (supernatant). A total of 10 to 40 μg of protein underwent 10% SDS–polyacrylamide gel electrophoresis (SDS-PAGE) and was transferred to a polyvinylidene difluoride membrane (PVDF;

#IPVH00010 Millipore, Billerica, MA). The resulting blots were probed with specific mouse or rabbit primary antibodies and either goat anti-mouse or –rabbit secondary antibodies conjugated to horseradish peroxidase (#17 2–1011 and#172-1019; Biorad, Hercules, CA), respectively. Blots were developed using SuperSignal West Pico Chemiluminescent Substrate (#34080; Thermo Scientific, Waltham, MA). Blots that were to be re-probed were stripped with Restore Western Blot Stripping Buffer (#21059; Thermo Scientific, Waltham, MA) for 40 minutes at room temperature prior to incubation with another primary antibody. Densitometry was performed on each blot using either ImageQuant or ImageJ.

Reverse transcripase-polymerase chain rection

RNA extraction and reverse transcription (RT)

RNA was extracted and purified using the RNeasy Mini Kit (#74104; Qiagen, Valencia, CA). RNA was reverse transcribed to complementary DNA (cDNA) using 200U of Moloney murine leukemia virus reverse transcriptase (#28025013; Invitrogen, Grand Island, NY) and incubating at 37°C for one hour.

Real-time PCR

mRNA expression analyses were carried out by real-time PCR using a DNA Opticon system (MJ Research, Waltham, MA) and using DyNAmo SYBR green qPCR mix (New England Biolabs, Ipswich, MA). Standard curves were generated by serially diluting the sample expected to have the most amount of the PCR product. The yield of product for each unknown sample was calculated by applying its threshold cycle, or C(T), value to the standard curve using the Opticon Monitor analysis software (version 1.01, MJ Research, Waltham, MA). Values were normalized to corresponding 18S rRNA values and expressed as the fold increase relative to controls. Primers for HER2, HIF-1α, BCRP, GAPDH, BMI-1, Nanog and TWIST were obtained from (Sigma, St. Louis, MO or Qiagen Valencia, CA).

Chromatin immunoprecipitation assay

For the *in vitro* chromatin immunoprecipitation (ChIP) assay, the treated cells were washed with DPBS and fixed with 1% formaldehyde/dulbecco's phosphate buffered saline (DPBS) for 10 minutes at 37°C, after which the cells were washed with ice-cold DPBS containing protease inhibitors. The cells were collected into 1 mL DPBS and pelleted by centrifugation at 6,000 rpm for five minutes at 4°C. The cell pellet was resuspended in nuclear lysis buffer (ChIP kit, #17–295 Millipore, Billerica, MA) and incubated on ice for 15 minutes. Samples were sonicated on ice for 7 × 10-second cycles, with 20-second pauses between each cycle. The sonicated samples were centrifuged at 14,000 rpm for 10 minutes at 4°C. The sonicated samples were diluted 1:10 with dilution buffer (ChIP kit) before being immunocleared in a solution containing protein A- or G-Sepharose slurry (#16-156 and #16-266, respectively; Millipore, Billerica, MA) in Tris/ethylenediaminetetraacetic acid (EDTA) buffer, salmon sperm DNA (#15632011; Invitrogen, Grand Island, NY), and normal mouse or rabbit serum (#M5905 and #R9133; Sigma, St. Louis, MO) for two hours at 4°C. Immunocleared supernatants were incubated overnight at 4°C with anti-HIF-1α antibody (#610959; BD Biosciences). Protein A- or G-Sepharose beads and salmon sperm DNA were then added and incubated for one hour at 4°C. The beads were then washed sequentially with 1 mL each of wash buffers (ChIP kit). The protein-DNA complexes were eluted by twice incubating the beads in an elution buffer for 10 minutes at room temperature with vigorous mixing. To separate immunoprecipitated protein and DNA, the pooled elutes were incubated at 65°C overnight. The DNA was purified using the QIAquick PCR Purification kit (#28106; Qiagen Valencia, CA). The yield of target region DNA in each sample after ChIP was analyzed by real-time PCR using primers for a region of BCRP promoter that contains a HIF-1 response element (Invitrogen, Grand Island, NY) or a negative control open reading frame (ORF)-free intergenic region (ChIP-qPCR Human IGX1A Negative Control primers (#GPH100001C(–)01A, Qiagen, Valencia, CA).

Mammosphere assay

The mammosphere assay was performed using reagents from Stem Cell Technologies (Vancouver, CA), according to the manufacturer's instructions. Single cells were suspended in complete Mammocult media according to the manufacturer's instructions (#05620) and plated in ultra low attachment plates (#CLS3471; Corning, Tewksbury, MA) at a density of 10,000 to 20,000 cells/mL. Media were replenished every three days. Mammospheres were counted after at least seven days and up to three to four weeks. Spheres with a colony count of at least 50 cells were considered mammospheres.

Statistical analysis

All experiments were performed two to three times, with multiple replicates at each time point (total of n = 4 to 6 independent samples). Thus, quantified values are means of n = 4 to 6 independent samples/group with standard deviations (SD). Statistical analyses were performed using Graph Pad Prism software and included: 1) a two-sided t-test to compare two groups (for example, MCF-7Ca versus LTLTCa); 2) a

one-way analysis of variance (ANOVA) with Tukey's adjustment to compare three or more groups (for example, different treatment types, time points, and so on); and 3) a two-way ANOVA with Bonferroni adjustment (for example, different cell types and treatments or genes). For mRNA stability, the linear mixed-effects models approach was used. To assure approximate normality, the logarithmic transformation was applied to the normalized value of mRNA, that is, for each cell line, mRNA expression at each actinomycin D time point was normalized using the corresponding vehicle-treated samples. Average mRNA expressions were estimated and compared at the prespecified time-points (Additional file 1: Table S1.1 and Table S1.2), the trends over time were determined for HIF-α mRNA and BCRP mRNA. All required models' diagnostics were performed. There were fixed effects for time, experiment, cell lines and interactions between time and cell lines. The models had hierarchical structure as repeated measurements were taken within a well, nested within time, cell line, and experiment. The compound symmetry was chosen as appropriate to model the variance structure of the random effects. Statistical tests were two-sided. Analyses were conducted using SAS (v.9.22, SAS Inc., NC, USA). The alpha level applied in all statistical analyses was P <0.05.

Results

LTLTCa cells have higher HIF-1α protein expression than MCF-7Ca cells under nonhypoxic conditions

Previous studies have shown that a decrease in ERα and an increase in HER2 protein expression is associated with acquired AI-resistance [9-11], represented in this current study by LTLTCa cells. To determine whether HIF-1 expression is also associated with acquired AI-resistance, protein expression of the inducible HIF-1α subunit in LTLTCa and MCF-7Ca cells was determined. As expected, LTLTCa cells had 0.3 ± 0.02-fold ERα (P <0.0001); and 18.0 ± 5.5-fold HER2 (P = 0.002) protein levels compared to letrozole-sensitive parental MCF-7Ca cells under normal cell culture conditions (that is, nonhypoxic; 20% O_2) (Figure 1A). LTLTCa cells also had 15.7 ± 5.9–fold (versus 1.0 ± 1.4 MCF-7Ca at 20% O_2) higher basal levels of HIF-1α protein than their parental MCF-7Ca cells, which expressed little to no HIF-1α (Figure 1A).

Since oxygen levels in normal tissue [39,40], including the breast [26,41], range from 2% to 5%, and HIF-1α protein is known to be sensitive to O_2 levels [17], protein expression at 5% O_2 was also determined (Figure 1A). ERα and HER2 levels in both LTLTCa and MCF-7Ca cells remained unchanged when the percent O_2 was reduced to more physiological levels. HIF-1α expression, in contrast and as expected, increased in both

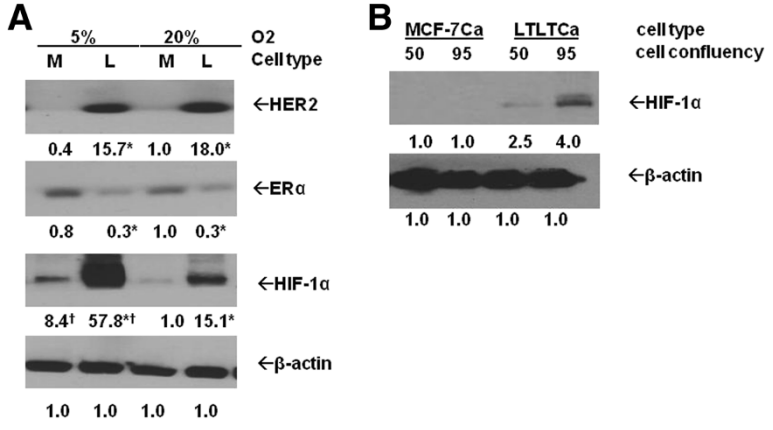

Figure 1 Comparison of protein expression in parental MCF-7Ca and LTLTCa cells under different oxygen tension and cell confluency. **A)** Parental MCF-7Ca and LTLTCa cells were plated and cultured in their respective passage media under either 5% O_2 (*in vivo* normoxic/physiological conditions) or 20% O_2 (normal, nonhypoxic cell culture conditions). Total protein was extracted and HER2, ERα, HIF-1α and β-actin were analyzed by Western blot analysis. Shown are representative blots and overall densitometry results of n = 6 independent cell samples/group. Densitometry results are expressed as mean fold-change in protein levels compared to MCF-7Ca cells in 20% O_2 after normalization to β-actin (mean ± SD of n = 6 independent cell samples/group; *versus MCF-7Ca and † versus 20% O_2; HER2 effect of cell type P = 0.0002, effect of % O_2 P = .5749, interaction between cell type and % O_2 P = .7337; ERα effect of cell type P <0.0001, effect of % O_2 P = .2879, interaction between cell type and% O_2 P = .2016; HIF-1α effect of cell type P = 0.0024, effect of % O_2 P = 0.0087, interaction between cell type and% O_2 P = 0.0413; two-way ANOVA). **B)** LTLTCa and parental MCF-7Ca cells were plated and cultured in their respective passage media at 1X or 2X density. Total protein was extracted when 2X density plates reached approximately 90% to 95% confluency, and, consequently, 1X density plates reached approximately 50% to 60% confluency. HIF-1α and β-actin protein were analyzed by Western blot. Densitometry results are expressed as mean fold-change compared to MCF-7Ca cells after normalization to β-actin. (mean ± SD, n = 6 independent cell samples/group; effect of cell confluency P = 0.0006, effect of cell type P < 0.0001, interaction between cell confluency and cell type P = 0.0006, two-way ANOVA). ANOVA, analysis of variance; ERα, estrogen receptor alpha; HER2, human epidermal growth factor receptor 2; HIF-1α, hypoxia inducible factor 1 α subunit; n, number; SD, standard deviation.

MCF-7Ca and LTLTCa cells (8.4 ± 3.1-fold and 57.8 ± 2.2-fold versus MCF-7Ca at 20% O_2, Figure 1A). Nevertheless the fold differences in HIF-1α expression between LTLTCa cells and MCF-7Ca persisted and were significant.

Lastly, since HIF-1α protein expression can also be affected by cell density/confluency [42,43], protein expression in LTLTCa and MCF-7Ca cells at both approximately 50% and 95% confluencies were also analyzed. LTLTCa cells had higher levels of HIF-1α protein than MCF-7Ca cells under nonhypoxic conditions at both cell densities (P <0.0001, Figure 1B). Furthermore, while MCF-7Ca cells still had little or no HIF-1α protein at 95% confluency, LTLTCa cells exhibited a significant increase in HIF-1α (P = 0.0006; Figure 1B). These results suggest that: 1) letrozole-resistant LTLTCa cells basally and inherently have higher HIF-1α protein expression than letrozole-sensitive MCF-7Ca cells regardless of O_2 levels or cell density; and 2) LTLTCa cells are more sensitive to inducers of HIF-1α expression, such as decreased O_2 levels and cell density/confluency.

HIF-1α expression in LTLTCa cells is due to increased protein synthesis

Elevated HIF-1α protein expression in cells can result from increased protein stability and/or synthesis [44]. In LTLTCa cells, higher levels of HIF-1α may be due to increased protein synthesis (for example, increased mRNA translation to protein) for several reasons. First, unlike HER2 and ERα mRNA, HIF-1α mRNA expression was not significantly different between LTLTCa cells and MCF-7Ca cells (Figure 2A). This rules out increased *HIF-1α* gene transcription as the basis for increased HIF-1α protein. Second, overall through 16 hours of actinomycin D treatment HIF-1α mRNA was not more stable in LTLTCa cells compared to MCF-7Ca cells (Figure 2B and Additional

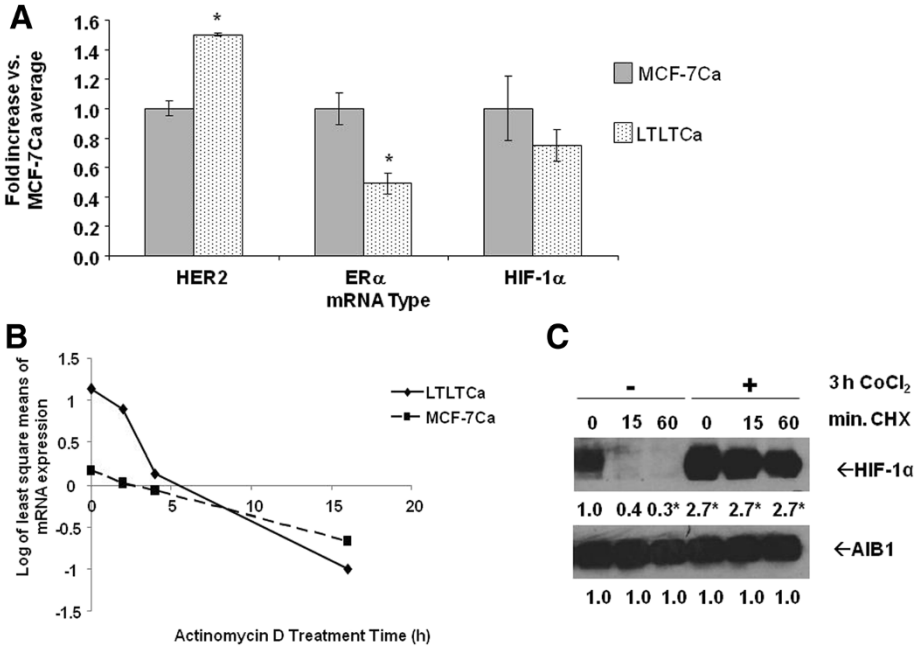

Figure 2 Comparison of HIF-1α mRNA expression and stability in LTLTCa and MCF-7Ca cells. A) LTLTCa and MCF-7Ca cells were plated and cultured in their respective passage media under normal cell culture (nonhypoxic) conditions. Total RNA was extracted and HER2, ERα, HIF-1α and 18S rRNA were analyzed by real-time RT-PCR analysis. Results shown are expressed as the mean fold-change in mRNA levels compared with MCF-7Ca cells after normalization to 18S rRNA (mean ± SD of n = 6 independent cell samples/group; *versus MCF-7Ca; effect of gene type P <0.0001, effect of cell type P = 0.1376, interaction between gene type and cell type P <0.0001; *MCF-7Ca versus LTLTCa for specific gene, P <0.0001; two-way ANOVA). **B)** LTLTCa and MCF-7Ca cells were treated with vehicle or 0.5 μg/ml actinomycin D for 0 to 16 hours. Total RNA was extracted and HIF-1α mRNA underwent real-time RT-PCR. Results are expressed as least square means of log transformed averages of mRNA expression at various timepoints (trend over time) after normalization to corresponding vehicle-treated samples and analysis by linear mixed effect model, adjusting for experiment, cell line and cell line*time interaction (means ± SD of n = 6 independent samples/group; P <0.001 for effect of cell line, time, their interaction and experiment). **C)** LTLTCa cells were treated with vehicle or 100 μM $CoCl_2$ for three hours and then with 100 uM cycloheximide for 0 to 60 minutes. Whole cell protein was extracted and underwent Western blot for HIF-1α and AIB1 protein. Shown are representative blots and overall densitometry results of n = 6 independent cell samples/group. Densitometry results are expressed as mean fold-change in protein levels compared to vehicle-treated-0 minutes cycloheximide cells after normalization to AIB1 (mean ± SD of n = 6 independent cell samples/group; *versus no $CoCl_2$-0 minutes CHX, P <0.0001, one-way ANOVA). ANOVA, analysis of variance; ERα, estrogen receptor alpha; HER2, human epidermal growth factor receptor 2; HIF-1α, hypoxia inducible factor 1 α subunit; n, number; SD, standard deviation.

file 1: Table S1.1). HIF-1α mRNA was more abundant in LTLTCa cells than MCF-7Ca cells prior to four hours of actinomycin D treatment, but it was less by sixteen hours (Figure 2B). Statistical analysis of HIF-1α mRNA expression over time in LTLTCa cells compared to MCF-7Ca cells showed significant effects of time, and cell line, and their interaction (P <0.001; linear mixed effect model of time regression analysis). Third, investigation of HIF-1α protein stability after treatment with the protein synthesis inhibitor cycloheximide with or without the HIF-1α protein stabilizer $CoCl_2$ [45], demonstrated that after addition of the protein synthesis inhibitor cycloheximide, HIF-1α protein in vehicle-treated LTLTCa cells rapidly degraded within 15 minutes (Figure 1C). In contrast, HIF-1α expression in $CoCl_2$-treated LTLTCa cells was elevated by 2.8 ± 0.0-fold compared to 1.0 ± 0.3-fold in vehicle-treated cells (P <0.0001), and did not decrease through 60 minutes of cycloheximide treatment (2- to 2.8-fold at each time point, P <0.001) (Figure 1C). These protein results are consistent with what is known about the rapid proteosomal degradation of HIF-1α protein in nonhypoxic cells [44], and the effect of $CoCl_2$ on HIF-1α protein stability [46]. These protein stability results further rule out increased protein stability as the basis for elevated HIF-1α levels in LTLTCa cells under nonhypoxic conditions.

HER2-activated PI3K/Akt/mTOR pathway regulates HIF-1α expression in LTLTCa cells

Since LTLTCa cells have significantly higher HER2 protein and mRNA expression compared to MCF-7Ca cells ([47], Figures 1A and 2A), this current study sought to determine whether endogenously overexpressed HER2 affects HIF-1α in LTLTCa cells. To do this, the effects of two types of HER2 inhibitors on HIF-1α were studied (Figure 3). Lapatinib is a HER2 kinase inhibitor that does not affect HER2 expression but does decrease HER2 activation of downstream kinase pathways (for example, MAPK, PI3K/Akt/mTOR pathway). Trastuzumab is a HER2 monoclonal antibody that decreases HER2 expression and its activation of downstream kinase pathways. As expected, only trastuzumab significantly reduced HER2 protein expression (0.4 ± 0.05 versus 1 ± 0.2 vehicle-treated), but both lapatinib and trastuzumab inhibited activation of the MAPK (0.2 ± 0.1-fold and 0.3 ± 0.01-fold,

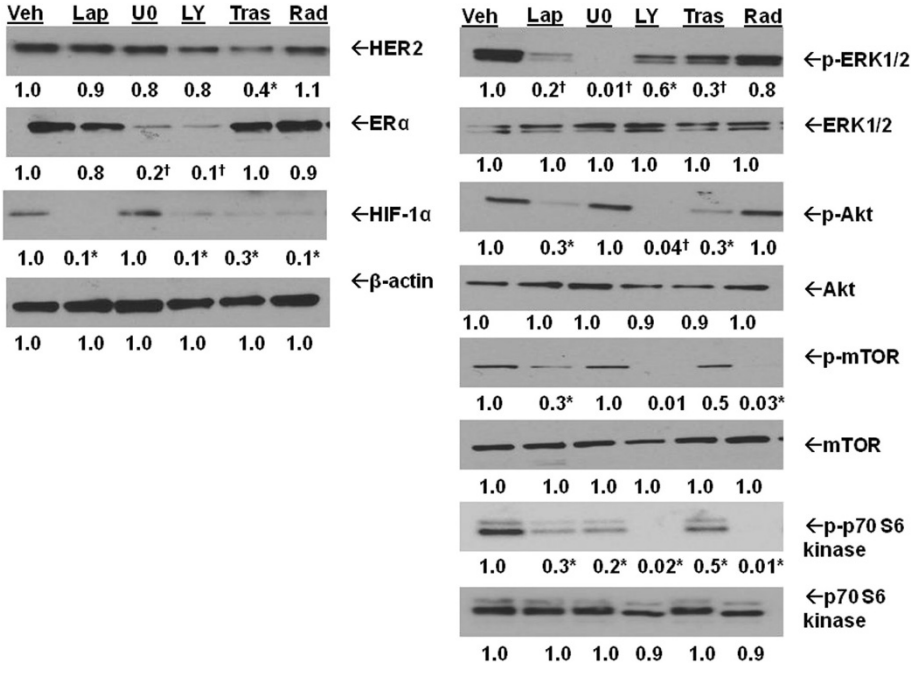

Figure 3 Regulation of HIF-1α protein in LTLTCa cells. A) LTLTCa cells were treated with either vehicle, 1 μM lapatinib, 20 μM MAPK pathway inhibitor U0126, 20 μM LY294002 PI3K pathway inhibitor, 500 μg/ml trastuzumab or 100 nM RAD001 for 24 hours. Total protein was extracted and HER2 (P = 0.128), phospho- and total-ERK1/2 (P <0.0001 for p-ERK), phospho- and total-Akt (P <0.0001 for p-Akt), phospho- and total mTOR (P = 0.0071), phospho- and total p70 S6 kinase (P <0.0001), ERα (P <0.0001), HIF-1α (P = 0.0003), and β-actin were analyzed by Western blot. Shown are representative blots and overall densitometry results of n = 6 independent cell samples/group. Densitometry results are expressed as mean fold-change in protein levels compared to vehicle-treated cells after normalization to β-actin (mean ± SD, n = 6 independent cell samples/group; *versus vehicle, P <0.05; † versus vehicle, P <0.001, one-way ANOVA). ANOVA, analysis of variance; ERα, estrogen receptor alpha; HER2, human epidermal growth factor receptor 2; HIF-1α, hypoxia inducible factor 1 α subunit; n, number; SD, standard deviation; mTOR, mammalian target of rapamycin.

respectively, versus 1 ± 0.2-fold vehicle-treated of p-ERK1/2, P <0.05) and PI3K/Akt pathways (0.2 ± 0.2-fold and 0.3 ± 0.08-fold versus 1 ± 0.09-fold vehicle of p-Akt, P <0.01) (Figure 3). Both inhibitors also significantly decreased HIF-1α protein expression in LTLTCa cells (0.2 ± 0.2-fold and 0.4 ± 0.2-fold, respectively, versus of 1 ± 0.1-fold vehicle-treated, P <0.001) (Figure 3).

Since both the MAPK and PI3K/Akt/mTOR pathways are activated by HER2 and known to regulate HIF-1α expression and activity [44,48,49], the effect of specific inhibition of each pathway on HIF-1α expression was also studied (Figure 3). As expected, the MAPK inhibitor U0126 effectively decreased p-ERK1/2 protein expression (0.01 ± 0.01-fold versus 1 ± 0.2-fold vehicle-treated, P <0.001), and the PI3K inhibitor LY294002 decreased p-Akt (0.01 ± 0.01-fold versus 1 ± 0.09-fold vehicle-treated), downstream Akt target p-mTOR (0.5 ± 0.2-fold versus 1 ± 0.2-fold vehicle-treated), downstream mTOR target p-70 S6 kinase (0.02 ± 0.02-fold versus 1 ± 0.1-fold vehicle-treated). Also as expected, the mTOR inhibitor Rad001 decreased phosphorylation of mTOR (0 ± 0.01 versus 1 ± 0.1-fold vehicle) and p70 S6 kinase (0.02 ± 0.02-fold versus 0.1 ± 0.1-fold vehicle) without affecting upstream Akt (Figure 3). HIF-1α protein expression was significantly decreased in LTLTCa cells with LY294002 (0.1 ± 0.1-fold versus 1 ± 0.1-fold vehicle-treated) and Rad001 (0.1 ± 0.06-fold versus 1 ± 0.1-fold vehicle-treated), but not by U0126. Overall, these results indicate that HER2 activation of the PI3K/Akt/mTOR pathway induces HIF-1α expression. They also suggest that the HER2-activated MAPK pathway in LTLTCa cells has distinct functions from that of the PI3K/Akt/mTOR pathway.

HIF-1α involvement in HER2 regulation of BCRP expression

As a transcription factor, HIF-1 may be mediating the effects of HER2 on target genes that contribute to the LTLTCa cell phenotype. One such gene may be the breast cancer resistance protein (*BCRP*), an efflux

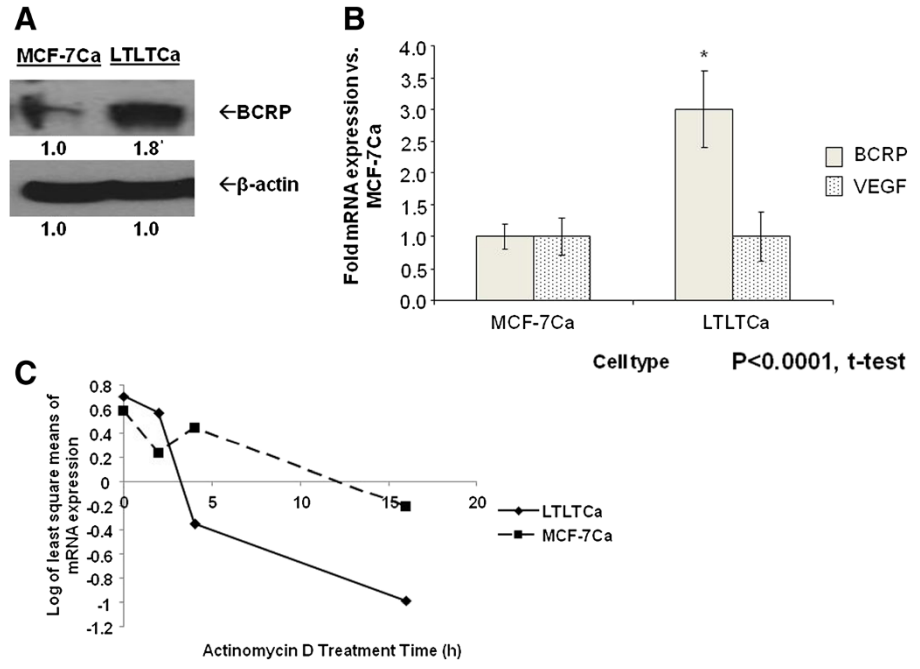

Figure 4 Comparison of BCRP protein and mRNA expression and stability in LTLTCa and MCF-7Ca cells. LTLTCa and parental MCF-7Ca cells were plated and cultured in their respective passage media under normal cell culture (nonhypoxic) conditions. **A)** Total protein was extracted and BCRP and β-actin were analyzed by Western blot analysis. Densitometry results are expressed as fold-change in protein levels compared to MCF-7Ca cells after normalization to β-actin (mean ± SD, n = 6 independent cell samples/group; *versus MCF-7Ca, P <0.0001, two-sided t test). **B)** Total RNA was extracted and BCRP mRNA, VEGF mRNA and 18S rRNA were analyzed by real-time RT-PCR analysis. Results are expressed as the fold-change in mRNA levels compared with MCF-7Ca cells after normalization to 18S rRNA (mean ± SD, n = 6 independent cell samples/group; *versus MCF-7Ca, P <0.0001, two-tailed t-test). **C)** LTLTCa and MCF-7Ca cells were treated with vehicle or 0.5 μg/ml actinomycin D for 0 to 16 hours. Total RNA was extracted and BCRP mRNA was analyzed by real-time RT-PCR. Results are expressed as least square means of log transformed averages of mRNA expression at various timepoints (trend over time) after normalization to corresponding vehicle-treated samples, and analysis by linear mixed effect model adjusting for experiment, cell line, and cell line*time interaction (mean ± SD of n = 6 independent cell samples/group; *versus MCF-7Ca; effect of gene type P = 0.0025, effect of cell type P = .3749, interaction between gene type and cell type P = 0.0025; two-way ANOVA). ANOVA, analysis of variance; BCRP, breast cancer resistant protein; n, number; SD, standard deviation; VEGF, vascular endothelial growth factor.

transporter protein and stem cell marker implicated in cancer cell chemoresistance [50,51]. *BCRP* is also known to be a HIF-1 target gene [31]. Recently, findings from our laboratory have shown that BCRP protein is overexpressed in LTLTCa cells compared to MCF-7Ca cells and that BCRP is important in stem cell characteristics of LTLTCa (for example, mammosphere formation, side population percentage) [52]. This current study confirms the overexpression of BCRP protein in LTLTCa cells, and further demonstrates that BCRP mRNA expression (3 ± 0.6-fold versus 1 ± 0.2-fold vehicle-treated, P <0.0001, one-way ANOVA) is also elevated compared to MCF-7Ca cells (Figure 4A-B). BCRP mRNA stability was also compared between the two cell types. Consistent with findings of others in MCF-7 cells [53], BCRP mRNA is fairly stable through 16 hours of actinomycin D treatment in MCF-7Ca cells (Figure 2C). Overall, BCRP mRNA in LTLTCa cells was not significantly more stable than in MCF-7Ca (Figure 4C). Statistical analysis of BCRP mRNA expression over time in LTLTCa cells compared to MCF-7Ca cells showed significant effects of time, but not cell line (effect of time $P < 0.001$; effect of cell line at $P = 0.049$; linear mixed effect model of time regression analysis). Thus, overexpression of BCRP in LTLTCa cells is attributed to increased synthesis at the gene transcription level.

In order to elucidate the factors and pathways involved in regulating BCRP expression, the effects of the HER2 kinase inhibitor lapatinib, HIF-1α stabilizer $CoCl_2$, and/or specific kinase pathway inhibitors U0126 (MAPK pathway) and LY294002 (PI3K/Akt pathway) on BCRP protein or mRNA expression were assessed (Figure 5A-B). Lapatinib reduced both BCRP protein (0.2-fold versus 1.0-fold vehicle, P <0.01) and mRNA (0.6 ± 0.2-fold versus 1.0

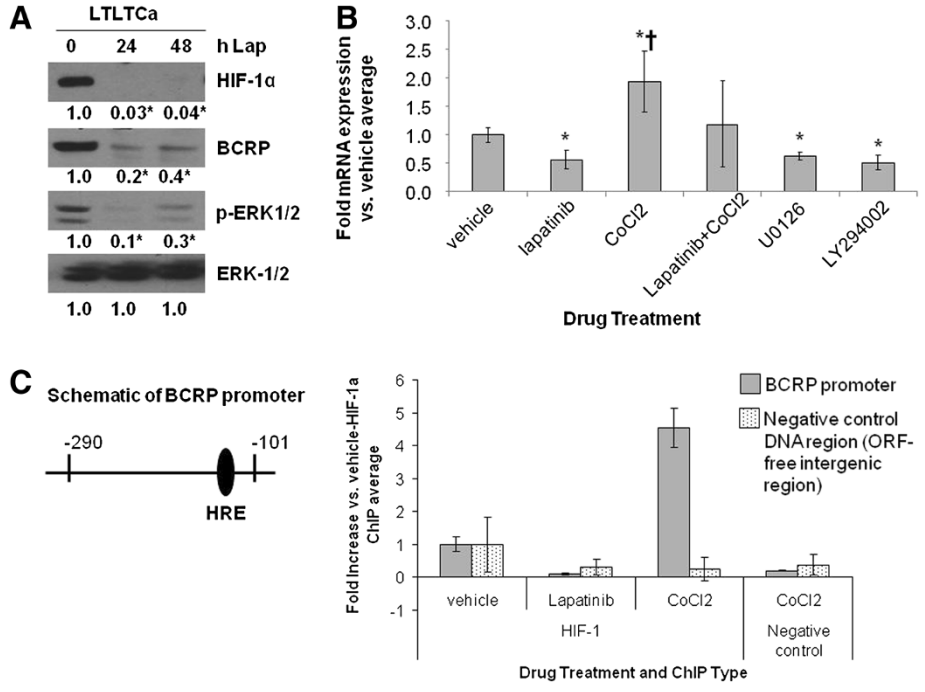

Figure 5 Effect of lapatinib and $CoCl_2$ on BCRP protein and mRNA expression and on HIF-1α binding to the BCRP promoter. A-B), A) LTLTCa cells were treated with 1 μM lapatinib for 0 to 48 hours. Total protein was extracted and underwent Western blot for HIF-1α, BCRP, p-ERK1/2, and ERK. Shown are representative blots and overall densitometry results of n = 6 independent cell samples/group. Densitometry results are expressed as mean fold-change compared to 0 hours after normalization to ERK (mean ± SD of n = 6 independent cell samples/group; *versus 0 hours lapatinib; $P = 0.0004$ for ERK for HIF-1α, $P = 0.0017$ for BCRP, $P = 0.0009$ for phospho-ERK1/2, $P = 1$ for ERK-1/2; one-way ANOVA). **B)** Total RNA was extracted and underwent real-time RT-PCR for BCRP mRNA and 18S rRNA. Real-time results are the mean fold-change in mRNA levels compared with vehicle after normalization to 18S rRNA (mean ± SD of n = 6 independent cell samples/group; *versus vehicle, P <0.05; † versus lapatinib, U0126 or LY294002, P <0.01; overall P <0.0001, one-way ANOVA). **C)** LTLTCa were treated with vehicle, 1 μM lapatinib, and/or 100 μM $CoCl_2$ for 24 hours. Protein-DNA complexes from LTLTCa cells were analyzed by ChIP analysis. Immunoprecipitation was done either with HIF-1α antibody or an equivalent volume of normal mouse serum (negative control). Primers for either the −290 to −101 region of the human BCRP promoter, which contains the HRE to which HIF-1 binds, or ORF-free intergenic region (negative control DNA region) were used for real-time PCR. Results are the mean fold increase compared with vehicle-treated cells after normalization to input samples of each (means ± SD, n = 6 independent cells sample/group; *versus vehicle-HIF-1 IP; $P = 0.004$ for BCRP promoter, $P = .2972$ for negative control ORF-free intergenic region; one-way ANOVA). ANOVA, analysis of variance; BCRP, breast cancer resistant protein; ChIP, chromatin immunoprecipitation; HIF-1α, hypoxia inducible factor 1 α subunit; n, number; SD, standard deviation.

± .0.02-fold vehicle-treated, P <0.01, one-way ANOVA) levels in LTLTCa cells. This decrease correlated with lapatinib's inhibitory effects on HIF-1α and p-ERK1/2 expression. Inhibition of either the MAPK or PI3K/Akt pathways also resulted in decreased BCRP mRNA levels (0.7 ± 0.05-fold and 0.55 ± 0.08-fold versus 1.0 ± .0.02 vehicle-treated, P <0.01, respectively; Figure 5B). $CoCl_2$ treatment conversely increased BCRP mRNA in LTLTCa cells. Co-treatment with lapatinib and $CoCl_2$ resulted in BCRP mRNA levels that tended to be intermediate of lapatinib-inhibited and $CoCl_2$-induced levels, but not significantly different from either one and from vehicle (Figure 5B).

Although results in Figure 5A-B suggested that HER2, via the MAPK and PI3K/Akt pathways, and HIF-1α are both involved in regulating BCRP expression in LTLTCa cells, these expression analyses did not test whether HIF-1α actually mediates the effects of HER2 on target genes. ChIP analysis was, therefore, performed to determine HIF-1α binding to the BCRP promoter under basal, non-hypoxic conditions and after lapatinib or $CoCl_2$ treatment. Real-time PCR analysis of immunoprecipitated DNA after ChIP showed that under basal, nonhypoxic conditions HIF-1α was bound to a hypoxia-response element (HRE)-containing region of the BCRP promoter in LTLTCa cells (Figure 5C). $CoCl_2$ significantly increased HIF-1α binding to the BCRP promoter, but lapatinib treatment prevented this binding (versus 1 ± 1.2-fold vehicle-treated, $P = 0.004$, one-way ANOVA). Specificity of immunoprecipitation was confirmed by the lack of immunoprecipitated DNA in the negative IP control samples, as well as on the negative control DNA ($P = 0.2972$, one-way ANOVA). In addition, samples in the BCRP promoter PCR (excluding input) amplified at cycles 20 to 30, while samples in the negative control DNA region PCR (excluding input) amplified at cycles 32 to 40. Correlation between HIF-1α binding to the BCRP promoter and changes in BCRP mRNA and protein expression in the absence or presence of lapatinib suggests that HER2-regulated HIF-1 is involved in *BCRP* gene expression in LTLTCa cells.

Such regulation, however, does not appear to be relevant to all known HIF-1 target genes. Vascular endothelial

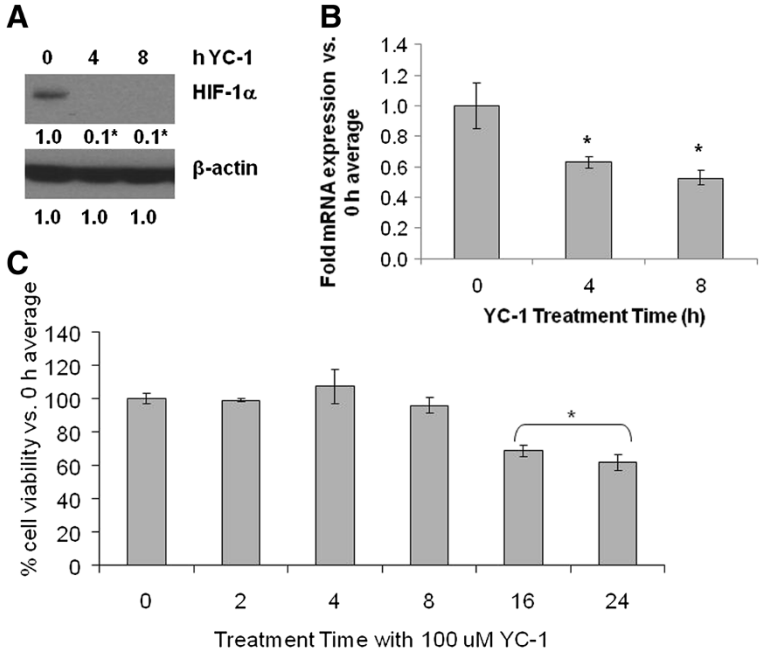

Figure 6 Effect of YC-1 on HIF-1α and BCRP expression and cell viability in LTLTCa cells. LTLTCa cells were treated with 100 μM YC-1 for 0 to 24 hours and effects on HIF-1α **(A)** and BCRP **(B)** expression and cell viability **(C)** were determined. **A)** After 0 to 4 hours of YC-1 treatment, total protein was extracted and HIF-1α and β-actin were analyzed by Western blot analysis. Shown are representative blots and overall densitometry results of n = 6 independent cell samples/group. Densitometry results are expressed as mean fold-change in protein levels compared to 0 hours after normalization to β-actin (mean ± SD of n = 6 independent cell samples/group; *versus 0 hours YC-1, P <0.001; overall P <0.0001, one-way ANOVA). **B)** After 0 to 8 hours YC-1 treatment, total RNA was extracted and BCRP mRNA and 18S rRNA were analyzed by real-time RT-PCR analysis. Real-time results are expressed as the mean fold-change in mRNA levels compared with vehicle after normalization to 18S rRNA (mean ± SD, n = 6 independent cell samples/group; *versus 0 hours YC-1, P <0.001; overall P <0.0001, one-way ANOVA). **C)** Viability of cells was measured by MTT assay after 0 to 24 hours treatment with YC-1. Results are expressed as mean percent of 0 hours average (mean ± SD, n = 4 independent cell samples/group; *versus 0 hours, P <0.001; overall P <0.0001, one-way ANOVA). ANOVA, analysis of variance; BCRP, breast cancer resistant protein; HIF-1α, hypoxia inducible factor 1 α subunit; MTT, 3-[4,5-dimethylthiazol-2-yl]-2,5 diphenyl tetrazolium bromide; n, number; SD, standard deviation.

growth factor (*VEGF*), another known HIF-1 target gene and important therapeutic target in cancer [17], is not upregulated in LTLTCa cells compared to MCF-7Ca cells (Figure 2B). Also, despite being induced by $CoCl_2$, VEGF mRNA expression was not sensitive to lapatinib (data not shown).

Effect of specific inhibition of HIF-1α on BCRP

To further support a connection between HIF-1α and BCRP, HIF-1α expression in LTLTCa cells was specifically inhibited by either YC-1, a known pharmacological inhibitor of HIF-1α [54,55] or siRNA. Similar to observations with lapatinib treatment, HIF-1α protein and BCRP mRNA expression were significantly decreased (0.1 ± 0.1-fold versus 0.1 ± 0.3-fold vehicle-treated and 0.5 ± 0.05-fold versus 1 ± 0.15-fold vehicle treated P <0.0001, respectively) in LTLTCa cells within eight hours of YC-1 treatment (Figure 6A-B). This correlated with a 30% to 40% decrease in LTLTCa cell viability by 16 and 24 hours, respectively (Figure 6C). Specific inhibition of HIF-1α expression by siRNAs also significantly decreased both HIF-1α mRNA (approximately 0.4 ± 0.04-fold versus 1 ± 0.2-fold negative control siRNA, P = 0.0057, one-way ANOVA) and protein (0.3 ± 0.1-fold to 0.03 ± 0.1-fold versus 1 ± 0.05-fold negative control, P <0.0001, one-way ANOVA), as well as BCRP mRNA (0.4- to 0.6-fold versus 1 ± 0.2-fold negative control siRNA, P <0.0001, one-way ANOVA) expression after 48 hours (Figure 7A-B).

Correlation between HER2, HIF-1α, and BCRP in HER2-transfected cells and another AI-resistant cell line

To further confirm the role of HER2 in regulating HIF-1α and BCRP and to determine if ERα is also involved, protein expression in Hc7 cells, ERα + MCF-7 cells transfected with *HER2* gene was also studied. Similar to ERα-/HER2+ LTLTCa cells, Hc7 cells overexpressed phospho-ERK, HIF-1α and BCRP protein expression compared to ERα+/HER2-parental MCF-7 cells (Figure 8A). Furthermore, HER2 inhibition by lapatinib decreased HIF-1α protein levels in Hc7 cells (0.1 ± 0.1-fold versus vehicle, P <0.0001; Figure 8B). Interestingly, inhibition of ERα alone by the ERα antagonist ICI 182,780 also reduced HIF-1α levels, but its effect on the protein level was significantly less than that of lapatinib alone or lapatinib and ICI182,780 in combination (Figure 8C). Another AI-resistant cell line, exemestane-resistant AC1-ExR breast cancer cells, was also analyzed. Despite retaining ERα, AC1-ExR cells also showed higher HER2, HIF-1α and BCRP protein levels. Overall, these results further indicate that increased HER2 and HER2-activated kinase pathways correlate with increased HIF-1α. They also indicate that while ERα can play a role in regulating HIF-1, as has been suggested by other studies [22], HER2 is likely to be the more important factor in the cells studied.

Functional importance of HIF-1α in LTLTCa cells

Effect of HIF-1α inhibition on LTLTCa cells

Lastly, the functional importance of HIF-1 to the letrozole-resistant cell phenotype was explored. In cancer cells,

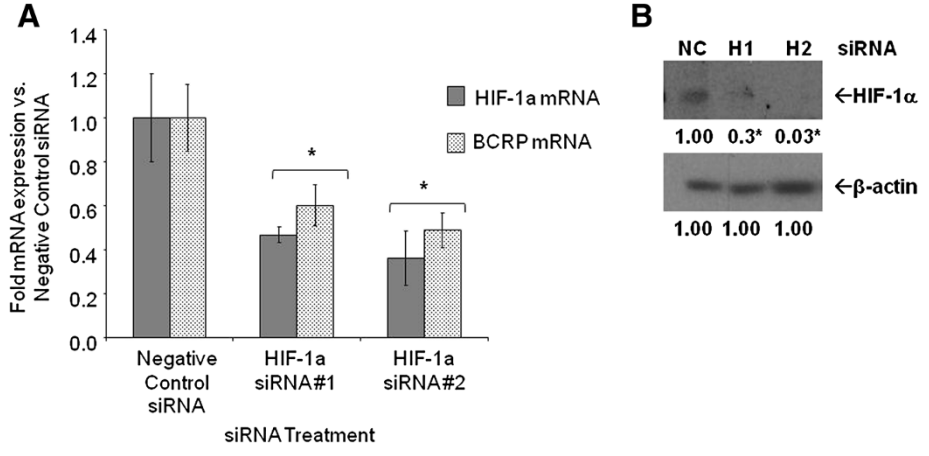

Figure 7 Effect of HIF-1α siRNA on mRNA expression in LTLTCa cells. A) LTLTCa cells were plated in passage media and then treated with two siRNAs for HIF-1α for 48 hours. Total mRNA was extracted and HIF-1α and BCRP mRNA, and 18S rRNA were analyzed by real-time RT-PCR. Real-time results are expressed as the mean fold-change in mRNA levels compared with negative control after normalization to 18S rRNA (mean ± SD, n = 6 independent samples/group; *versus negative control, P = 0.0057 for HIF-1α; P = 0.0026 for BCRP; one-way ANOVA). **B)** LTLTCa cells were plated in passage media and then treated with two siRNAs for HIF-1α for 48 hours. Total protein was extracted and HIF-1α and β-actin protein were analyzed by Western blot. Shown are representative blots and overall densitometry results of n = 6 independent cell samples/group. Densitometry results are expressed as mean fold-change in protein levels compared to negative control after normalization to β-actin (mean ± SD, n = 6 independent cell samples/group; *versus negative control (NC), P <0.0001, one-way ANOVA). ANOVA, analysis of variance; BCRP, breast cancer resistant protein; HIF-1α, hypoxia inducible factor 1 α subunit; n, number; SD, standard deviation.

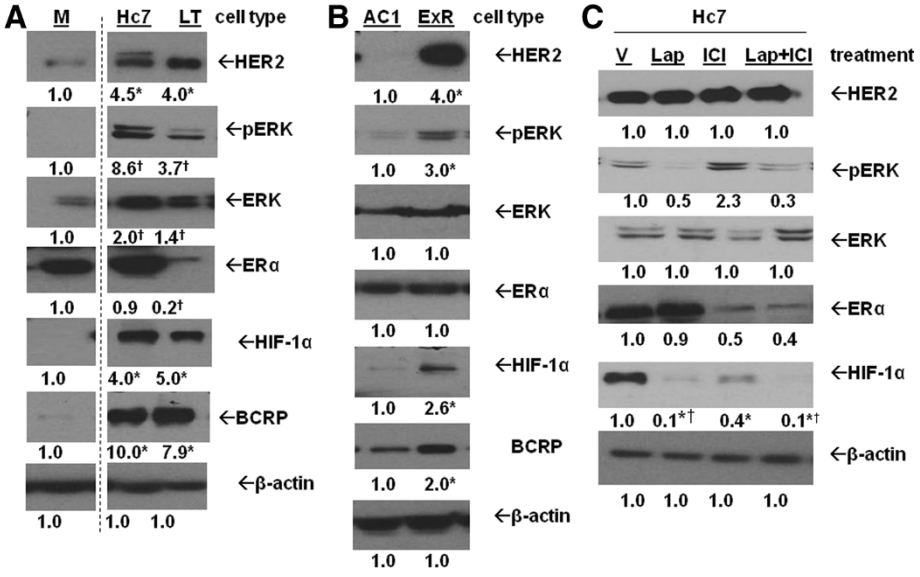

Figure 8 Protein expression in HER2+ cells and exemestane-resistant cells. A) MCF-7Ca (M), Hc7 and LTLTCa (LT) cells were plated in their respective passage media. Total protein was extracted and HER2, phosphorylated- and total-ERK, ERα, HIF-1α, BCRP and β-actin protein were analyzed by Western blot. Shown are representative blots and overall densitometry results of n = 6 independent cell samples/group. Densitometry results are expressed as mean fold-change compared to MCF-7Ca after normalization to ERK (mean ± SD of n = 6 independent cell samples/group; *versus MCF-7Ca, P <0.05; † versus MCF-7Ca, P <0.001, one-way ANOVA). Dashed lines indicate omitted lane in between M and Hc7 of the same blots. **B)** AC1 (AC1) and AC1-ExR (ExR) cells were plated in their respective passage media. Total protein was extracted and HER2, phosphorylated- and total-ERK, ERα, HIF-1α and β-actin protein were analyzed by Western blot. Shown are representative blots and overall densitometry results of n = 6 independent cell samples/group. Densitometry results are expressed as mean fold-change compared to vehicle-treated cells after normalization to β-actin (mean ± SD of n = 6 independent cell samples/group; *versus vehicle, P <0.0001, two-sided t-test). **C)** MCF-7/HER2 cells were treated with either vehicle (V), 1 μM lapatinib (Lap), 100 nM ICI 182,780 (ICI) or 1 μM lapatinib + 100 nM ICI 182,780 (Lap + ICI) for 24 hours. Total protein was extracted and HER2, phospho- and total-ERK1/2, ERα, HIF-1α and β-actin were analyzed by Western blot. Shown are representative blots and overall densitometry results of n = 6 independent cell samples/group. Densitometry results are expressed as mean fold-change compared to vehicle-treated cells after normalization to β-actin (mean ± SD of n = 6 independent cell samples/group; *versus vehicle, P <0.0001, one-way ANOVA). ANOVA, analysis of variance; BCRP, breast cancer resistant protein; ERα, estrogen receptor alpha; HER2, human epidermal growth factor receptor 2; HIF-1α, hypoxia inducible factor 1 α subunit; n, number; SD, standard deviation.

hypoxia and HIF-1 are known to be involved in increased cell survival, chemoresistance [56,57], resistance to apoptosis [58] and maintenance of cancer stem cell characteristics [59,60]. Previous findings from our laboratory [52] have already demonstrated that letrozole resistance and cancer stem cell characteristics of LTLTCa cells are reduced by inhibition of HER2 and/or BCRP. Although Gilani *et al.* did not specifically test for the involvement of HIF-1, results of this study combined with those of our current study demonstrating the HER2-HIF-1-BCRP pathway, supports a role for HIF-1 in determining the letrozole-resistant cell phenotype.

To determine the functional significance of HIF-1 in LTLTCa cells, the effect of specific inhibition of HIF-1α expression by siRNA on mammosphere formation and cell viability was analyzed (Figure 9). Consistent with our previous study [52], LTLTCa cells formed mammospheres (306 mammospheres/20,000 cells ± 5) (Figure 9B), and this was decreased by BCRP siRNA treatment (64 mammospheres/20,000 cells ± 9; P <0.001, one-way ANOVA). HIF-1α siRNA treatment similarly decreased mammosphere formation in LTLTCa cells (101 mammospheres/20,000 cells ± 18), while $CoCl_2$ increased formation (500 mammospheres/20,000 cells ± 20) compared to negative control-treated siRNA (P <0.001, one-way ANOVA). These results correlated with the effect of HIF-1α inhibition on other genes. HIF-1α siRNA treatment decreased BCRP mRNA (P = 0.0377, one-way ANOVA), as well as expression of GAPDH [61] (P = 0.0058, one-way ANOVA), another known HIF-1 target gene, and BMI-1 (P = 0.0214, one-way ANOVA), another stem cell marker [62] (Figure 9A). HIF-1α siRNA treatment also significantly decreased LTLTCa cell viability (P <0.0001, one-way ANOVA) in the presence of increasing concentrations of letrozole (Figure 9C).

Effect of HIF-1α upregulation on MCF-7Ca cells

To further confirm the physiological role of HIF-1 and BCRP, converse experiments were done to investigate whether MCF-7Ca cells could become more letrozole-resistant with increased HIF-1α. $CoCl_2$ was used to

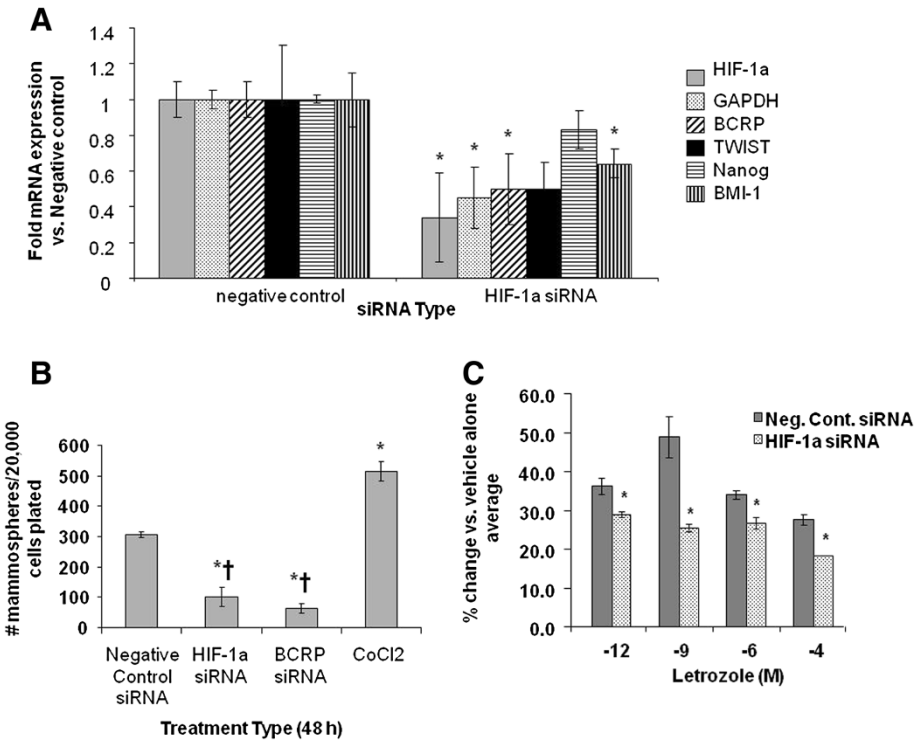

Figure 9 Effect of HIF-1α and/or BCRP siRNA on mammosphere formation and cell proliferation in LTLTCa cells. A) LTLTCa cells were treated with either negative control siRNA or HIF-1α siRNA for 48 hours. Total mRNA was extracted and HIF-1α, BCRP, GAPDH, Nanog, BMI-1 and TWIST mRNA, and 18S rRNA were analyzed by real-time RT-PCR. Real-time results are expressed as the fold-change in mRNA levels compared with negative control after normalization to 18S rRNA (mean ± SD, n = 6 independent cell samples/group; *versus vehicle; $P = 0.0.132$ HIF-1; $P = 0.0058$ GAPDH, $P = 0.0377$ BCRP, $P = 0.0612$ TWIST, $P = 0.058$ Nanog, $P = 0.0214$ BMI-1; two-sided t-test). **B)** LTLTCa cells were plated in passage media and then treated with negative control siRNA, HIF-1α siRNA, BCRP siRNA, or 100 μM $CoCl_2$ for 48 hours. Cells were then collected and resuspended in mammosphere media on low-attachment cell culture wells. Results are expressed as number of mammospheres counted per 20,000 cells plated (mean ± SD, n = 6 independent cell samples/group; *versus negative control, $P < 0.001$; † versus $CoCl_2$, $P < 0.001$; overall $P < 0.0001$, one-way ANOVA). BCRP siRNA confirmed to decrease BCRP expression (0.35- and 0.15-fold versus negative control, $P < 0.01$, one-way ANOVA; data not shown). **C)** Viability of the cells was measured by the MTT assay after 48 hours treatment with negative control or HIF-1 alpha siRNA and subsequently 6 day treatment with increasing doses of letrozole. Results are expressed as percent of 0 μM letrozole (vehicle) (mean ± SD, n = 4 independent cell samples/group; *versus 0 μM letrozole, $P < 0.001$; overall $P < 0.0001$ one way ANOVA). ANOVA, analysis of variance; BCRP, breast cancer resistant protein; HIF-1α, hypoxia inducible factor 1 α subunit; MTT, 3-[4,5-dimethylthiazol-2-yl]-2,5 diphenyl tetrazolium bromide; n, number; SD, standard deviation.

increase HIF-1α expression in MCF-7Ca cells and the efficacy of $CoCl_2$ was confirmed by Western blot analysis and RT-PCR. Within 24 hours of $CoCl_2$ treatment, HIF-1α protein and BCRP mRNA and protein expression were increased in MCF-7Ca cells (Figure 10A-B). Cell viability experiments in the presence of increasing concentrations of letrozole were then performed ($P < 0.0001$, one-way ANOVA). Consistent with previous findings from our laboratory [12], MCF-7Ca cells not treated with $CoCl_2$ were sensitive to the growth inhibitory effects of letrozole (Figure 10C). Additional treatment of MCF-7Ca cells with $CoCl_2$ significantly increased their resistance to letrozole. The effects of $CoCl_2$ were attributable to HIF-1, as co-treatment of MCF-7Ca cells with $CoCl_2$ and HIF-1α siRNA returned their sensitivity to letrozole. Overall, the physiological experiments on LTLTCa and MCF-7Ca cells indicate that HIF-1 is likely involved in both cancer stem cell characteristics and cell viability.

Discussion

Prior to this study, AI resistance was associated with increased dependence on growth factors and decreased dependence on ERα. However, the role that such molecular changes play in AI resistance and the mechanism by which they elicit their effects were not known. Novel results from this study demonstrated that nonhypoxic expression of HIF-1 mediates HER2's effects on letrozole-resistance. Specifically, the HER2-activated PI3K/Akt pathway increases HIF-1α protein synthesis in LTLTCa cells. HIF-1α, in turn, upregulates expression of BCRP and other genes and contributes to letrozole resistance and stem cell characteristics of LTLTCa cells.

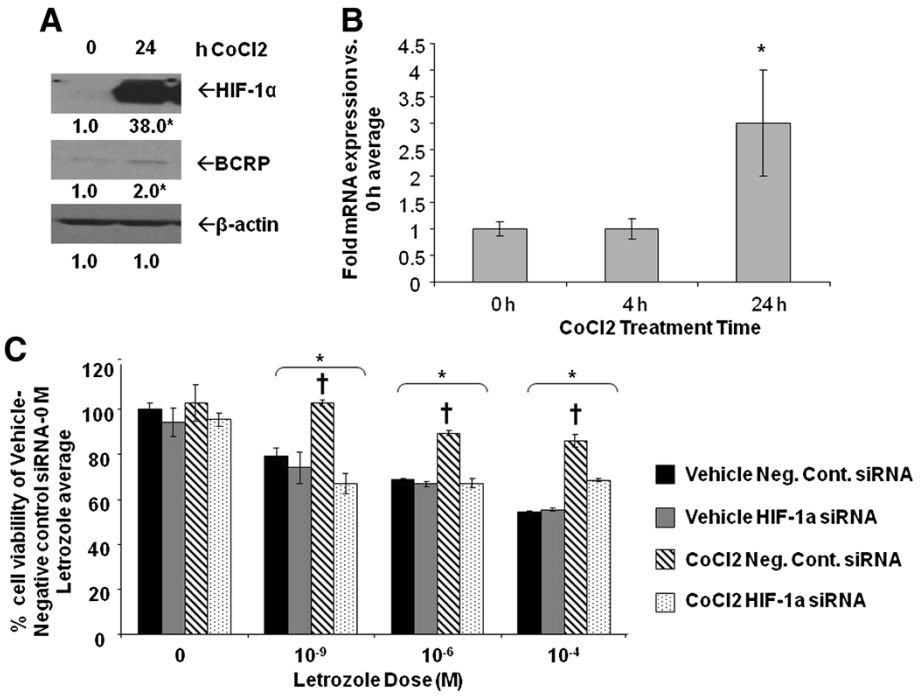

Figure 10 Effect of $CoCl_2$ on MCF-7Ca protein expression and cell viability. A-B, MCF-7Ca cells were incubated in steroid-free media and then treated with 100 μM $CoCl_2$ for 0 to 24 hours. **A)** Total protein was extracted and HIF-1α, BCRP, and β-actin were analyzed by Western blot analysis. Shown are representative blots and overall densitometry results of n = 6 independent cell samples/group. Densitometry results are expressed as mean fold-change in protein levels compared to 0 hours after normalization to β-actin (mean ± SD of n = 4 independent cell samples/group, *versus 0 hours; $P = 0.0005$ for HIF-1a; $P = 0.0065$ for BCRP, two-sided t-test). **B)** Total RNA was extracted and BCRP mRNA and 18S rRNA were analyzed by real-time RT-PCR analysis. Results are expressed as the mean fold-change in mRNA levels compared with 0 hours after normalization to 18S rRNA (mean ± SD, n = 4 independent cell samples/group; *versus 0 hours, $P < 0.001$; overall $P = 0.0002$, one-way ANOVA). **C)** Viability of cells was measured by MTT assay after five days of treatment with increasing doses of letrozole following 48 hours pre-treatment with or without 100 μM $CoCl_2$ and HIF-1α siRNA. Results are expressed as mean percent of 0 μM letrozole-without $CoCl_2$-with negative control siRNA (mean ± SD of n = 6 independent samples/group; *versus vehicle-negative control siRNA-0 μM letrozole, $P < 0.001$; † versus vehicle-HIF-1α siRNA and $CoCl_2$-HIF-1α siRNA; effect of letrozole $P < 0.0001$, effect of pre-treatment (vehicle/$CoCl_2$ and negative control siRNA/HIF-1α siRNA) $P < 0.0001$, interaction between letrozole dose and pre-treatment $P < 0.0001$; two-way ANOVA). ANOVA, analysis of variance; BCRP, breast cancer resistant protein; HIF-1α, hypoxia inducible factor 1 α subunit; MTT, 3-[4,5-dimethylthiazol-2-yl]-2,5 diphenyl tetrazolium bromide; n, number; SD, standard deviation.

Nonhypoxic regulation of HIF-1 expression and activity in LTLTCa cells is due to the HER2-activated PI3K/Akt/mTOR pathway. This is consistent with findings by others indicating hypoxia independent upregulation of HIF-1α in cancer cells by loss of function of tumor suppressor genes and gain of function of oncogenes [27]. The oncogene *HER2/neu*, in particular, has been previously associated with nonhypoxic HIF-1 [24,25]. Laughner *et al*. and Li *et al*. have demonstrated that transfection of HER2 into NIH/3 T3 cells or activation of HER2 in MCF-7 cells led to activation of the PI3K/Akt pathway, and the subsequent increased HIF-1 expression via protein synthesis and HIF-1 transcriptional activity. Previous studies have also demonstrated the importance of mTOR [48,49]. In addition, mTOR has been explored in two randomized trials (BOLERO-2 and TAMRAD) as a potential therapeutic target for overcoming endocrine therapy resistance [63]. Our current study provides evidence that this HER2-PI3K/Akt-mTOR-HIF-1 signaling mechanism can indeed occur endogenously in HER2+ cells (Figures 3, 4, and 8), leads to upregulation of BCRP (Figure 2), and has physiological relevance as well as potential clinical implications (for example, AI resistance; Figures 9 and 10).

Despite providing evidence that HER2 activation of the PI3K/Akt-mTOR pathway regulates HIF-1α, this study cannot completely exclude the involvement of ERα or the MAPK pathway. In addition to overexpressing HER2, LTLTCa cells also have decreased expression of ERα (Figure 3). It is possible that ERα can also regulate nonhypoxic HIF-1α expression in LTLTCa cells. Indeed, ERα- and HIF-1-mediated signaling pathways are known to interact antagonistically [18,19] and cooperatively [20-23]. Although this current study did not directly investigate ERα's role, the overexpression of HIF-1α observed in both ERα + (Hc7 and Ac1-ExR) and ERα- (LTLTCa) HER2+ breast cancer cell lines, suggests that ERα status may not

affect HER2 regulation of non-hypoxic HIF-1α levels. With regard to the MAPK pathway, inhibition of this pathway did not affect HIF-1α expression in LTLTCa cells, but it did decrease BCRP mRNA expression under basal, non-hypoxic conditions. It is possible that the MAPK pathway is involved in phosphorylation of HIF-1α rather than its synthesis. Previous studies have shown that MAPK pathway-mediated phosphorylation of HIF-1α occurs under non-hypoxic conditions and can increase HIF-1α expression and transcriptional activity [64,65]. These results could also indicate the MAPK and PI3K/Akt pathways have very distinct functions in AI-resistant breast cancer cells, regulating different subsets of genes. For example, the MAPK pathway may be involved in HER2 regulation of genes that require activation by phosphorylated $ER\alpha^{Ser118}$. In contrast, the PI3K/Akt pathway may be involved in HER2 regulation of genes that require HIF-1.

Inherent upregulation of HIF-1α protein expression under nonhypoxic conditions is another novel finding in AI-resistant breast cancer. There is precedence for associating HIF-1 expression with drug resistance in different cancer cell types, including chronic myeloid leukemia cells [66], gastric cancer cells [67], non-small cell lung cancer cells [68], and even breast cancer cells [58]. However, these previous cases involved hypoxia-induced, HIF-1α rather than the non-hypoxic HIF-1. Our findings are also consistent with previous clinical evidence that HIF-1α is associated with letrozole resistance. Generali *et al*. demonstrated that increased p-MAPK and HIF-1α protein expression were significant determinants of primary letrozole resistance in breast cancer patients. In contrast, increased ERα and decreased p-MAPK were significant determinants of response to letrozole treatment [56]. The protein expression patterns observed by Generali *et al*. are similar to what is observed in letrozole-resistant LTLTCa and –sensitive MCF-7Ca cells, respectively (Figures 3 and 6). Although these clinical findings involve *de novo* letrozole resistance, they still correlate with, and likely pertain to, our laboratory's results on acquired letrozole resistance. These results combined suggest that HIF-1 is involved in both *de novo* and acquired AI resistance and, therefore, could be therapeutically targeted to prevent and treat resistance to letrozole and the other AIs.

Lastly, this study indicates that HIF-1 may contribute to letrozole resistance by mediating the effects of HER2 on target genes, such as BCRP. Previous findings by our laboratory had implicated HER2 and BCRP in resistance to the growth inhibitory effects of letrozole and to maintenance of stem cell characteristics in letrozole-resistant breast cancer, and had demonstrated that its expression was dependent on HER2 [35,52], but it was unclear until now how HER2 regulated BCRP. Moreover, HIF-1 may mediate the effects of HER2 on many other genes. Besides, BCRP, other known HIF-1 target genes that may serve as markers of letrozole resistance include: 1) cancer stem cell maintenance markers (*Oct-4, kit ligand, JARID1B*); 2) epithelial-mesenchymal-transition (EMT) markers (*Snail, vimentin*); and 3) invasion markers (*c-Met, endothelin 1, fibronectin, MMP-2 and –4*) [27,69]. Interestingly, another known HIF-1 target gene, *VEGF,* was not upregulated in LTLTCa cells compared to MCF-7Ca cells. It is possible that nonhypoxic HIF-1 expression has different levels of influence on different HIF-1 target genes, particularly

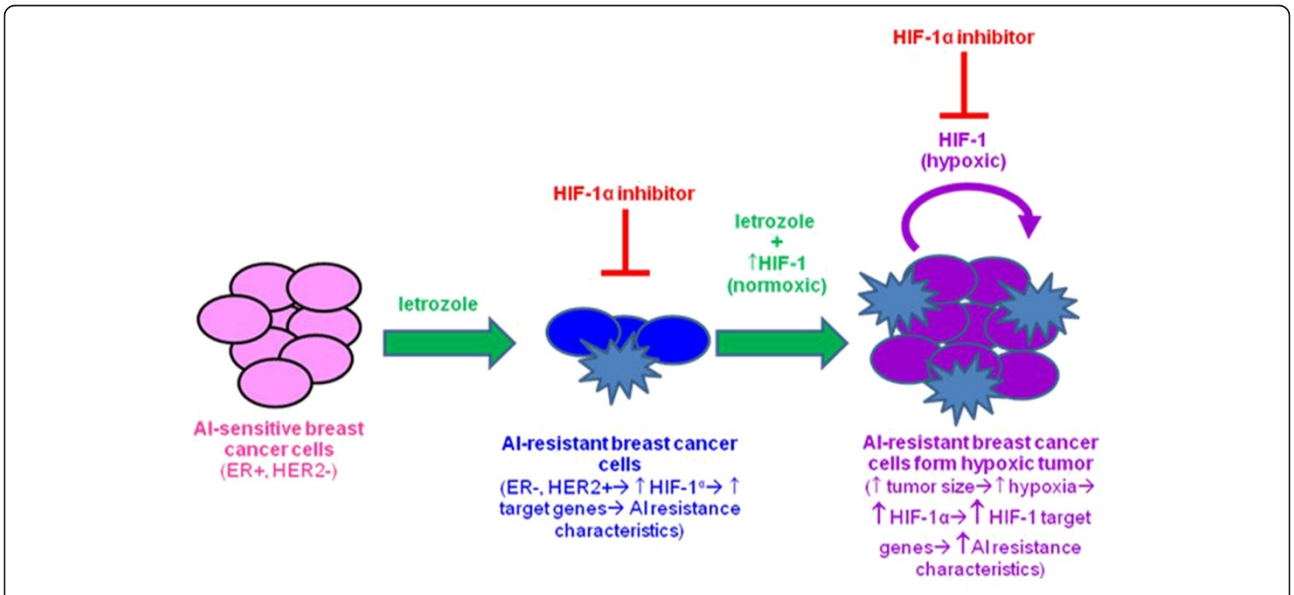

Figure 11 Proposed model of regulation and role of HIF-1α in AI resistant breast cancer.

those that can be regulated by multiple transcription factors. Indeed BCRP and VEGF both are known to be regulated by additional transcription factors, such as ERα [22,70].

Conclusions

Overall, this study provides novel evidence that non-hypoxic HIF-1α is inherently expressed in AI-resistant cells, upregulated by HER2-PI3K/Akt-mTOR pathway and is an important factor in letrozole-resistant breast cancer cells, regulating target genes such as *BCRP* and regulating AI responsiveness and cancer stem cell characteristic expression. Thus, HIF-1α could be used as a diagnostic marker and/or therapeutic target. Based on this, a proposed model of acquired AI-resistance may involve the following scenario: under non-hypoxic conditions, when the breast cancer cell population and tumor size have been reduced by letrozole treatment and prior to significant tumor hypoxia, a switch from ERα- to growth factor (for example, HER2)-mediated signaling occurs via PI3K/Akt and mTOR, which leads to increased HIF-1α expression and activation of HIF-1 target genes (for example, *BCRP*) that contribute to AI resistance (Figure 11). Consequently, inhibition of HIF-1 expression and/or activity would prolong cancer cell sensitivity to AIs and prevent recurrence and metastasis. Indeed, a number of anti-cancer drugs in clinical use are also known to inhibit HIF-1 [27]. They include HER2 inhibitor, trastuzumab [24] and lapatinib. Furthermore, as demonstrated in this study that HIF-1 is regulated mainly via the PI3K/Akt/mTOR pathway, inhibition of the downstream affecter of this pathway using mTOR inhibitors, such as rapamycin, temsirolimus/CCI-779 and everolimus/RAD-001, can also be considered [24,71-73]. There is also EZN-2968, a specific HIF-1α mRNA inhibitor, shown to reduce cancer cell viability and xenograft tumor growth, which is currently under phase I clinical trial [74]. Any of these anti-cancer drugs could now potentially, based on the evidence provided by this study, be applied to the prevention and treatment of AI-resistant breast cancer.

Additional file

Additional file 1: Table S1.1. Test results conducted to compare mean differences of normalized, log-transformed HIF-1α mRNA expression at various time points of actinomycin D for LTLTCa and MCF-7Ca cells. Shown are estimated mean differences in log transformed, normalized HIF-1α mRNA expression between different timepoints of actinomycin D treatment. Table results are estimated mean differences in log transformed, normalized HIF-1α mRNA expression between different timepoints of actinomycin D treatment calculated from the same data as shown Figure 1B data, which indicates trend over time. Pre-specified timepoints compared within each cell line were 0 versus 2 hours, 2 versus 4 hours, or 4 versus 16 hours. Data were analyzed by linear mixed effect model adjusting for experiment, cell line, and cell line*time interaction mRNA. Fixed effects for time, experiment, cell lines and interactions between time and cell lines were determined (means ± SD of n = 6 independent samples/group; P <0.001 for effect of cell line, time, their interaction and experiment). NS, not significant, P >0.05. **Table S1.2.** Test results conducted to compare mean differences of normalized, log-transformed BCRP mRNA expression at various time points of actinomycin D for both LTLTCa and MCF-7Ca cells. Table results are estimated mean differences in log transformed, normalized BCRP mRNA expression between different timepoints of actinomycin D treatment calculated from the same data as shown in Figure 2C. Pre-specified timepoints compared within each cell line were 0 versus 2 hours, 2 versus 4 hours, or 4 versus 16 hours. Data were analyzed by linear mixed effect model adjusting for experiment, cell line, and cell line*time interaction mRNA. Fixed effects for time, experiment, cell lines and interactions between time and cell lines were determined (means ± SD of n = 6 independent samples/group; P <0.001 for effect of time and cell line*time interaction). NS, not significant, P >0.05.

Abbreviations

AC1: MCF-7 cells transfected with the aromatase gene by the laboratory of Dr. Brodie; AC1-ExR: long-term exemestane treated AC1 cells; AI: aromatase inhibitor; Akt: also known as protein kinase B; ANOVA: analysis of variance; BCRP: breast cancer resistance protein; CDT: charcoal-dextran treated; ChIP: chromatin immunoprecipitation; (D)MEM: (Dulbecco's) modified Eagle's medium; EGFR: epidermal growth factor receptor; ERα: estrogen receptor alpha; FBS: fetal bovine serum; Hc7: MCF-7 cells transfected with HER2 gene by the laboratory of Dr. Brodie; HER2: human epidermal growth factor receptor 2; HIF-1: hypoxia inducible factor 1; HIF-1α: hypoxia inducible factor 1 α subunit; HRE: hypoxia-response element; LTLTCa: long-term letrozole treated MCF-7Ca cells; MAPK: mitogen-activated protein kinase; MCF-7Ca: MCF-7 cells transfected with the aromatase gene by the laboratory of Dr. Chen; mTOR: mammalian target of rapamycin; PBS: phosphate-buffered saline; PI3K: phosphatidylinositide 3-kinase; PRF: phenol red-free; ORF: open reading frame; siRNA: small interfering RNA; RT-PCR: reverse transcriptase-polymerase chain reaction; VEGF: vascular endothelial growth factor.

Competing interests

The authors declare that they have no competing interests.

Authors' contributions

AK conceived of and designed the study, performed all experiments, and drafted the manuscript. RG participated in RT-PCR in Figure 1A and western blot 1B. AS participated in densitometry analysis of Figure 3A and helped to draft the manuscript. SC coordinated obtaining lapatinib and trastuzumab and participated in discussions of study design. GS participated in the analysis and interpretation of Western blot data for Figures 3, 4, and 8 and statistical analyses for Figures 1B and 2C. PS participated in the mammosphere assay and selection of cancer stem cell markers in Figure 9A. OG performed statistical analyses for Figures 1B and 2C. SK performed statistical analyses for Figures 1B and 2C. AB participated in the design of the study, interpretation of all results, and the critical review and revision of the manuscript. All authors read and approved final manuscript.

Acknowledgements

Funding for this study was provided by the Department of Defense Breast Cancer Research Program Postdoctoral Award (BC1039031).

Author details

[1]Department of Pharmacology and Experimental Therapeutics, University of Maryland, Baltimore, MD 21201, USA. [2]Department of Medicine, University of Maryland, Baltimore, MD 21201, USA. [3]School of Medicine, University of Maryland Marlene and Stewart Greenebaum Cancer Center, Baltimore, MD 21201, USA. [4]Division of Biostatistics and Bioinformatics Department of Epidemiology and Public Health, University of Maryland, Baltimore, MD 21201, USA. [5]Department of Biology, Loyola University Maryland, Baltimore, MD 21210, USA. [6]Department of Pharmacology and Experimental Therapeutics, University of Maryland School of Medicine, Health Science Facilities, Room 580G, 685 West Baltimore Street, Baltimore, MD 21201, USA.

Received: 23 October 2012 Accepted: 2 January 2014
Published: 29 January 2014

References

1. United States Cancer Statistics: 1999–2008 Incidence and Mortality Web-based Report. [http://www.cdc.gov/uscs.]
2. Chumsri S, Howes T, Bao T, Sabnis G, Brodie A: **Aromatase, aromatase inhibitors, and breast cancer.** *J Steroid Biochem Mol Biol* 2011, **125:**13–22.
3. Santen RJ, Brodie H, Simpson ER, Siiteri PK, Brodie A: **History of aromatase: saga of an important biological mediator and therapeutic target.** *Endocr Rev* 2009, **30:**343–375.
4. Nabholtz JM, Mouret-Reynier MA, Durando X, Van Praagh I, Al-Sukhun S, Ferriere JP, Chollet P: **Comparative review of anastrozole, letrozole and exemestane in the management of early breast cancer.** *Expert Opin Pharmacother* 2009, **10:**1435–1447.
5. Dowsett M, Cuzick J, Ingle J, Coates A, Forbes J, Bliss J, Buyse M, Baum M, Buzdar A, Colleoni M, Coombes C, Snowdon C, Gnant M, Jakesz R, Kaufmann M, Boccardo F, Godwin J, Davies C, Peto R: **Meta-analysis of breast cancer outcomes in adjuvant trials of aromatase inhibitors versus tamoxifen.** *J Clin Oncol* 2010, **28:**509–518.
6. Winer EP, Hudis C, Burstein HJ, Wolff AC, Pritchard KI, Ingle JN, Chlebowski RT, Gelber R, Edge SB, Gralow J, Cobleigh MA, Mamounas EP, Goldstein LJ, Whelan TJ, Powles TJ, Bryant J, Perkins C, Perotti J, Braun S, Langer AS, Browman GP, Somerfield MR: **American Society of Clinical Oncology technology assessment on the use of aromatase inhibitors as adjuvant therapy for postmenopausal women with hormone receptor-positive breast cancer: status report 2004.** *J Clin Oncol* 2005, **23:**619–629.
7. Miller WR, Larionov AA: **Understanding the mechanisms of aromatase inhibitor resistance.** *Breast Cancer Res* 2012, **14:**201.
8. Kubo M, Kanaya N, Petrossian K, Ye J, Warden C, Liu Z, Nishimura R, Osako T, Okido M, Shimada K, Takahashi M, Chu P, Yuan YC, Chen S: **Inhibition of the proliferation of acquired aromatase inhibitor-resistant breast cancer cells by histone deacetylase inhibitor LBH589 (panobinostat).** *Breast Cancer Res Treat* 2013, **137:**93–107.
9. Sabnis G, Brodie A: **Adaptive changes results in activation of alternate signaling pathways and resistance to aromatase inhibitor resistance.** *Mol Cell Endocrinol*, **340:**142–147.
10. Johnston SR, Martin LA, Leary A, Head J, Dowsett M: **Clinical strategies for rationale combinations of aromatase inhibitors with novel therapies for breast cancer.** *J Steroid Biochem Mol Biol* 2007, **106:**180–186.
11. Macedo LF, Sabnis GJ, Goloubeva OG, Brodie A: **Combination of anastrozole with fulvestrant in the intratumoral aromatase xenograft model.** *Cancer Res* 2008, **68:**3516–3522.
12. Sabnis G, Schayowitz A, Goloubeva O, Macedo L, Brodie A: **Trastuzumab reverses letrozole resistance and amplifies the sensitivity of breast cancer cells to estrogen.** *Cancer Res* 2009, **69:**1416–1428.
13. Brodie A, Macedo L, Sabnis G: **Aromatase resistance mechanisms in model systems in vivo.** *J Steroid Biochem Mol Biol* 2010, **118:**283–287.
14. Schwartzberg LS, Franco SX, Florance A, O'Rourke L, Maltzman J, Johnston S: **Lapatinib plus letrozole as first-line therapy for HER-2+ hormone receptor-positive metastatic breast cancer.** *Oncologist* 2010, **15:**122–129.
15. Hynes NE, Lane HA: **ERBB receptors and cancer: the complexity of targeted inhibitors.** *Nat Rev Cancer* 2005, **5:**341–354.
16. Mukohara T: **Mechanisms of resistance to anti-human epidermal growth factor receptor 2 agents in breast cancer.** *Cancer Sci* 2011, **102:**1–8.
17. Semenza GL: **Targeting HIF-1 for cancer therapy.** *Nat Rev Cancer* 2003, **3:**721–732.
18. Cho J, Kim D, Lee S, Lee Y: **Cobalt chloride-induced estrogen receptor alpha down-regulation involves hypoxia-inducible factor-1alpha in MCF-7 human breast cancer cells.** *Mol Endocrinol (Baltimore, Md)* 2005, **19:**1191–1199.
19. Mukundan H, Kanagy NL, Resta TC: **17-beta estradiol attenuates hypoxic induction of HIF-1alpha and erythropoietin in Hep3B cells.** *J Cardiovasc Pharmacol* 2004, **44:**93–100.
20. Kazi AA, Jones JM, Koos RD: **Chromatin immunoprecipitation analysis of gene expression in the rat uterus in vivo: estrogen-induced recruitment of both estrogen receptor alpha and hypoxia-inducible factor 1 to the vascular endothelial growth factor promoter.** *Mol Endocrinol (Baltimore, Md)* 2005, **19:**2006–2019.
21. Cho J, Bahn JJ, Park M, Ahn W, Lee YJ: **Hypoxic activation of unoccupied estrogen-receptor-alpha is mediated by hypoxia-inducible factor-1 alpha.** *J Steroid Biochem Mol Biol* 2006, **100:**18–23.
22. Kazi AA, Koos RD: **Estrogen-induced activation of hypoxia-inducible factor-1alpha, vascular endothelial growth factor expression, and edema in the uterus are mediated by the phosphatidylinositol 3-kinase/Akt pathway.** *Endocrinology* 2007, **148:**2363–2374.
23. Hua K, Din J, Cao Q, Feng W, Zhang Y, Yao L, Huang Y, Zhao Y, Feng Y: **Estrogen and progestin regulate HIF-1alpha expression in ovarian cancer cell lines via the activation of Akt signaling transduction pathway.** *Oncol Rep* 2009, **21:**893–898.
24. Laughner E, Taghavi P, Chiles K, Mahon PC, Semenza GL: **HER2 (neu) signaling increases the rate of hypoxia-inducible factor 1alpha (HIF-1alpha) synthesis: novel mechanism for HIF-1-mediated vascular endothelial growth factor expression.** *Mol Cell Biol* 2001, **21:**3995–4004.
25. Li YM, Zhou BP, Deng J, Pan Y, Hay N, Hung MC: **A hypoxia-independent hypoxia-inducible factor-1 activation pathway induced by phosphatidylinositol-3 kinase/Akt in HER2 overexpressing cells.** *Cancer Res* 2005, **65:**3257–3263.
26. Vaupel P, Mayer A, Hockel M: **Tumor hypoxia and malignant progression.** *Methods Enzymol* 2004, **381:**335–354.
27. Semenza GL: **Defining the role of hypoxia-inducible factor 1 in cancer biology and therapeutics.** *Oncogene* 2010, **29:**625–634.
28. Mendez O, Zavadil J, Esencay M, Lukyanov Y, Santovasi D, Wang SC, Newcomb EW, Zagzag D: **Knock down of HIF-1alpha in glioma cells reduces migration in vitro and invasion in vivo and impairs their ability to form tumor spheres.** *Mol Cancer* 2010, **9:**133.
29. Lu X, Yan CH, Yuan M, Wei Y, Hu G, Kang Y: **In vivo dynamics and distinct functions of hypoxia in primary tumor growth and organotropic metastasis of breast cancer.** *Cancer Res* 2010, **70:**3905–3914.
30. Mazumdar J, Dondeti V, Simon MC: **Hypoxia-inducible factors in stem cells and cancer.** *J Cell Mol Med* 2009, **13:**4319–4328.
31. Krishnamurthy P, Ross DD, Nakanishi T, Bailey-Dell K, Zhou S, Mercer KE, Sarkadi B, Sorrentino BP, Schuetz JD: **The stem cell marker Bcrp/ABCG2 enhances hypoxic cell survival through interactions with heme.** *J Biol Chem* 2004, **279:**24218–24225.
32. Zhou DJ, Pompon D, Chen SA: **Stable expression of human aromatase complementary DNA in mammalian cells: a useful system for aromatase inhibitor screening.** *Cancer Res* 1990, **50:**6949–6954.
33. Yue W, Zhou D, Chen S, Brodie A: **A new nude mouse model for postmenopausal breast cancer using MCF-7 cells transfected with the human aromatase gene.** *Cancer Res* 1994, **54:**5092–5095.
34. Jelovac D, Sabnis G, Long BJ, Macedo L, Goloubeva OG, Brodie AM: **Activation of mitogen-activated protein kinase in xenografts and cells during prolonged treatment with aromatase inhibitor letrozole.** *Cancer Res* 2005, **65:**5380–5389.
35. Sabnis G, Goloubeva O, Gilani R, Macedo L, Brodie A: **Sensitivity to the aromatase inhibitor letrozole is prolonged after a "break" in treatment.** *Mol Cancer Ther* 2010, **9:**46–56.
36. Burks SR, Macedo LF, Barth ED, Tkaczuk KH, Martin SS, Rosen GM, Halpern HJ, Brodie AM, Kao JP: **Anti-HER2 immunoliposomes for selective delivery of electron paramagnetic resonance imaging probes to HER2-overexpressing breast tumor cells.** *Breast Cancer Res Treat* 2010, **124:**121–131.
37. Macedo LF, Guo Z, Tilghman SL, Sabnis GJ, Qiu Y, Brodie A: **Role of androgens on MCF-7 breast cancer cell growth and on the inhibitory effect of letrozole.** *Cancer Res* 2006, **66:**7775–7782.
38. Schech AJ, Nemieboka BE, Brodie AH: **Zoledronic acid inhibits aromatase activity and phosphorylation: potential mechanism for additive zoledronic acid and letrozole drug interaction.** *J Steroid Biochem Mol Biol* 2012, **132:**195–202.
39. Stroka DM, Burkhardt T, Desbaillets I, Wenger RH, Neil DA, Bauer C, Gassmann M, Candinas D: **HIF-1 is expressed in normoxic tissue and displays an organ-specific regulation under systemic hypoxia.** *FASEB J* 2001, **15:**2445–2453.
40. Jiang BH, Semenza GL, Bauer C, Marti HH: **Hypoxia-inducible factor 1 levels vary exponentially over a physiologically relevant range of O2 tension.** *Am J Physiol* 1996, **271:**C1172–C1180.
41. Bergstraesser LM, Weitzman SA: **Culture of normal and malignant primary human mammary epithelial cells in a physiological manner simulates in vivo growth patterns and allows discrimination of cell type.** *Cancer Res* 1993, **53:**2644–2654.
42. Fang Y, Sullivan R, Graham CH: **Confluence-dependent resistance to doxorubicin in human MDA-MB-231 breast carcinoma cells requires hypoxia-inducible factor-1 activity.** *Exp Cell Res* 2007, **313:**867–877.
43. Paltoglou SM, Roberts BJ: **Role of the von Hippel-Lindau tumour suppressor protein in the regulation of HIF-1alpha and its oxygen-**

regulated transactivation domains at high cell density. *Oncogene* 2005, **24:**3830–3835.
44. Semenza G: **Signal transduction to hypoxia-inducible factor 1.** *Biochem Pharmacol* 2002, **64:**993–998.
45. Yuan Y, Hilliard G, Ferguson T, Millhorn DE: **Cobalt inhibits the interaction between hypoxia-inducible factor-alpha and von Hippel-Lindau protein by direct binding to hypoxia-inducible factor-alpha.** *J Biol Chem* 2003, **278:**15911–15916.
46. Wang GL, Semenza GL: **General involvement of hypoxia-inducible factor 1 in transcriptional response to hypoxia.** *Proc Natl Acad Sci U S A* 1993, **90:**4304–4308.
47. Sabnis G, Brodie A: **Understanding resistance to endocrine agents: molecular mechanisms and potential for intervention.** *Clin Breast Cancer* 2010, **10:**E6–E15.
48. Pore N, Jiang Z, Shu HK, Bernhard E, Kao GD, Maity A: **Akt1 activation can augment hypoxia-inducible factor-1alpha expression by increasing protein translation through a mammalian target of rapamycin-independent pathway.** *Mol Cancer Res* 2006, **4:**471–479.
49. Sudhagar S, Sathya S, Lakshmi BS: **Rapid non-genomic signalling by 17beta-oestradiol through c-Src involves mTOR-dependent expression of HIF-1alpha in breast cancer cells.** *Br J Cancer* 2011, **105:**953–960.
50. Allen JD, Schinkel AH: **Multidrug resistance and pharmacological protection mediated by the breast cancer resistance protein (BCRP/ABCG2).** *Mol Cancer Ther* 2002, **1:**427–434.
51. Doyle LA, Ross DD: **Multidrug resistance mediated by the breast cancer resistance protein BCRP (ABCG2).** *Oncogene* 2003, **22:**7340–7358.
52. Gilani RA, Kazi AA, Shah P, Schech AJ, Chumsri S, Sabnis G, Jaiswal AK, Brodie AH: **The importance of HER2 signaling in the tumor-initiating cell population in aromatase inhibitor-resistant breast cancer.** *Breast Cancer Res Treat* 2012, **135:**681–692.
53. Li X, Pan YZ, Seigel GM, Hu ZH, Huang M, Yu AM: **Breast cancer resistance protein BCRP/ABCG2 regulatory microRNAs (hsa-miR-328, -519c and −520 h) and their differential expression in stem-like ABCG2+ cancer cells.** *Biochem Pharmacol* 2011, **81:**783–792.
54. Yeo EJ, Chun YS, Park JW: **New anticancer strategies targeting HIF-1.** *Biochem Pharmacol* 2004, **68:**1061–1069.
55. Feng Y, Zhu H, Ling T, Hao B, Zhang G, Shi R: **Effects of YC-1 targeting hypoxia-inducible factor 1 alpha in oesophageal squamous carcinoma cell line Eca109 cells.** *Cell Biol Int* 2011, **35:**491–497.
56. Generali D, Buffa FM, Berruti A, Brizzi MP, Campo L, Bonardi S, Bersiga A, Allevi G, Milani M, Aguggini S, Papotti M, Dogliotti L, Bottini A, Harris AL, Fox SB: **Phosphorylated ERalpha, HIF-1alpha, and MAPK signaling as predictors of primary endocrine treatment response and resistance in patients with breast cancer.** *J Clin Oncol* 2009, **27:**227–234.
57. Rohwer N, Cramer T: **Hypoxia-mediated drug resistance: novel insights on the functional interaction of HIFs and cell death pathways.** *Drug Resist Updat* 2011, **14:**191–201.
58. Flamant L, Notte A, Ninane N, Raes M, Michiels C: **Anti-apoptotic role of HIF-1 and AP-1 in paclitaxel exposed breast cancer cells under hypoxia.** *Mol Cancer* 2010, **9:**191.
59. Mathieu J, Zhang Z, Zhou W, Wang AJ, Heddleston JM, Pinna CM, Hubaud A, Stadler B, Choi M, Bar M, Tewari M, Liu A, Vessella R, Rostomily R, Born D, Horwitz M, Ware C, Blau CA, Cleary MA, Rich JN, Ruohola-Baker H: **HIF induces human embryonic stem cell markers in cancer cells.** *Cancer Res* 2011, **71:**4640–4652.
60. Oliveira-Costa JP, Zanetti JS, Silveira GG, Soave DF, Oliveira LR, Zorgetto VA, Soares FA, Zucoloto S, Ribeiro-Silva A: **Differential expression of HIF-1alpha in CD44 + CD24-/low breast ductal carcinomas.** *Diagn Pathol* 2011, **6:**73.
61. Higashimura Y, Nakajima Y, Yamaji R, Harada N, Shibasaki F, Nakano Y, Inui H: **Up-regulation of glyceraldehyde-3-phosphate dehydrogenase gene expression by HIF-1 activity depending on Sp1 in hypoxic breast cancer cells.** *Arch Biochem Biophys* 2011, **509:**1–8.
62. Wu KJ, Yang MH: **Epithelial-mesenchymal transition and cancer stemness: the Twist1–Bmi1 connection.** *Biosci Rep*, **31:**449–455.
63. Fedele P, Calvani N, Marino A, Orlando L, Schiavone P, Quaranta A, Cinieri S: **Targeted agents to reverse resistance to endocrine therapy in metastatic breast cancer: where are we now and where are we going?** *Crit Rev Oncol Hematol* 2012, **84:**243–251.
64. Berra E, Pages G, Pouyssegur J: **MAP kinases and hypoxia in the control of VEGF expression.** *Cancer Metastasis Rev* 2000, **19:**139–145.
65. Minet E, Michel G, Mottet D, Raes M, Michiels C: **Transduction pathways involved in Hypoxia-Inducible Factor-1 phosphorylation and activation.** *Free Radic Biol Med* 2001, **31:**847–855.
66. Zhao F, Mancuso A, Bui TV, Tong X, Gruber JJ, Swider CR, Sanchez PV, Lum JJ, Sayed N, Melo JV, Perl AE, Carroll M, Tuttle SW, Thompson CB: **Imatinib resistance associated with BCR-ABL upregulation is dependent on HIF-1alpha-induced metabolic reprograming.** *Oncogene* 2010, **29:**2962–2972.
67. Liu L, Ning X, Sun L, Shi Y, Han S, Guo C, Chen Y, Sun S, Yin F, Wu K, Fan D: **Involvement of MGr1-Ag/37LRP in the vincristine-induced HIF-1 expression in gastric cancer cells.** *Mol Cell Biochem* 2007, **303:**151–160.
68. Song X, Liu X, Chi W, Liu Y, Wei L, Wang X, Yu J: **Hypoxia-induced resistance to cisplatin and doxorubicin in non-small cell lung cancer is inhibited by silencing of HIF-1alpha gene.** *Cancer Chemother Pharmacol* 2006, **58:**776–784.
69. Whipple RA, Matrone MA, Cho EH, Balzer EM, Vitolo MI, Yoon JR, Ioffe OB, Tuttle KC, Yang J, Martin SS: **Epithelial-to-mesenchymal transition promotes tubulin detyrosination and microtentacles that enhance endothelial engagement.** *Cancer Res* 2010, **70:**8127–8137.
70. Zhang Y, Zhou G, Wang H, Zhang X, Wei F, Cai Y, Yin D: **Transcriptional upregulation of breast cancer resistance protein by 17beta-estradiol in ERalpha-positive MCF-7 breast cancer cells.** *Oncology* 2006, **71:**446–455.
71. Majumder PK, Febbo PG, Bikoff R, Berger R, Xue Q, McMahon LM, Manola J, Brugarolas J, McDonnell TJ, Golub TR, Loda M, Lane HA, Sellers WR: **mTOR inhibition reverses Akt-dependent prostate intraepithelial neoplasia through regulation of apoptotic and HIF-1-dependent pathways.** *Nat Med* 2004, **10:**594–601.
72. Faivre S, Kroemer G, Raymond E: **Current development of mTOR inhibitors as anticancer agents.** *Nat Rev Drug Discov* 2006, **5:**671–688.
73. Thomas GV, Tran C, Mellinghoff IK, Welsbie DS, Chan E, Fueger B, Czernin J, Sawyers CL: **Hypoxia-inducible factor determines sensitivity to inhibitors of mTOR in kidney cancer.** *Nat Med* 2006, **12:**122–127.
74. Greenberger LM, Horak ID, Filpula D, Sapra P, Westergaard M, Frydenlund HF, Albaek C, Schroder H, Orum H: **A RNA antagonist of hypoxia-inducible factor-1alpha, EZN-2968, inhibits tumor cell growth.** *Mol Cancer Ther* 2008, **7:**3598–3608.

doi:10.1186/bcr3609
Cite this article as: Kazi *et al.*: Nonhypoxic regulation and role of hypoxia-inducible factor 1 in aromatase inhibitor resistant breast cancer. *Breast Cancer Research* 2014 **16:**R15.